

The role of caspase-7 during infection with *Listeria monocytogenes* and during intoxication with listeriolysin O.

By

Sara Kathryn Bondi Cassidy

**A dissertation submitted in partial fulfillment
of the requirements for the degree of
Doctor of Philosophy
(Microbiology and Immunology)
in the University of Michigan
2013**

Doctoral Committee:

**Associate Professor Mary X.D. O'Riordan, Chair
Professor Victor J. DiRita
Professor Colin S. Duckett
Professor Michele S. Swanson**

Dedication

This work is dedicated to my daughter, Rosemarie Katherine Cassidy. May it inspire her with the courage to follow her dreams, whatever they may be.

Acknowledgements

My sincerest thanks to Gabriel Nuñez and Thirumala-Devi Kannaganti for contributing mice and expertise to the data outlined in Chapter 2. I'm also grateful to Jon Hagar for his contribution to Chapter 2, and to Darren Higgins, who provided bacterial strains that helped to make this work possible.

Special thanks go to Luigi Franchi, who provided not only mice to this project, but served as my supervisor during my internship at Lycera, Corp. Luigi has been fantastically supportive of my development as a scientist, both academically and professionally.

Thanks to Marie-Ève Charbonneau for major contributions to Chapter 3 and for being a stellar role model.

Special thanks go to my committee, whose insight has made substantial contributions to this body of work. Thanks to Vic, for keeping this project grounded and honest. Thanks to Colin, for teaching me about caspase biology and apoptosis, and for providing a framework on which to mold my experiments. Thanks to Michele, for helping me think about the cell biology in a meaningful way, for providing expertise and reagents, and for being a professional and personal role model. And my deepest thanks to Mary, who has shaped my professional development in such a positive way, I am confident I will succeed in any future scientific endeavors.

Finally, I must acknowledge the contribution of my husband, Eugene Cassidy, to the completion of this work. He, pursuing his own Ph. D. in History, has faithfully taken on well more than his share of the household chores and childcare. For the past 6 months, he has worked every night at the kitchen table on his own dissertation to compensate

for the time he spends during the day making sure the wheels don't fall off our wagon. I am more confident and more beautiful than I have ever been at any other time in my life. I shine because I have the love of a person who shares my values and my passions, who is not above lending his t-shirt to a snotty toddler when she needs a tissue, or lending a hand to his wife when she needs a boost. I got so lucky snagging him, and I hope I never forget it. Without him, certainly, this work would not exist.

Table of Contents

Dedication	ii
Acknowledgements	iii
List of figures	vii
Chapter 1	
More than a pore: The cellular response to cholesterol-dependent cytolysins	1
Abstract	1
1. Introduction	2
2. The physical properties of the CDCs	4
2.1 Structure and membrane binding	4
2.2 Oligomerization and pore formation	5
3. Membrane response to CDC intoxication	10
3.1 Endocytosis of pores	10
3.2 Membrane blebbing	12
4. Intracellular effects of CDC intoxication	15
4.1 Effects on the endoplasmic reticulum and Golgi	15
4.2 Effects on the mitochondria and nucleus	16
4.3 Endolysosomal network	20
4.4 Immune signaling	21
5. Conclusions	24
6. References	25
Chapter 2	
Membrane damage during <i>Listeria monocytogenes</i> infection triggers a caspase-7 dependent cytoprotective response	34
Abstract	34
1. Introduction	36

2. Results	39
3. Discussion	56
4. Methods and materials	59
5. References	66
Chapter 3	
Transient activation of caspase-7 promotes blebbing and survival in response to damage by pore-forming toxins	71
Abstract	71
1. Introduction	73
2. Results	76
3. Discussion	91
4. Materials and methods	95
5. References	101
Chapter 4	
The contribution of cellular processes to membrane repair after LLO damage	106
1. Introduction	106
2. Results	107
3. Discussion	125
4. References	128
Chapter 5	
Perspectives	131
References	143
Appendix	147

List of Figures

Chapter 1

- 1.1. CDC pore-dependent membrane repair 11
- 1.2. CDC pore-dependent signaling responses 19

Chapter 2

- 2.1. Caspase-7 is activated in macrophages during infection with *L. monocytogenes*. 40
- 2.2. Caspase-7 activation during infection with *L. monocytogenes* induces minimal apoptosis. 42
- 2.3. Caspase-1 and other key mediators of innate immunity are individually dispensable for caspase-7 cleavage. 44
- 2.4. Caspase-7 deficient BMDM are permeable to small molecules during infection. 47
- 2.5. Caspase-7 enhances host resistance to LLO-mediated plasma membrane damage. 49
- 2.6. Caspase-7 is cleaved in response to membrane damage in the absence of infection. 52
- 2.7. Damage caused by pore-forming toxins stimulates caspase-7 cleavage. 54

Chapter 3

- 3.1. Transient caspase-7 activity promotes survival and membrane integrity in LLO-intoxicated cells. 77
- 3.2. *csp7^{-/-}* cells display altered blebbing compared to BL/6 cells in response to LLO treatment. 81
- 3.3. ROCK I is cleaved in a caspase-dependent manner in response to LLO damage. 83
- 3.4. Inhibition of ROCK and myosin impedes toxin-induced blebbing 85

3.5. Annexin A1 aggregation is reduced in <i>csp7^{-/-}</i> BMDMs post intoxication.	88
3.6. ROCK I and myosin II promote membrane fidelity during infection with <i>L. monocytogenes</i> .	90

Chapter 4

4.1. LAMP-1 staining of BMDMs in response to infection.	108
4.2. ASM treatment of <i>L. monocytogenes</i> infected BMDMs.	111
4.3. Cholesterol biosynthesis regulation during <i>L. monocytogenes</i> infection.	113
4.4. Monitoring PDI as a marker of ER stress in response to PFT damage.	116
4.5. Activation of the UPR in response to LLO damage.	119
4.6 Autophagy is activated by exogenous LLO treatment and is reduced by myosin II inhibition.	123

Chapter 5

5.1. Models of caspase-7 activation	135
5.2. Caspase-3 is activated with slower kinetics than caspase-7 in response to toxin treatment.	138
5.2. A schematic of the dichotomous roles of activated caspase-7.	142

Appendix

A1. Infection at MOI1 and MOI5 results in equivalent intracellular CFU by 8h pi.	148
A2. Caspase-3 is weakly cleaved in response to <i>L. monocytogenes</i> infection.	149
A3. Most <i>L. monocytogenes</i> infected cells do not display common markers of apoptosis.	150
A4. Caspase-7 deficient cells retain LDH at similar levels as BL/6 cells during infection.	151
A5. WT and iLLO strains grow to equivalent intracellular CFU by 8 h pi.	152
A6. BMDM treated with low concentrations of exogenous LLO do not release LDH by 5 h pi.	153
A7. BMDM treated with α -hemolysin release little LDH 8 h post treatment.	154
A8. Treatment of BMDMs with LLO results in transient caspase-7	

activation.	155
A9. Caspase-7 deficient cells display slower recovery after LLO intoxication compared to BL/6 cells.	156

Chapter 1

More than a pore: The cellular response to cholesterol-dependent cytolysins

(Published: Cassidy SKB and O’Riordan MXD (2013) Toxins 5:618-636)

Abstract: Targeted disruption of the plasma membrane is a ubiquitous form of attack used in all three domains of life. Many bacteria secrete pore-forming proteins during infection with broad implications for pathogenesis. The cholesterol-dependent cytolysins (CDC) are a family of pore-forming toxins expressed predominately by Gram-positive bacterial pathogens. The structure and assembly of some of these oligomeric toxins on the host membrane have been described, but how the targeted cell responds to intoxication by the CDCs is not as clearly understood. Many CDCs induce lysis of their target cell and can activate apoptotic cascades to promote cell death. However, the extent to which intoxication causes cell death is both CDC- and host cell-dependent, and at lower concentrations of toxin, survival of intoxicated host cells is well documented. Additionally, the effect of CDCs can be seen beyond the plasma membrane, and it is becoming increasingly clear that these toxins are potent regulators of signaling and immunity, beyond their role in intoxication. In this review, we discuss the cellular response to CDC intoxication with emphasis on the effects of pore formation on the host cell plasma membrane and subcellular organelles and whether subsequent cellular responses contribute to the survival of the affected cell.

1. Introduction

The cholesterol-dependent cytolysins (CDCs) are a family of pore-forming proteins expressed by several genera of pathogenic, primarily Gram-positive bacteria that cause very different diseases. Examples include *Streptococcus pyogenes*, a common cause of upper respiratory infections, *Bacillus anthracis*, which mostly causes cutaneous infections, and *Listeria monocytogenes*, which causes gastroenteritis. The CDCs are secreted as soluble monomers, which upon binding to host cell membranes, can oligomerize to form β -barrel pores of large diameter. Although the CDCs share structural similarity, the role of these toxins during infection largely depends on the pathogen and the context of infection. For instance, data suggest the secretion of Streptolysin O (SLO) may protect the extracellular pathogen, *S. pyogenes*, from phagocytic killing by lysing target cells [1]. SLO translocates the *S. pyogenes* secreted effector, SPN, into target cells resulting in cytotoxicity [2]. In contrast, Listeriolysin O (LLO) is necessary for the intracellular pathogen, *Listeria monocytogenes*, to escape the primary vacuole and replicate within the cytosol of intact macrophages [3]. Thus, bacteria can exploit a common mechanism of pore formation to drive divergent cellular outcomes during pathogenesis.

CDC intoxication may result in some characteristic hallmarks of membrane damage, such as ion flux across the targeted cell membrane, loss of cytosolic contents, stimulation of repair mechanisms, and host cell lysis. However, many cellular responses to CDCs are poorly explained by pore-formation alone. For instance, Tetanolysin O (TLO) from *Clostridium tetani*, stimulates the release of IL-1 β , a pro-inflammatory cytokine, from target cells, but only at sub-lytic doses [4], which may contribute to host clearance of the bacteria. Others have shown that a non-cytolytic allele of pneumolysin

(PLY) retained the capacity to stimulate IFN γ , a cytokine capable of activating macrophages, in the absence of the ability to form pores [5]. Thus, the CDCs can trigger adaptive or inflammatory pathways within the targeted cell, independently from or in addition to, the damage they cause. It is also apparent that some cell types are able to withstand and repair lesions caused by pore-forming toxins, the molecular mechanisms of which are incompletely elucidated [6].

Many studies have used direct mutation of the CDC protein or pre-treatment with cholesterol to assess the signal transduction capabilities of CDC treatment in the absence of pore-formation. Pre-treatment with cholesterol was reported to abrogate pore formation, but not monomer binding of LLO [7]. Typically, loss of pore-formation is measured via the lysis of red blood cells [7], the release of lactate dehydrogenase (LDH) from target cells [2,5] and/or the visualization of pores on the target cell surface [7]. However, a more recent study by Hamon and Cossart demonstrated that LLO pre-treated with cholesterol still allowed K⁺ flux across the plasma membrane, which suggests that cholesterol-treated LLO may retain some membrane damaging capacity [8]. Moreover, mutations in these pore-forming proteins that destroy their ability to lyse red blood cells may still allow some activity in other cell types, as demonstrated for the perfringolysin O (PFO) G461D mutant protein [9]. Thus, we note that caution should be taken in concluding unequivocally which host response pathways are stimulated by pore-formation and which are not, but include in this chapter some studies indicating that pore-formation is likely not the only property of the CDC proteins that can drive host responses.

Macromolecular pore-forming proteins are not unique to bacteria. Members of the MACPF family, including mammalian perforin and the C9 protein of the complement

cascade, share strikingly similar structural topology and pore-forming mechanisms with the CDCs [10]. The parasite, *Toxoplasma gondii*, secretes a pore-forming protein, PLP1, to promote egress from infected cells [11]. *Enterolobium contortisiliquum*, a tree native to Brazil, produces a pore-forming toxin, which functions as an insecticide and deterrent from ingestion [12]. The structural similarities between CDCs, perforin, and PLP1, for example, suggest that the target cell may sense membrane damage caused by these toxins in similar ways. For instance the pores produced by both CDCs and perforin are rapidly resealed [13,14]. As such, there are likely conserved mechanisms in the adaptive cellular response to intoxication by these proteins. Given that plasma membrane disruption is ubiquitous among all forms of life, the study of the cellular response to the insult of pore formation may provide insight into broadly relevant mechanisms for cellular preservation and survival.

2. Physical properties of the CDCs

2.1 Structure and membrane binding

Alignment of the amino acid sequences of CDCs reveals significant identity (from 28-99%) and similarity (> 45%) among family members [15], suggesting conservation of activity and structure. The four CDC proteins from different bacterial species that have been crystallized in their soluble monomeric form, PFO [16], intermedilysin (ILY) [17], anthrolysin O (ALO) [18], and suilysin (SLY) [19], all display markedly similar topology (CDC membrane assembly is reviewed in detail here [20]). One of the defining characteristics of the CDC family is a structural motif of 11 residues (ECTGLAWEWWR), termed the undecapeptide or tryptophan rich motif, situated at the membrane-binding portion of the protein. Single amino acid mutations in this motif alter pore formation, but recent work suggests that other elements and not the undecapeptide are necessary for cholesterol recognition [21]. Instead, this motif is proposed to control structural reorientation after cholesterol binding [22].

The CDC monomers are rich in β -sheets and their structures are divided into four domains of which D2-4 are responsible for cholesterol recognition and membrane insertion. The contribution of D1 is not well characterized. For all but two CDCs, cholesterol is necessary and sufficient for membrane binding. The exceptions are intermedilysin (ILY) and vaginolysin (VLY), which require an additional receptor, human CD59, for membrane recognition [23,24], imparting species specificity to these two toxins.

2.2 Oligomerization and pore formation

Many studies support a model where CDC monomers preferentially bind in lipid rafts, which are microdomains of the plasma membrane enriched for cholesterol and signaling molecules, because of the requirement for membrane cholesterol in pore formation [25-27]. Coalescence of rafts containing monomers increases the likelihood of monomer-monomer interaction to promote oligomerization and subsequent pore formation. Concurrently, raft fusion is also likely to stimulate signal transduction within the cell [28] (some cellular responses to CDC intoxication that occur independently from full pore-formation are listed in Table 1). Whether raft fusion upon monomer binding is host- or CDC-directed is unknown. It is possible that raft fusion stimulates signal transduction that occurs upon CDC membrane binding in the absence of pore formation [5], but this hypothesis has not been tested directly. It is interesting to speculate that the coalescence of lipid rafts upon CDC binding may spur signaling cascades that could function to trigger adaptive signaling mechanisms. For example, Gekara *et al* demonstrated that treatment of cells with LLO protein deficient in pore formation, but not membrane binding, retained the ability to coalesce rafts and activate tyrosine phosphorylation [25]. CDCs are not unique in using cholesterol or other components of lipid rafts for membrane binding; cholera toxin and shiga toxins use gangliosides enriched in lipid rafts as receptors [29,30]. The signal transduction stimulated by CDC binding may in part reflect a universal response to raft fusion. The signaling generated upon raft fusion may then license a specific survival response, such as membrane repair in the case of CDC binding. The specificity of the response would likely be ligand-receptor and context dependent, but may reflect a universal response to membrane lateral trafficking and perturbation.

When CDC monomers interact in the membrane, they undergo extensive changes in their secondary structure for proper membrane insertion orientation [31,32]. As

TABLE 1: Pore-independent cellular responses to CDC treatment.

Response	Outcome	Toxin	Ref
Translocation of a bacterial effector	Hydrolysis of NAD ⁺	SLO	[2]
Lipid raft fusion	Tyrosine phosphorylation	LLO	[20]
IFN γ secretion	Inflammation	PLY	[5]
iNOS production	Anti-microbial	PLY	[5]
Histone dephosphorylation	Transcriptional modification	LLO	[71]
Vaccine adjuvant	Improved tumor clearance	LLO	[97]
MHC presentation	Adaptive immunity	LLO	[96]

monomers oligomerize they form a ring on the cell surface, termed the pre-pore complex. Pore formation occurs upon a conformational change that drives insertion of a β -barrel hairpin into the membrane bilayer. [33]. Much of our understanding of the physical characteristics of the CDC pores comes from cryo-electron microscopy and atomic force microscopy visualizing toxin pores on membranes [34-36], and these micrographs reveal both fully formed circular pores and what appear to be partial pores, or arcs. The argument could be made that the arcs arise as artifacts of sample preparation and non-native membrane conditions. However, there is evidence to suggest that some CDCs may form arcs under native conditions as well. A study by Shaughnessey *et al* demonstrated the sequential release of a small dye (Lucifer Yellow, MW 522), termed perforation, followed by a large dye (TRDx average MW 10,000) in *Listeria*-containing phagosomes of macrophages. This perforation of the phagosomal membrane required the *L. monocytogenes* CDC, LLO [37]. These data suggest that lesions of different sizes occur in the phagosomal membrane during infection. It is possible that CDC arcs in the membrane allow the leakage of the smaller dye, whereas full pores, which would have a greater diameter, allow for loss of the larger dye. Others have provided evidence supporting the biological existence of CDC arcs as well [34,38,39]. Using genetic techniques, Palmer *et al* demonstrated that SLO mutant proteins that preferentially formed arcs prevented the influx of large dextran molecules into erythrocytes, whereas SLO proteins that preferentially formed circular pores did not [38]. The role of arcs in the cellular response to toxin is not well understood. Nonetheless, the formation of arcs might trigger different signaling mechanisms and cellular responses compared to formation of the full pore, which forms a channel lined with protein. The uneven disruption of the plasma membrane during arc insertion

would expose hydrophobic sections of membrane to the cytosol. This hydrophobicity could then serve as a danger signal to activate an immune response [40], a repair response, or both.

The full CDC pore is large, composed of ~35-50 monomers with a diameter of 250-300Å, and has been used as a delivery mechanism to introduce foreign matter, such as antibodies, into the cytosol [41]. Despite their size, the holes formed by CDCs are rapidly sealed [13,42], suggesting that the host cell has efficient adaptive mechanisms to withstand this type of membrane attack.

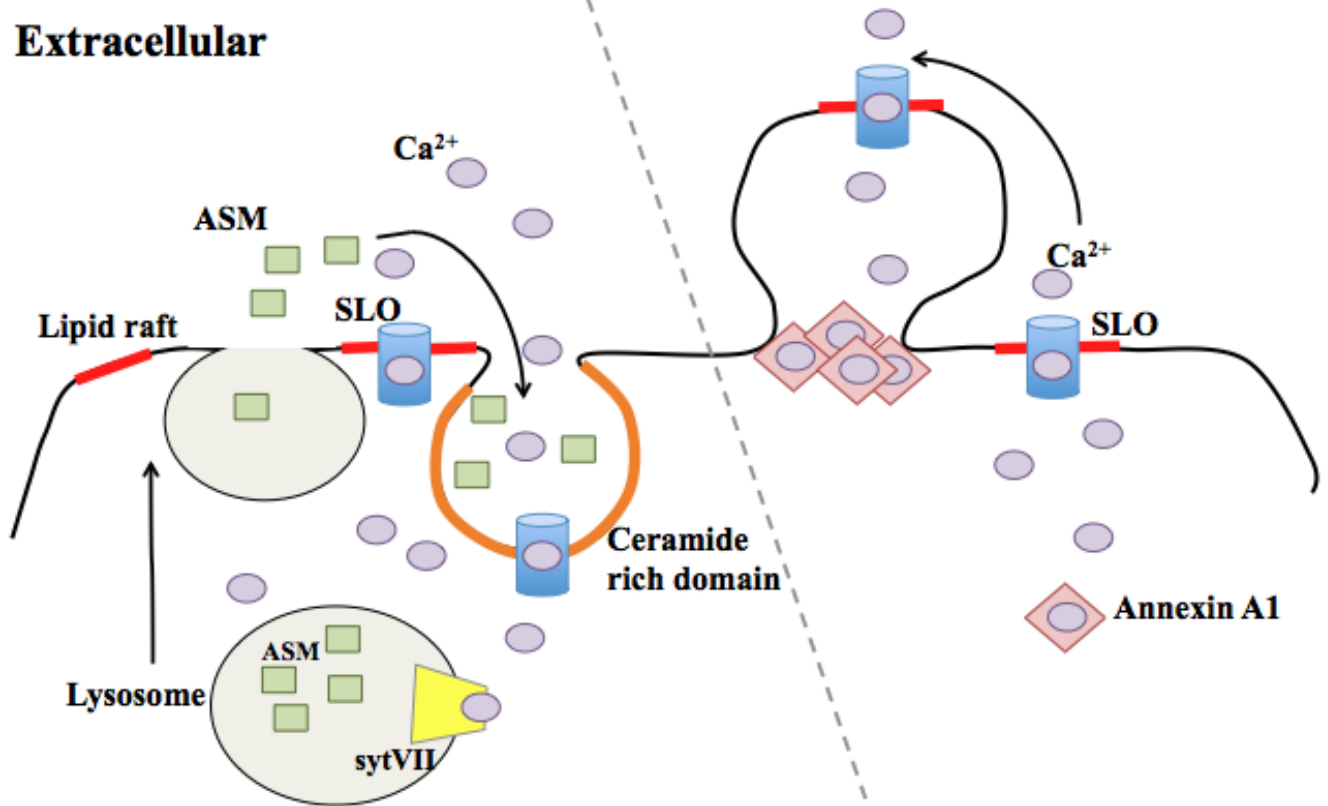
3. Membrane response to CDC intoxication

3.1 Endocytosis of pores

Once a CDC pore is inserted into the membrane, the damaged cell must heal or remove the lesion to maintain viability. One mechanism to achieve this is to internalize the damaged section of membrane via endocytosis (Fig. 1.1). Work from Norma Andrews and colleagues has demonstrated that when SLO inserts into the membrane, Ca^{2+} flux across the damaged membrane stimulates lysosomal exocytosis, delivering additional membrane to the vicinity of the lesion [43]. This process is critically dependent on Ca^{2+} [44], as is the resealing process [13]. Lysosomes contain acid sphingomyelinase (ASM), which hydrolyzes sphingomyelin to form ceramide. Release of ASM into the extracellular space after lysosomal fusion with the plasma membrane generates a ceramide-rich platform that can invaginate to initiate endocytosis [45,46]. The molecular mechanism that pinches off invaginated membrane for endocytosis is not fully understood. Sphingomyelin tends to cluster with cholesterol in the plasma membrane [47], and thus has a high likelihood of being in close proximity to cholesterol-bound CDC pores. The ceramide-rich domains generated by ASM release can spatially reorganize receptors to activate intracellular signaling [48]. Therefore, the generation of ceramide-rich platforms may also act as a mechanism by which the cell can signal during CDC intoxication. Once internalized, SLO-containing vesicles traffic through the endocytic pathway to promote the degradation of the pore-forming protein [49]. endocytosis [45,46]. The molecular mechanism that pinches off invaginated membrane for endocytosis is not fully understood. Sphingomyelin tends to cluster with cholesterol in the plasma membrane [47], and thus has a high likelihood of being in close proximity to cholesterol-bound CDC pores. The ceramide-rich domains generated

Figure 1.1. CDC pore-dependent membrane repair.

Extracellular



Intracellular

Figure 1.1. A schematic of endocytosis and ectocytosis in response to CDC-induced plasma membrane damage. The SLO pore (blue barrel) allows for the influx of Ca²⁺ (light purple) into the cytosol. Synaptotagmin VII (sytVII, yellow) binding of Ca²⁺ stimulates the fusion of lysosomes with the plasma membrane. Fused lysosomes release acid sphingomyelinase (ASM, green) into the extracellular space. ASM converts sphingomyelin in the membrane to ceramide, which allows for invagination and endocytosis of toxin into the cell. Damaged caused by the SLO pore can also stimulate ectocytosis. Increases in cytosolic Ca²⁺ are sensed by annexin A1 which aggregate at the neck of the blebbed membrane to limit cytosolic leakage from the damage bilayer.

by ASM release can spatially reorganize receptors to activate intracellular signaling [48]. Therefore, the generation of ceramide-rich platforms may also act as a mechanism by which the cell can signal during CDC intoxication. Once internalized, SLO-containing vesicles traffic through the endocytic pathway to promote the degradation of the pore-forming protein [49].

This model of repair is not unique to CDC-mediated membrane damage, as introducing a scratch wound on the cell also stimulates lysosome fusion and rapid repair [50]. However, this model does not apply to all types of PFT damage. For instance, pores formed by aerolysin, a small heptameric toxin whose pore size is 1.5-2 nm, from *Aeromonas hydrophila*, are very stable in the membrane [51], and cause prolonged intracellular ion dysregulation compared to CDCs [42].

3.2 Membrane blebbing

Membrane blebbing, or ectocytosis, is commonly used as a hallmark of apoptosis [52], but blebbing in viable cells can also promote motility and cytokinesis [53]. Blebbing occurs when the membrane separates from the cytoskeletal scaffold, which confers rigidity to the bilayer when attached. Cytoplasmic hydrostatic pressure causes the outward protrusion of detached membrane to form a spherical bleb (Fig. 1.1). Recent data suggest that membrane blebbing can also protect cells from CDC-induced lysis. Babyichuk et al demonstrated that treatment of cells with SLO induced membrane blebbing, and that this process, much like lysosomal exocytosis, was dependent on sufficient Ca^{2+} concentration in the extracellular medium [54]. Blebbing protected intoxicated cells by isolating the damaged section of membrane, and cells that underwent blebbing were more likely to survive the insult [54]. These experiments supported blebbing as a process by which cells could protect themselves from

membrane perturbation. Keyel *et al* used “deep-etch” electron microscopy to demonstrate that blebs formed in response to SLO bud from the cell surface [55]. The shed vesicles appeared to be enriched for SLO protein compared to lysates derived from whole cells. The authors concluded that membrane blebbing promotes the shedding of SLO-damaged membranes to promote cell survival [55]. Therefore, the cellular response to CDC intoxication, in this case membrane blebbing and shedding, can promote the survival of the affected cell. The host pathways that control detachment of the plasma membrane from the cortical cytoskeleton to promote blebbing during intoxication have yet to be determined. Additionally, the mechanisms by which cells that undergo blebbing and shedding replenish the plasma membrane are not known. Recent data revealed a role for caspase-7 in promoting plasma membrane integrity during CDC intoxication [56]. Since caspases promote blebbing during apoptosis [57,58], it is possible that CDC-induced and apoptosis-associated blebbing are governed by a shared molecular mechanism, although this has not yet been tested directly.

The two mechanisms of membrane repair outlined here, endocytosis and ectocytosis, are not inherently discordant. Although Keyel *et al* found no evidence of endocytosis in their experiments [55], it is possible that different cell types favor one mechanism over the other, or that the amount of damage dictates the predominant repair mechanism. It is also possible that these two mechanisms work in concert. Cells that bleb and shed damaged membrane would likely need to replace that membrane to maintain cell surface area and hydrostatic homeostasis, and lysosomal exocytosis could supply this membrane faster than making new membrane *de novo*. Additionally, in all cases, extracellular Ca^{2+} was critical for repair. In the endocytosis model, synaptotagmin VII, a calcium binding protein present in lysosomes, was required for directing the fusion of

these vesicles with the plasma membrane for lesion repair [50]. In the ectocytosis model, annexins, a family of calcium binding proteins present in the cytosol, act as a plug at the neck of the bleb to seal off the contents of the cytosol away from the damaged membrane [54]. Different concentrations of intracellular Ca^{2+} may trigger different mechanisms of membrane repair, or the relative abundance of calcium sensors in different cell types may drive one repair response over another.

4. Intracellular effects of CDC intoxication

4.1 Effects on the endoplasmic reticulum and Golgi

Beyond the effects of CDC perturbation at the plasma membrane, there are hints that CDCs can also affect intracellular compartments. Pillich *et al* recently published a report suggesting that infection with *L. monocytogenes* can activate the unfolded protein response (UPR) in the endoplasmic reticulum (ER) [59]. The UPR is a stress response which acts to balance protein synthesis and protein folding in the ER to maintain cellular homeostasis [60]. UPR activation was dependent on secretion of LLO by *L. monocytogenes* [59]. Others have shown that UPR activation during intoxication with other pore-forming toxins is protective at the level of the organism. Loss of *ire-1* or *atf-6*, two UPR sensors, in *Caenorhabditis elegans* results in hypersensitivity to the PFT, Cry5B [61]. How activation of the UPR protects cells during intoxication is not known, but there are several possible explanations. UPR stimulation activates autophagy [62], a degradative pathway responsible for the turnover of cellular contents and organelles, and autophagy may contribute to the degradation of PFTs, damaged membrane, or both. UPR activation can also stimulate lipid synthesis [63], which could enhance membrane repair and replenishment after toxin-induced damage. Finally, the UPR promotes increased vesicular traffic between the ER and the Golgi [64]. Vesicles derived from these compartments may contribute to membrane repair in a manner analogous to lysosomal exocytosis.

In addition to activation of the UPR, there are some clues that suggest CDCs act on the ER membrane directly. PFO perforates the ER [65] despite the low concentration of cholesterol in this bilayer [66]. LLO stimulates the rapid release of Ca^{2+} from the ER of mast cells by Ca^{2+} channel-dependent and -independent mechanisms [67] (Fig. 1.2),

indicating that LLO may act on the ER membrane as well. However, LLO pores were not directly detected on the ER membrane [67]. Although CDC binding to internal stores of membrane is an appealing model to explain aspects of CDC-mediated signaling, most of the data remains speculative. It is inherently difficult to tease apart the cellular response to CDC-damaged organelles from the signaling that occurs as a result of plasma membrane damage, since the former cannot be detected without inducing the latter. Better tools are needed to determine if CDCs act on intracellular compartments directly, and whether these organelles can drive CDC-specific responses in the absence of plasma membrane damage.

Although the Golgi and ER are intimately connected within the cell, less is known about CDC interactions with the Golgi. Treatment of cells with SLO increases Golgi-derived trafficking to the damaged membrane [68], but this response is not likely specific to CDC-intoxication. Nonetheless, given the critical role for the Golgi apparatus in lipid metabolism and transport [69], the Golgi may play a role in modulating responses to CDC-derived damage. Infection with some bacterial pathogens has shed light on Golgi-plasma membrane interactions. Divangahi *et al* elegantly demonstrated that *Mycobacterium tuberculosis* infection induces plasma membrane damage and requires translocation of Golgi-derived vesicles to the bilayer to successfully seal lesions [70]. Thus, vesicular traffic from the Golgi represents an attractive source of new membrane and newly synthesized lipids to replace membrane lost during endo- or ectocytosis in response to CDC perturbation.

4.2 Effects on the mitochondria and nucleus

CDCs exert effects on many intracellular compartments. For instance, Goldmann *et al* determined that SLO treatment of macrophages had profound effects on the

mitochondria of the cell, including loss of mitochondrial membrane potential, which led to the oncotic death of the intoxicated cell [71]. Interestingly, loss of plasma membrane integrity was not the sole trigger for mitochondrial dysfunction, as cell death was not inhibited by increased osmolarity in the culture media. Also, the pore size at the plasma membrane was significantly smaller than what is estimated for the SLO pore [71], indicating that either the pores were of mammalian origin, or that SLO arcs might be the predominant form of damage. Together, these results suggest that SLO potentially acts as a signaling molecule, in addition to its role as a PFT, with negative implications for the function of cellular mitochondria.

Another study showed that PLY intoxication affects the mitochondria of neuronal cells to induce apoptotic cell death, and PLY protein was detected on the mitochondrial membrane using immuno-EM [72]. The authors demonstrated that the ability to form pores at the plasma membrane was necessary to induce mitochondrial dysregulation, but whether PLY protein formed pores on the mitochondrial membrane was not assessed. It is possible that monomer binding to the mitochondrial membrane was sufficient to induce the response, and that pore-formation at the plasma membrane was needed to introduce monomers into the cytoplasmic space. Considering that the sterol content of the mitochondrial membrane is very low [66], it is plausible that PLY oligomerization in this membrane would also be low.

LLO alters the mitochondria as well, but differently from SLO and PLY. Stavru *et al* demonstrated that treatment of cells with non-lytic concentrations of LLO induced fragmentation of the mitochondrial network [73] (Fig. 1.2). Although mitochondrial fragmentation is sometimes used as a hallmark of programmed cell death, markers of apoptosis were not observed in these cells. In fact, the LLO-induced changes in mitochondrial morphology were transient, leading the authors to hypothesize that

altering mitochondrial dynamics would slow the metabolism of the cell to promote the early stages of *L. monocytogenes* infection [73]. Whether other CDCs induce a similar morphological change is not known. The authors implicated Ca^{2+} flux as important in eliciting this response [73]. In conclusion, it is clear that intoxication with CDCs can significantly alter the mitochondria of intoxicated cells, but the outcome of that alteration is likely cell type- and potentially CDC-specific.

Most of the existing knowledge of the effects of CDCs on the nucleus has come from the exogenous treatment of cells with LLO. LLO binding to the plasma membrane can stimulate specific dephosphorylation of histone H3 in the nucleus [74]. PFO and PLY were also able to spur histone modification, but treatment with detergents and an unrelated PFT was not, indicating that the response is specific to CDC membrane binding. These data supply direct evidence for the hypothesis that CDCs can act as signal transducers. Using microarrays to monitor changes in transcription, Hamon *et al* found that epigenetic changes caused by LLO binding resulted in altered expression of ~150 genes [74]. The authors found that pre-treatment of LLO with cholesterol inhibited the ability of the CDC to stimulate the release of LDH from these cells, but not the dephosphorylation of histone H3, indicating that full pore formation was not needed to induce this response. In a subsequent paper Hamon *et al* determined that cholesterol-treated LLO retained the ability to stimulate K^{+} flux across the plasma membrane, and that this ion flux was sufficient to stimulate histone modification [8].

Treatment of cells with LLO can induce the nuclear translocation of the master transcriptional regulator, NF- κ B [75], as well as activate the MAPK cascade [76], both of which have the capacity to globally alter gene transcription and activate immune signaling (discussed below). Recent data suggest that LLO stimulates degradation of

Figure 1.2. CDC pore-dependent signaling responses

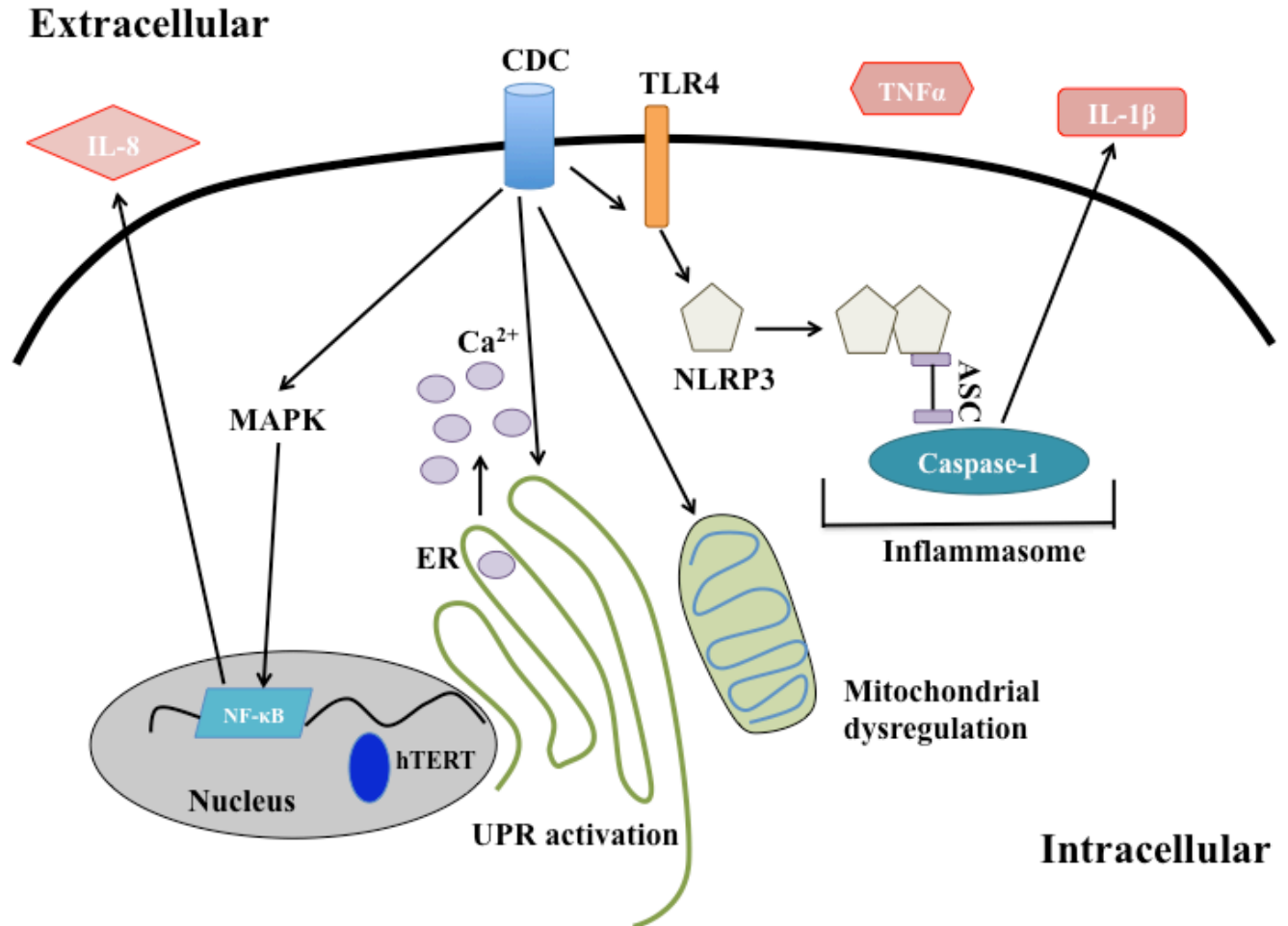


Figure 1.2. A schematic of the different signaling responses activated by CDC damage. CDC intoxicated cells activate the inflammasome, stimulating the release of IL-1 β . CDC perforated cells also secrete TNF α . Calcium is released by the ER and the UPR is activated in response to intoxication. CDC treatment results in loss of mitochondrial membrane potential and transient fragmentation of the mitochondrial network. IL-8 is secreted in a MAPK and NF- κ B dependent manner.

human telomerase reverse transcriptase [77], although that regulation is due in part to Ca^{2+} flux as a result of membrane perturbation. Taken together, these data suggest that CDCs can have profound influence on transcriptional regulation of the intoxicated cell, which would likely affect the outcome of infection.

4.3 Endolysosomal network

The endolysosomal network is a key cellular defense system that traps bacterial pathogens within a membrane bound compartment through phagocytosis or autophagy, and a CDC toxin, LLO from *L. monocytogenes*, is crucial for escape from this restrictive environment [78]. LLO perforates the phagosome, stimulating ion flux and cellular signaling [37,79]. One outcome of LLO perforation of the phagosome is to delay phagosome maturation [80]. While escape is the primary function of LLO-induced membrane damage within the vacuole, it is conceivable that pore formation permits the passage of other *L. monocytogenes* virulence factors, like PI-PLC and PC-PLC, across the phagosomal membrane to trigger host signaling pathways [81,82]. Phagosomal membrane damage induced by LLO activates autophagy, a scavenging pathway that targets cytoplasmic components for lysosomal degradation [83,84]. Although LLO is the only CDC expressed by a pathogen that is largely intracellular, some extracellular pathogens expressing CDC toxins, like *S. pyogenes*, can be found within host cells and their entry and survival may be influenced by CDC expression [85,86]. The structurally related mammalian MACPF protein, perforin, which confers cytolytic activity to T lymphocytes and natural killer cells, also acts from within the endolysosome, delivering granzyme B to the cytosol of infected target cells [87]. Damage of the lysosomal compartment, as a consequence of pore formation, is a potent trigger of the

inflammasome resulting in secretion of the pro-inflammatory cytokine IL-1 β [88,89]. Thus, LLO pore formation is critical for *L. monocytogenes* to escape the endosomal compartment, but in doing so alerts the host to its presence.

4.4 Immune signaling

There is a large body of evidence that cells can mount an inflammatory response to non-lytic intoxication with CDCs, and that CDCs themselves may act as pathogen-associated molecular patterns (PAMPs). Intoxication with LLO can activate the MAPK pathway [76], a signaling cascade that promotes both innate and adaptive immune responses [90]. Nasopharyngeal epithelial cells secrete a neutrophil chemoattractant, IL-8, upon intoxication with PLY, which is dependent on MAPK signaling [91]. SLO intoxication of neutrophils stimulates their secretion of antimicrobial peptides and inflammatory proteins via the activation of the MAPK cascade [92]. Treatment of macrophages with heat killed bacteria and either LLO or SLO activates MAPK-dependent secretion of IL-10 [93], an anti-inflammatory cytokine, which suggests that the immune response to CDC intoxication is tempered by the presence of additional stimuli.

In the early 1990s, it was demonstrated that monocytes secrete TNF α and IL1 β in response to treatment with SLO or PLY [94,95]. Approximately 10 years later, this cytokine release was linked to Toll-like receptor signaling, as macrophages lacking Toll-like receptor 4 (TLR4) failed to respond to purified PLY [96]. Similar results were obtained treating macrophages with recombinant ALO, LLO, PFO, and SLO [97]. Blocking the binding of lipopolysaccharide to TLR4 did not abrogate cytokine secretion, suggesting that activation of TLR4 by these toxins was not due to endotoxin

contamination [97]. Whether CDCs act directly as a ligand of TLR4 is still not known. Another possibility is that binding or oligomerization of CDCs at the plasma membrane induces rearrangement of membrane microdomains. Coalescence of lipid microdomains could promote TLR4 dimerization spurring immune signaling [98]. In this way, binding or oligomerization of CDCs at the membrane may enhance PAMP-like signaling cascades.

In addition to activation of pattern recognition receptors at the cell surface, CDCs can also stimulate intracellular immune signaling. TLO treatment of LPS-primed macrophages activates the NLRP3 inflammasome, inducing the processing and secretion of IL-1 β [4]. The authors concluded that full pore formation was necessary for cytokine secretion as pretreatment of the toxin with cholesterol was insufficient to stimulate the response. Whether cholesterol-treated TLO retains the ability to alter intracellular K⁺ similar to cholesterol-treated LLO [8] has not been studied. Later it was determined that SLO-induced inflammasome activation required TLR signaling, but infection with the bacterial pathogen that produces the toxin, *S. pyogenes*, does not [99]. Therefore, TLR signaling may represent a mechanism by which macrophages can distinguish between intoxication and direct infection with a particular pathogen in order to guide the proper immune response. It is important to note that NLRP3 can be activated by low intracellular K⁺ [100] and treatment of cells with CDCs can result in the depletion of cytosolic K⁺ [41]. Thus, activation of NLRP3 could represent a general response to membrane damage, which could be altered by additional virulence factors secreted by the bacterium or by a dynamic host response in the context of infection. However, murine splenic cells secrete IFN γ and produce iNOS in response to mutant PLY that appears to lack the ability to form pores [5], so cytokine secretion in response

to intoxication with CDCs may have damage-dependent and damage-independent triggers.

Treatment of immune cells with CDCs can modulate adaptive immune function. When macrophages are exposed to SLO-rich plasma membrane-derived vesicles, they secrete less TNF upon LPS stimulation and present fewer peptides to B cells [101]. Non-hemolytic LLO has potent immunogenic [102] and adjuvant properties for anti-cancer vaccination [103]. LLO-derived epitopes were presented to CD4 and to a lesser extent CD8+ T cells [102], an interesting finding since CD8+ cells are responsible for anti-tumor immunity as well as *L. monocytogenes* clearance [103-105]. However, when CD4+ T cells were directly exposed to LLO that retained pore-forming capabilities, these cells became anergic [106] or apoptotic [107]. Therefore, the relative levels and activity of CDC toxin present during infection, as well as its cellular context, regulate the magnitude and outcome of the resulting immune response.

5. Conclusions

An intact eukaryotic cell membrane is critical for cell survival and yet this barrier is routinely assaulted by CDC toxins during infection. Studies using these toxins have elucidated previously uncharacterized membrane repair mechanisms that also function to repair mechanical stresses, such as scratch wounds. Therefore, the damage responses discovered as a result of CDC pore formation may shed light on the mechanisms cells use to protect the bilayer in response to diverse insults. Studies on the morphological and transcriptional differences that occur during CDC treatment of cells will continue to guide our understanding of the host response to intoxication. Finally, signaling cascades activated by target cells upon CDC exposure indicate these toxins may be important modulators of innate and adaptive immunity, in addition to their specific functions in virulence. The CDC toxins have been a valuable model to study key aspects of host-pathogen interactions and continue to be versatile tools to investigate the cellular response to damage and infection, improving our understanding of host-pathogen interactions and immunity.

6. References

1. Sierig, G.; Cywes, C.; Wessels, M. R.; Ashbaugh, C. D. Cytotoxic effects of streptolysin O and streptolysin S enhance the virulence of poorly encapsulated group A streptococci. *Infect. Immun.* 2003, 71, 446–455.
2. Magassa, N. A. G.; Chandrasekaran, S.; Caparon, M. G. *Streptococcus pyogenes* cytolysin-mediated translocation does not require pore formation by streptolysin O. *EMBO reports* 2010, 11, 400–405.
3. Portnoy, D. A.; Jacks, P. S.; Hinrichs, D. J. Role of hemolysin for the intracellular growth of *Listeria monocytogenes*. *J. Exp. Med.* 1988, 167, 1459–1471.
4. Chu, J.; Thomas, L. M.; Watkins, S. C.; Franchi, L.; Núñez, G.; Salter, R. D. Cholesterol-dependent cytolysins induce rapid release of mature IL-1 β from murine macrophages in a NLRP3 inflammasome and cathepsin B-dependent manner. *J. Leukoc. Biol.* 2009, 86, 1227–1238.
5. Baba, H.; Kawamura, I.; Kohda, C.; Nomura, T.; Ito, Y.; Kimoto, T.; Watanabe, I.; Ichiyama, S.; Mitsuyama, M. Induction of gamma interferon and nitric oxide by truncated pneumolysin that lacks pore-forming activity. *Infect. Immun.* 2002, 70, 107–113.
6. Walev, I.; Palmer, M.; Martin, E.; Jonas, D.; Weller, U.; Höhn-Bentz, H.; Husmann, M.; Bhakdi, S. Recovery of human fibroblasts from attack by the pore-forming alpha-toxin of *Staphylococcus aureus*. *Microb. Pathog.* 1994, 17, 187–201.
7. Jacobs, T.; Darji, A.; Frahm, N.; Rohde, M.; Wehland, J.; Chakraborty, T.; Weiss, S. Listeriolysin O: cholesterol inhibits cytolysis but not binding to cellular membranes. *Mol. Microbiol.* 1998, 28, 1081–1089.
8. Hamon, M.A.; Cossart, P. K⁺ efflux is necessary for histone H3 dephosphorylation by *Listeria monocytogenes* listeriolysin O and other pore forming toxins. *Infect. Immun.* 2011, 79, 2839–2846.
9. Jones, S.; Prieter, K.; Portnoy, D.A. Conversion of an extracellular cytolysin into a phagosome-specific lysin which supports the growth of an intracellular pathogen. *Mol. Micro.* 1996, 21, 1219–1225.
10. Dunstone, M. A.; Tweten, R. K. Packing a punch: the mechanism of pore formation by cholesterol dependent cytolysins and membrane attack complex/perforin-like proteins. *Curr. Opin. Struct. Biol.* 2012, 22, 342–349.
11. Kafsack, B. F. C.; Pena, J. D. O.; Coppens, I.; Ravindran, S.; Boothroyd, J. C.; Carruthers, V. B. Rapid membrane disruption by a perforin-like protein facilitates parasite exit from host cells. *Science* 2009, 323, 530–533.
12. Sousa, M. V.; Richardson, M.; Fontes, W.; Morhy, L. Homology between the seed cytolysin enterolysin and bacterial aerolysins. *J. Protein Chem.* 1994, 13, 659–667.

13. Walev, I.; Bhakdi, S. C.; Hofmann, F.; Djonder, N.; Valeva, A.; Aktories, K.; Bhakdi, S. Delivery of proteins into living cells by reversible membrane permeabilization with streptolysin-O. *Proc. Natl. Acad. Sci. U.S.A.* 2001, 98, 3185–3190.
14. Lopez, J. A.; Susanto, O.; Jenkins M.R.; Lukoyanova, N.; Sutton, V.R.; Law, R.H.P.; Johnston, A.; Bird, C.H.; Bird, P.I.; Whisstock, J.C.; Trapani, J.A.; Saibil, H.R.; Voskoboinik, I. Perforin forms transient pores on the target cell plasma membrane to facilitate rapid access of granzymes during killer cell attack. *Blood* 2013, doi:10.1182/blood-2012-07-446146.
15. Heuck, A. P.; Moe, P. C.; Johnson, B. B. The cholesterol-dependent cytolysin family of gram-positive bacterial toxins. *Subcell. Biochem.* 2010, 51, 551–577.
16. Rossjohn, J.; Feil, S. C.; McKinstry, W. J.; Tweten, R. K.; Parker, M. W. Structure of a cholesterol-binding, thiol-activated cytolysin and a model of its membrane form. *Cell* 1997, 89, 685–692.
17. Polekhina, G.; Giddings, K. S.; Tweten, R. K.; Parker, M. W. Insights into the action of the superfamily of cholesterol-dependent cytolysins from studies of intermedilysin. *Proc. Natl. Acad. Sci. U.S.A.* 2005, 102, 600–605.
18. Bourdeau, R. W.; Malito, E.; Chenal, A.; Bishop, B. L.; Musch, M. W.; Villereal, M. L.; Chang, E. B.; Mosser, E. M.; Rest, R. F.; Tang, W.-J. Cellular functions and X-ray structure of anthrolysin O, a cholesterol-dependent cytolysin secreted by *Bacillus anthracis*. *J. Biol. Chem.* 2009, 284, 14645–14656.
19. Xu, L.; Huang, B.; Du, H.; Zhang, X. C.; Xu, J.; Li, X.; Rao, Z. Crystal structure of cytotoxin protein suilysin from *Streptococcus suis*. *Protein Cell* 2010, 1, 96–105.
20. Hotze, E. M.; Tweten, R. K. Membrane assembly of the cholesterol-dependent cytolysin pore complex. *Biochim. Biophys. Acta* 2012, 1818, 1028–1038.
21. Soltani, C. E.; Hotze, E. M.; Johnson, A. E.; Tweten, R. K. Structural elements of the cholesterol-dependent cytolysins that are responsible for their cholesterol-sensitive membrane interactions. *Proc. Natl. Acad. Sci. U.S.A.* 2007, 104, 20226–20231.
22. Dowd, K. J.; Tweten, R. K. The cholesterol-dependent cytolysin signature motif: a critical element in the allosteric pathway that couples membrane binding to pore assembly. *PLoS Pathog.* 2012, 8, e1002787.
23. Giddings, K. S.; Zhao, J.; Sims, P. J.; Tweten, R. K. Human CD59 is a receptor for the cholesterol-dependent cytolysin intermedilysin. *Nat. Struct. Mol. Biol.* 2004, 11, 1173–1178.
24. Gelber, S. E.; Aguilar, J. L.; Lewis, K. L. T.; Ratner, A. J. Functional and phylogenetic characterization of Vaginolysin, the human-specific cytolysin from *Gardnerella vaginalis*. *J. Bacteriol.* 2008, 190, 3896–3903.

25. Gekara, N. O.; Weiss, S. Lipid rafts clustering and signalling by listeriolysin O. *Biochem. Soc. Trans.* 2004, 32, 712–714.
26. Gekara, N. O.; Jacobs, T.; Chakraborty, T.; Weiss, S. The cholesterol-dependent cytolysin listeriolysin O aggregates rafts via oligomerization. *Cell. Microbiol.* 2005, 7, 1345–1356.
27. Nelson, L. D.; Chiantia, S.; London, E. Perfringolysin O association with ordered lipid domains: implications for transmembrane protein raft affinity. *Biophys. J.* 2010, 99, 3255–3263.
28. Simons, K.; Toomre, D. Lipid rafts and signal transduction. *Nat. Rev. Mol. Cell Biol.* 2000, 1, 31–39.
29. Zitzer, A.; Bittman, R.; Verbicky, C. A.; Erukulla, R. K.; Bhakdi, S.; Weis, S.; Valeva, A.; Palmer, M. Coupling of cholesterol and cone-shaped lipids in bilayers augments membrane permeabilization by the cholesterol-specific toxins streptolysin O and *Vibrio cholerae* cytolysin. *J. Biol. Chem.* 2001, 276, 14628–14633.
30. Kouzel, I. U.; Pohlentz, G.; Storck, W.; Radamm, L.; Hoffmann, P.; Bielaszewska, M.; Bauwens, A.; Cichon, C.; Schmidt, M. A.; Mormann, M.; Karch, H.; Müthing, J. Association of Shiga toxin glycosphingolipid receptors with membrane microdomains of toxin-sensitive lymphoid and myeloid cells. *J. Lipid Res.* 2013, 54, 692–710.
31. Tilley, S. J.; Orlova, E. V.; Gilbert, R. J. C.; Andrew, P. W.; Saibil, H. R. Structural basis of pore formation by the bacterial toxin pneumolysin. *Cell* 2005, 121, 247–256.
32. Ramachandran, R.; Heuck, A. P.; Tweten, R. K.; Johnson, A. E. Structural insights into the membrane-anchoring mechanism of a cholesterol-dependent cytolysin. *Nat. Struct. Biol.* 2002, 9, 823–827.
33. Tweten, R. K. Cholesterol-dependent cytolysins, a family of versatile pore-forming toxins. *Infect. Immun.* 2005, 73, 6199–6209.
34. Bhakdi, S.; Trantum-Jensen, J.; Sziegoleit, A. Mechanism of membrane damage by streptolysin-O. *Infect. Immun.* 1985, 47, 52–60.
35. Schuerch, D. W.; Wilson-Kubalek, E. M.; Tweten, R. K. Molecular basis of listeriolysin O pH dependence. *Proc. Natl. Acad. Sci. U.S.A.* 2005, 102, 12537–12542.
36. Czajkowsky, D. M.; Hotze, E. M.; Shao, Z.; Tweten, R. K. Vertical collapse of a cytolysin prepore moves its transmembrane beta-hairpins to the membrane. *EMBO J.* 2004, 23, 3206–3215.
37. Shaughnessy, L. M.; Hoppe, A. D.; Christensen, K. A.; Swanson, J. A. Membrane perforations inhibit lysosome fusion by altering pH and calcium in *Listeria monocytogenes* vacuoles. *Cell. Microbiol.* 2006, 8, 781–792.

38. Palmer, M.; Harris, R.; Freytag, C.; Kehoe, M.; Trandum-Jensen, J.; Bhakdi, S. Assembly mechanism of the oligomeric streptolysin O pore: the early membrane lesion is lined by a free edge of the lipid membrane and is extended gradually during oligomerization. *EMBO J.* 1998, 17, 1598–1605.
39. Gilbert, R. J. C.; Mikelj, M.; Dalla Serra, M.; Froelich, C. J.; Anderlüh, G. Effects of MACPF/CDC proteins on lipid membranes. *Cell. Mol. Life Sci.* 2012.
40. Seong, S.-Y.; Matzinger, P. Hydrophobicity: an ancient damage-associated molecular pattern that initiates innate immune responses. *Nat. Rev. Immunol.* 2004, 4, 469–478.
41. Bhakdi, S.; Weller, U.; Walev, I.; Martin, E.; Jonas, D.; Palmer, M. A guide to the use of pore-forming toxins for controlled permeabilization of cell membranes. *Med. Microbiol. Immunol.* 1993, 182, 167–175.
42. Gonzalez, M. R.; Bischofberger, M.; Frêche, B.; Ho, S.; Parton, R. G.; van der Goot, F. G. Pore-forming toxins induce multiple cellular responses promoting survival. *Cell. Microbiol.* 2011, 13, 1026–1043.
43. Rao, S. K.; Huynh, C.; Proux-Gillardeaux, V.; Galli, T.; Andrews, N. W. Identification of SNAREs involved in synaptotagmin VII-regulated lysosomal exocytosis. *J. Biol. Chem.* 2004, 279, 20471–20479.
44. Rodríguez, A.; Webster, P.; Ortego, J.; Andrews, N. W. Lysosomes behave as Ca²⁺-regulated exocytic vesicles in fibroblasts and epithelial cells. *J. Cell Biol.* 1997, 137, 93–104.
45. Idone, V.; Tam, C.; Goss, J. W.; Toomre, D.; Pypaert, M.; Andrews, N. W. Repair of injured plasma membrane by rapid Ca²⁺-dependent endocytosis. *J. Cell Biol.* 2008, 180, 905–914.
46. Tam, C.; Idone, V.; Devlin, C.; Fernandes, M. C.; Flannery, A.; He, X.; Schuchman, E.; Tabas, I.; Andrews, N. W. Exocytosis of acid sphingomyelinase by wounded cells promotes endocytosis and plasma membrane repair. *J. Cell Biol.* 2010, 189, 1027–1038.
47. Truman, J.-P.; Gadban, A. M. M.; Smith, K. J.; Hammad, S. M. Acid sphingomyelinase in macrophage biology. *Cell. Mol. Life Sci.* 2011, 68, 3293–3305.
48. Grassme, H.; Jendrossek, V.; Bock, J.; Riehle, A.; Gulbins, E. Ceramide-rich membrane rafts mediate CD40 clustering. *J. Immunol.* 2002, 168, 298–307.
49. Corrotte, M.; Fernandes, M. C.; Tam, C.; Andrews, N. W. Toxin Pores Endocytosed During Plasma Membrane Repair Traffic into the Lumen of MVBs for Degradation. *Traffic* 2012, 13, 483–494.
50. Reddy, A.; Caler, E. V.; Andrews, N. W. Plasma membrane repair is mediated by Ca²⁺-regulated exocytosis of lysosomes. *Cell* 2001, 106, 157–169.

51. Lesieur, C.; Frutiger, S.; Hughes, G.; Kellner, R.; Pattus, F.; van der Goot, F. G. Increased stability upon heptamerization of the pore-forming toxin aerolysin. *J. Biol. Chem.* 1999, 274, 36722–36728.
52. Kerr, J. F.; Wyllie, A. H.; Currie, A. R. Apoptosis: a basic biological phenomenon with wide-ranging implications in tissue kinetics. *Br. J. Cancer* 1972, 26, 239–257.
53. Charras, G.; Paluch, E. Blebs lead the way: how to migrate without lamellipodia. *Nat. Rev. Mol. Cell Biol.* 2008, 9, 730–736.
54. Babiychuk, E. B.; Monastyrskaya, K.; Potez, S.; Draeger, A. Blebbing confers resistance against cell lysis. *Cell Death Differ.* 2011, 18, 80–89.
55. Keyel, P. A.; Loutcheva, L.; Roth, R.; Salter, R. D.; Watkins, S. C.; Yokoyama, W. M.; Heuser, J. E. Streptolysin O clearance through sequestration into blebs that bud passively from the plasma membrane. *J. Cell Sci.* 2011, 124, 2414–2423.
56. Cassidy, S. K. B.; Hagar, J. A.; Kanneganti, T.-D.; Franchi, L.; Núñez, G.; O’Riordan, M. X. D. Membrane damage during *Listeria monocytogenes* infection triggers a caspase-7 dependent cytoprotective response. *PLoS Pathog* 2012, 8, e1002628.
57. Sebbagh, M.; Renvoizé, C.; Hamelin, J.; Riché, N.; Bertoglio, J.; Bréard, J. Caspase-3-mediated cleavage of ROCK I induces MLC phosphorylation and apoptotic membrane blebbing. *Nat. Cell Biol.* 2001, 3, 346–352.
58. Coleman, M. L.; Sahai, E. A.; Yeo, M.; Bosch, M.; Dewar, A.; Olson, M. F. Membrane blebbing during apoptosis results from caspase-mediated activation of ROCK I. *Nat. Cell Biol.* 2001, 3, 339–345.
59. Pillich, H.; Loose, M.; Zimmer, K.-P.; Chakraborty, T. Activation of the unfolded protein response by *Listeria monocytogenes*. *Cell. Microbiol.* 2012, 14, 949–964.
60. Todd, D. J.; Lee, A.-H.; Glimcher, L. H. The endoplasmic reticulum stress response in immunity and autoimmunity. *Nat. Rev. Immunol.* 2008, 8, 663–674.
61. Bischof, L. J.; Kao, C.-Y.; Los, F. C. O.; Gonzalez, M. R.; Shen, Z.; Briggs, S. P.; van der Goot, F. G.; Aroian, R. V. Activation of the unfolded protein response is required for defenses against bacterial pore-forming toxin in vivo. *PLoS Pathog* 2008, 4, e1000176.
62. Høyer-Hansen, M.; Jäättelä, M. Connecting endoplasmic reticulum stress to autophagy by unfolded protein response and calcium. *Cell Death Differ* 2007, 14, 1576–1582.
63. Ron, D.; Walter, P. Signal integration in the endoplasmic reticulum unfolded protein response. *Nat. Rev. Mol. Cell Biol.* 2007, 8, 519–529.
64. Schröder, M.; Kaufman, R. J. The mammalian unfolded protein response. *Annu. Rev. Biochem.* 2005, 74, 739–789.

65. Flanagan, J. J.; Tweten, R. K.; Johnson, A. E.; Heuck, A. P. Cholesterol exposure at the membrane surface is necessary and sufficient to trigger perfringolysin O binding. *Biochemistry* 2009, 48, 3977–3987.
66. van Meer, G.; Voelker, D. R.; Feigenson, G. W. Membrane lipids: where they are and how they behave. *Nat. Rev. Mol. Cell Biol.* 2008, 9, 112–124.
67. Gekara, N. O.; Westphal, K.; Ma, B.; Rohde, M.; Groebe, L.; Weiss, S. The multiple mechanisms of Ca²⁺ signalling by listeriolysin O, the cholesterol-dependent cytolysin of *Listeria monocytogenes*. *Cell. Microbiol.* 2007, 9, 2008–2021.
68. Kobayashi, T.; Pimplikar, S. W.; Parton, R. G.; Bhakdi, S.; Simons, K. Sphingolipid transport from the trans-Golgi network to the apical surface in permeabilized MDCK cells. *FEBS Letters* 1992, 300, 227–231.
69. Bankaitis, V. A.; Garcia-Mata, R.; Mousley, C. J. Golgi membrane dynamics and lipid metabolism. *Curr. Biol.* 2012, 22, R414–24.
70. Divangahi, M.; Chen, M.; Gan, H.; Desjardins, D.; Hickman, T. T.; Lee, D. M.; Fortune, S.; Behar, S. M.; Remold, H. G. *Mycobacterium tuberculosis* evades macrophage defenses by inhibiting plasma membrane repair. *Nat. Immunol.* 2009, 10, 899–906.
71. Goldmann, O.; Sastalla, I.; Wos-Oxley, M.; Rohde, M.; Medina, E. *Streptococcus pyogenes* induces oncosis in macrophages through the activation of an inflammatory programmed cell death pathway. *Cell. Microbiol.* 2009, 11, 138–155.
72. Braun, J. S.; Hoffmann, O.; Schickhaus, M.; Freyer, D.; Dagand, E.; Bermpohl, D.; Mitchell, T. J.; Bechmann, I.; Weber, J. R. Pneumolysin causes neuronal cell death through mitochondrial damage. *Infect Immun* 2007, 75, 4245–4254.
73. Stavru, F.; Bouillaud, F.; Sartori, A.; Ricquier, D.; Cossart, P. *Listeria monocytogenes* transiently alters mitochondrial dynamics during infection. *Proc. Natl. Acad. Sci. U.S.A.* 2011, 108, 3612–3617.
74. Hamon, M. A.; Batsché, E.; Régnault, B.; Tham, T. N.; Seveau, S.; Muchardt, C.; Cossart, P. Histone modifications induced by a family of bacterial toxins. *Proc. Natl. Acad. Sci. U.S.A.* 2007, 104, 13467–13472.
75. Kayal, S.; Lilienbaum, A.; Poyart, C.; Memet, S.; Israel, A.; Berche, P. Listeriolysin O-dependent activation of endothelial cells during infection with *Listeria monocytogenes*: activation of NF-kappa B and upregulation of adhesion molecules and chemokines. *Mol. Microbiol.* 1999, 31, 1709–1722.
76. Tang, P.; Rosenshine, I.; Cossart, P.; Finlay, B. B. Listeriolysin O activates mitogen-activated protein kinase in eucaryotic cells. *Infect. Immun.* 1996, 64, 2359–2361.
77. Samba-Louaka, A.; Stavru, F.; Cossart, P. Role for telomerase in *Listeria monocytogenes* infection. *Infect. Immun.* 2012, 80, 4257–4263.

78. Schnupf, P.; Portnoy, D. A. Listeriolysin O: a phagosome-specific lysin. *Microbes Infect.* 2007, 9, 1176–1187.
79. Shaughnessy, L. M.; Lipp, P.; Lee, K.-D.; Swanson, J. A. Localization of protein kinase C epsilon to macrophage vacuoles perforated by *Listeria monocytogenes* cytolysin. *Cell. Microbiol.* 2007, 9, 1695–1704.
80. Henry, R.; Shaughnessy, L.; Loessner, M. J.; Alberti-Segui, C.; Higgins, D. E.; Swanson, J. A. Cytolysin-dependent delay of vacuole maturation in macrophages infected with *Listeria monocytogenes*. *Cell. Microbiol.* 2006, 8, 107–119.
81. Marquis, H.; Goldfine, H.; Portnoy, D. A. Proteolytic pathways of activation and degradation of a bacterial phospholipase C during intracellular infection by *Listeria monocytogenes*. *J. Cell Biol.* 1997, 137, 1381–1392.
82. Wadsworth, S. J.; Goldfine, H. Mobilization of protein kinase C in macrophages induced by *Listeria monocytogenes* affects its internalization and escape from the phagosome. *Infect. Immun.* 2002, 70, 4650–4660.
83. Birmingham, C. L.; Canadien, V.; Gouin, E.; Troy, E. B.; Yoshimori, T.; Cossart, P.; Higgins, D. E.; Brumell, J. H. *Listeria monocytogenes* evades killing by autophagy during colonization of host cells. *Autophagy* 2007, 3, 442–451.
84. Meyer-Morse, N.; Robbins, J. R.; Rae, C. S.; Mochevova, S. N.; Swanson, M. S.; Zhao, Z.; Virgin, H. W.; Portnoy, D. Listeriolysin O is necessary and sufficient to induce autophagy during *Listeria monocytogenes* infection. *PLoS ONE* 2010, 5, e8610.
85. Logsdon, L. K.; Håkansson, A. P.; Cortés, G.; Wessels, M. R. Streptolysin O inhibits clathrin-dependent internalization of group A Streptococcus. *MBio* 2011, 2, e00332–10.
86. Sakurai, A.; Maruyama, F.; Funao, J.; Nozawa, T.; Aikawa, C.; Okahashi, N.; Shintani, S.; Hamada, S.; Ooshima, T.; Nakagawa, I. Specific behavior of intracellular *Streptococcus pyogenes* that has undergone autophagic degradation is associated with bacterial streptolysin O and host small G proteins Rab5 and Rab7. *J. Biol. Chem.* 2010, 285, 22666–22675.
87. Thiery, J.; Keefe, D.; Boulant, S.; Boucrot, E.; Walch, M.; Martinvalet, D.; Goping, I. S.; Bleackley, R. C.; Kirchhausen, T.; Lieberman, J. Perforin pores in the endosomal membrane trigger the release of endocytosed granzyme B into the cytosol of target cells. *Nat. Immunol.* 2011, 12, 770–U146.
88. Davis, M. J.; Swanson, J. A. Technical advance: Caspase-1 activation and IL-1 β release correlate with the degree of lysosome damage, as illustrated by a novel imaging method to quantify phagolysosome damage. *J. Leukoc. Biol.* 2010, 88, 813–822.
89. Hornung, V.; Bauernfeind, F.; Halle, A.; Samstad, E. O.; Kono, H.; Rock, K. L.; Fitzgerald, K. A.; Latz, E. Silica crystals and aluminum salts activate the NALP3 inflammasome through phagosomal destabilization. *Nat. Immunol.* 2008, 9, 847–856.

90. Dong, C.; Davis, R. J.; Flavell, R. A. MAP kinases in the immune response. *Annu. Rev. Immunol.* 2002, 20, 55–72.
91. Dogan, S.; Zhang, Q.; Pridmore, A. C.; Mitchell, T. J.; Finn, A.; Murdoch, C. Pneumolysin-induced CXCL8 production by nasopharyngeal epithelial cells is dependent on calcium flux and MAPK activation by Toll-like receptor 4. *Microbes Infect.* 2011, 13, 65-75.
92. Nilsson, M.; Sørensen, O. E.; Mörgelin, M.; Weineisen, M.; Sjöbring, U.; Herwald, H. Activation of human polymorphonuclear neutrophils by streptolysin O from *Streptococcus pyogenes* leads to the release of proinflammatory mediators. *Thromb. Haemost.* 2006, 95, 982-990.
93. Bebien, M.; Hensler, M. E.; Davanture, S.; Hsu, L.-C.; Karin, M.; Park, J. M.; Alexopoulou, L.; Liu, G. Y.; Nizet, V.; Lawrence, T. The pore-forming toxin β hemolysin/ cytolysin triggers p38 MAPK-dependent IL-10 production in macrophages and inhibits innate immunity. *PLoS Pathog* 2012, 8, e1002812.
94. Hackett, S. P.; Stevens, D. L. Streptococcal toxic shock syndrome: synthesis of tumor necrosis factor and interleukin-1 by monocytes stimulated with pyrogenic exotoxin A and streptolysin O. *J. Infect. Dis.* 1992, 165, 879–885.
95. Houldsworth, S.; Andrew, P. W.; Mitchell, T. J. Pneumolysin stimulates production of tumor necrosis factor alpha and interleukin-1 beta by human mononuclear phagocytes. *Infect. Immun.* 1994, 62, 1501–1503.
96. Malley, R.; Henneke, P.; Morse, S. C.; Cieslewicz, M. J.; Lipsitch, M.; Thompson, C. M.; Kurt-Jones, E.; Paton, J. C.; Wessels, M. R.; Golenbock, D. T. Recognition of pneumolysin by Toll-like receptor 4 confers resistance to pneumococcal infection. *Proc. Natl. Acad. Sci. U.S.A.* 2003, 100, 1966–1971.
97. Park, J. M.; Ng, V. H.; Maeda, S.; Rest, R. F.; Karin, M. Anthrolysin O and other gram-positive cytolysins are toll-like receptor 4 agonists. *J. Exp. Med.* 2004, 200, 1647–1655.
98. Zhang, H.; Tay, P. N.; Cao, W.; Li, W.; Lu, J. Integrin-nucleated Toll-like receptor (TLR) dimerization reveals subcellular targeting of TLRs and distinct mechanisms of TLR4 activation and signaling. *FEBS Letters* 2002, 532, 171–176.
99. Harder, J.; Franchi, L.; Muñoz-Planillo, R.; Park, J.-H.; Reimer, T.; Núñez, G. Activation of the Nlrp3 inflammasome by *Streptococcus pyogenes* requires streptolysin O and NF-kappa B activation but proceeds independently of TLR signaling and P2X7 receptor. *J. Immunol.* 2009, 183, 5823–5829.
100. Pétrilli, V.; Papin, S.; Dostert, C.; Mayor, A.; Martinon, F.; Tschopp, J. Activation of the NALP3 inflammasome is triggered by low intracellular potassium concentration. *Cell Death Differ.* 2007, 14, 1583–1589.

101. Keyel, P. A.; Heid, M. E.; Salter, R. D. Macrophage responses to bacterial toxins: a balance between activation and suppression. *Immunol. Res.* 2011, 50, 118–123.
102. Carrero, J. A.; Vivanco-Cid, H.; Unanue, E. R. Listeriolysin O is strongly immunogenic independently of its cytotoxic activity. *PLoS ONE* 2012, 7, e32310.
103. Wallecha, A.; Wood, L.; Pan, Z.-K.; Maciag, P. C.; Shahabi, V.; Paterson, Y. *Listeria monocytogenes*-derived listeriolysin O has pathogen-associated molecular pattern-like properties independent of its hemolytic ability. *Clin. Vaccine Immunol.* 2013, 20, 77–84.
104. Harty, J. T.; Schreiber, R. D.; Bevan, M. J. CD8 T cells can protect against an intracellular bacterium in an interferon gamma-independent fashion. *Proc. Natl. Acad. Sci. U.S.A.* 1992, 89, 11612–11616.
105. Ladel, C. H.; Flesch, I. E.; Arnoldi, J.; Kaufmann, S. H. Studies with MHC-deficient knock-out mice reveal impact of both MHC I- and MHC II-dependent T cell responses on *Listeria monocytogenes* infection. *J. Immunol.* 1994, 153, 3116–3122.
106. Gekara, N. O.; Zietara, N.; Geffers, R.; Weiss, S. *Listeria monocytogenes* induces T cell receptor unresponsiveness through pore-forming toxin listeriolysin O. *J. Infect. Dis.* 2010, 202, 1698–1707.
107. Carrero, J. A.; Calderon, B.; Unanue, E. R. Listeriolysin O from *Listeria monocytogenes* is a lymphocyte apoptogenic molecule. *J. Immunol.* 2004, 172, 4866–4874.

Chapter 2

Membrane damage during *Listeria monocytogenes* infection triggers a caspase-7 dependent cytoprotective response

(Published: Cassidy SKB *et al* (2012) PLoS Pathog 8, e1002628)

Abstract: The cysteine protease caspase-7 has an established role in the execution of apoptotic cell death, but recent findings also suggest involvement of caspase-7 during the host response to microbial infection. Caspase-7 can be cleaved by the inflammatory caspase, caspase-1, and has been implicated in processing and activation of microbial virulence factors. Thus, caspase-7 function during microbial infection may be complex, and its role in infection and immunity has yet to be fully elucidated. Here we demonstrate that caspase-7 is cleaved during cytosolic infection with the intracellular bacterial pathogen, *Listeria monocytogenes*. Cleavage of caspase-7 during *L. monocytogenes* infection did not require caspase-1 or key adaptors of the primary pathways of innate immune signaling in this infection, ASC, RIP2 and MyD88. Caspase-7 protected infected macrophages against plasma membrane damage attributable to the bacterial pore-forming toxin Listeriolysin O (LLO). LLO-mediated membrane damage could itself trigger caspase-7 cleavage, independently of infection or overt cell death. We also detected caspase-7 cleavage upon treatment with other bacterial pore-forming toxins, but not in response to detergents. Taken together, our results support a model where cleavage of caspase-7 is a consequence of toxin-mediated membrane damage, a common occurrence during infection. We propose that host

activation of caspase-7 in response to pore formation represents an adaptive mechanism by which host cells can protect membrane integrity during infection.

1. Introduction

Pore-forming toxins are integral to the virulence of many microbial pathogens, including the Gram-positive bacterium, *Listeria monocytogenes*. This facultative intracellular pathogen can cause life-threatening disease in humans, particularly in the very old and very young, the immunocompromised, and pregnant women [1]. In macrophages, *L. monocytogenes* gains access to its replicative niche via the action of a pore-forming cholesterol-dependent cytolysin, Listeriolysin O (LLO) [2]. LLO-dependent perforation of the primary phagosomal membrane allows the pathogen to escape into the cytosol, where it grows to high titers in the apparent absence of overt cell damage until late in infection [3,4]. Virulence of *L. monocytogenes* therefore requires a delicate balance between expressing virulence factors, such as LLO, to survive host cell defenses while maintaining an intact host cell niche. Infection with *L. monocytogenes* expressing an overactive allele of LLO [5,6] or with a strain that overproduces LLO [7] results in host cell damage and attenuation *in vivo*, primarily due to killing of extracellular *L. monocytogenes* by neutrophils [6]. It can therefore be inferred that the integrity and survival of infected host cells affects virulence of *L. monocytogenes*.

The infected macrophage plays a dichotomous role during *L. monocytogenes* infection, acting both as a reservoir for bacterial replication and as a source for inflammatory signals that result from recognition of microbial ligands or cellular stress. *L. monocytogenes* activates many inflammatory pathways in the cell that promote eventual bacterial clearance and immunity. Infection stimulates Toll-like receptors TLR2 and possibly TLR5, and the Nod-like receptors (NLRs) Nod1 and Nod2, resulting in NF- κ B-dependent pro-inflammatory gene transcription [8-12]. Cytosolic *L. monocytogenes* triggers assembly of the caspase-1 associated inflammasome, a

multiprotein complex whose formation can lead to an inflammatory cell death termed pyroptosis [13]. Active caspase-1 processes pro-IL-1 β and pro-IL-18, inflammatory cytokines that promote antimicrobial properties of phagocytes and stimulate adaptive immunity [14-16]. Several NLRs activate caspase-1 as a result of *L. monocytogenes* infection, including NLRC4, NLRP3 and AIM2, all of which require the adaptor protein ASC [17-20]. Studies in knockout mice have demonstrated that caspase-1 is important for primary clearance of *L. monocytogenes*, but the role of other caspases in the innate immune response to infection is less well defined [21].

Caspase-7 is a member of a family of cytosolic cysteine proteases that promulgate diverse biological responses, including programmed cell death and inflammation. Caspases can also promote cell survival, as caspase-1 positively regulates cholesterol biosynthesis in response to a bacterial pore-forming toxin, aerolysin [22]. A defining characteristic of caspases is specific cleavage of substrates at aspartic acid residues using a cysteine side chain as a nucleophile for peptide hydrolysis [23]. Caspases reside in the cytosol as zymogens that require dimerization and/or proteolytic cleavage before becoming catalytically active. Cleavage of caspase-7 results in a large and a small fragment; proteolysis between the large and small subunit is considered the fundamental activating event [24]. Caspase-7 was initially characterized as an “executioner” caspase whose activity directs the highly regulated cascade of events leading to cellular disassembly during apoptotic cell death ([25,26] and recently reviewed in [27]). Recent studies have implicated maturation of caspase-7 as a consequence of infection or inflammatory stimulation. Caspase-7 cleavage occurs during infection by the Gram-negative intracellular bacterial pathogens *Salmonella enterica* serovar Typhimurium and *Legionella pneumophila* [28,29]. In these contexts,

caspase-7 was cleaved by inflammasome-associated caspase-1. Caspase-7-deficient macrophages allowed increased *L. pneumophila* intracellular growth, possibly due to delayed macrophage cell death [29]. These studies provide evidence that caspase-7 is involved in host-pathogen interactions.

Here we show that caspase-7 cleavage is triggered by membrane damage during *L. monocytogenes* infection, and is dissociated from canonical markers of apoptosis. Caspase-7 cleavage occurred in the absence of caspase-1, distinct from the activation cascade observed during infection by *S. Typhimurium* and *L. pneumophila* [28,29]. Infected macrophages lacking caspase-7 exhibited increased plasma membrane permeability, which required ongoing production of LLO. Treatment of host cells with sublytic concentrations of recombinant LLO, as well as a pore-forming toxin from *Staphylococcus aureus*, α -hemolysin, triggered caspase-7 activation in the absence of infection. Together, these data lead us to propose that caspase-7 activation is protective host response to plasma membrane damage that limits subsequent cytotoxicity during bacterial infection.

2. Results

Caspase-7 cleavage is induced by *L. monocytogenes* infection without concomitant induction of apoptosis.

We first investigated whether hallmarks of proteolysis associated with caspase-7 activity could be detected in *L. monocytogenes* infected cells. To this end, we infected bone marrow derived macrophages (BMDM) from C57BL/6 (BL/6) mice with either a WT strain of *L. monocytogenes*, or with a strain lacking the *hly* gene, which encodes the pore-forming toxin Listeriolysin O (LLO⁻ strain). The LLO⁻ strain cannot escape the primary phagosome and does not replicate within macrophages. At 8 h pi, we assessed DEVDase activity, an indicator of caspase-3/7 proteolytic activity, by measuring cleavage of a luminescent DEVD containing substrate in cell lysates (Fig. 2.1A). Both caspase-3 and -7 are able to cleave exogenous DEVD substrate, but recent studies suggest that proteases have overlapping but distinct physiological substrates within the host cell [30]. We detected an increase in DEVD-specific enzymatic activity in response to infection with WT, but not the LLO⁻ mutant, indicating that bacterial uptake per se was insufficient to stimulate DEVDase activity. The difference in DEVDase activity between cells infected at MOI1 vs MOI5 was not attributable to differences in the number of infected cells (Fig. 2.1B) nor the number of bacteria, as we isolated nearly equivalent CFU from cultures infected under these conditions at 8 h pi (Fig. A1). At MOI1 and MOI5, 80-90% of cells were infected, although at MOI5, macrophages contained higher numbers of bacteria at early time points. To specifically determine if caspase-7 was activated during *L. monocytogenes* infection, we investigated whether *L. monocytogenes* infection induced caspase-7 cleavage in BMDM by lysing infected cells at 8 h pi and analyzing caspase-7 by immunoblot using an antibody that recognizes both the full length protein and the larger cleavage product (Fig. 2.1C). We observed cleaved

Figure 2.1.

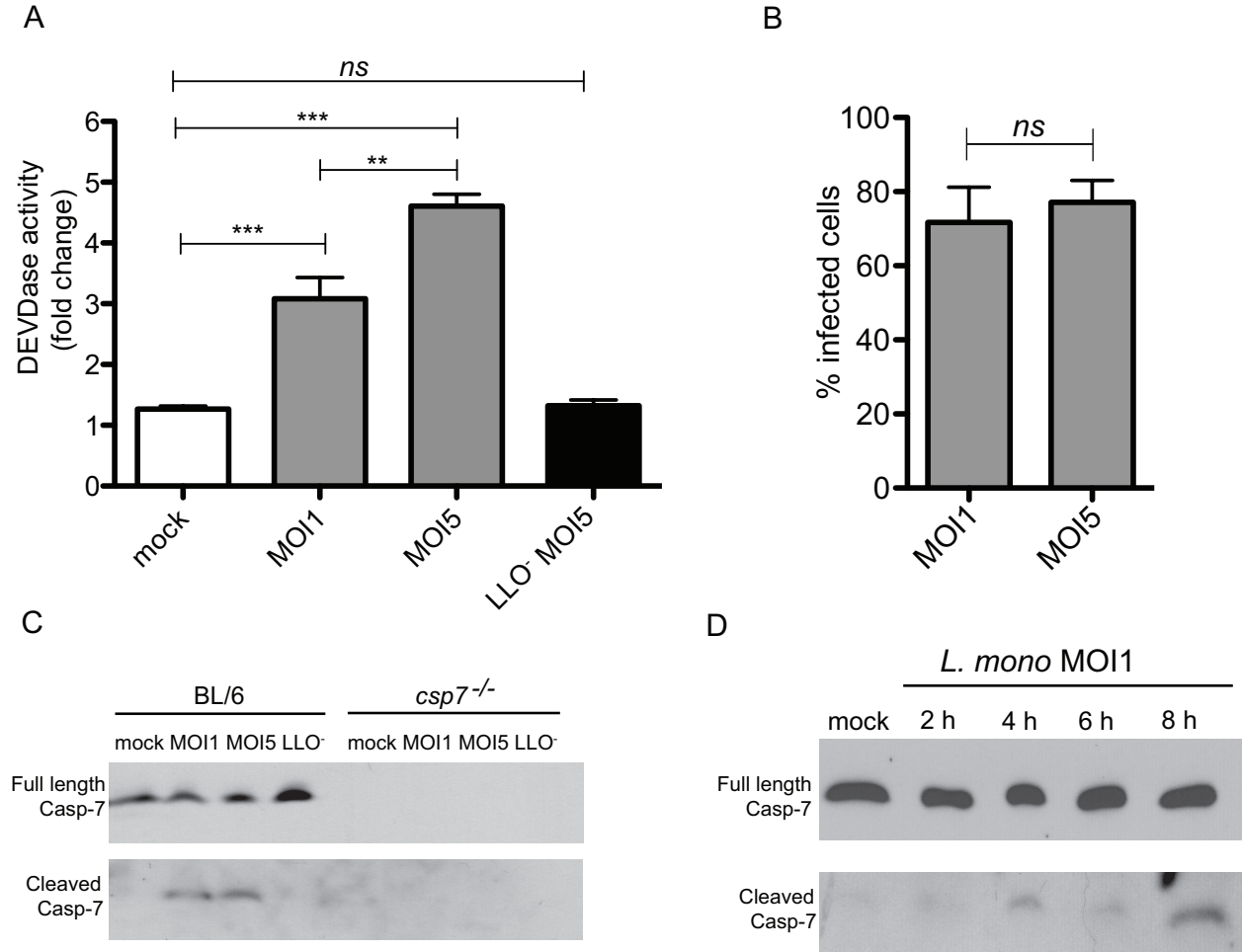


Figure 2.1. Caspase-7 is activated in macrophages during infection with *L. monocytogenes*. (A) BL/6 BMDMs were infected at the indicated MOI with either WT *L. monocytogenes* or with a mutant strain lacking the *hly* gene encoding listeriolysin O (LLO⁻). For this and all future experiments, BMDMs infected with the LLO⁻ strain were infected at MOI5. Cells were assessed for enzymatic activity 8 h pi. (B) The percentage of cells infected with *L. monocytogenes* at 8 h pi at the given MOI was assessed using fluorescence microscopy and Metamorph software. (C) BL/6 and *csp7*^{-/-} BMDMs were infected and cell lysates were probed for the cleavage of caspase-7 by immunoblot using an antibody that recognizes both full length and cleaved caspase-7 protein. The paired panels for full length and cleaved caspase-7 shown in this and all other immunoblots are from the same blot, but were cut to allow for longer exposure of the cleaved fragment. (D) BL/6 macrophages were infected with *L. monocytogenes*, lysates were harvested at the indicated times post infection and probed for caspase-7 protein. (A-D) are representative of no less than three independent experiments. * P < 0.05, ** P < 0.01 and *** P < 0.001, generated using unpaired t-tests. *ns* = not significant.

caspase-7 protein in BL/6 cells infected with WT at MOI1 and MOI5, but not in

uninfected (mock) BMDM or BMDM infected with the LLO⁻ strain (MOI 5), suggesting bacterial occupancy of the phagosome was insufficient to stimulate cleavage of this protease. Full-length caspase-7 protein was detected in BL/6 BMDM in all samples and was used as a protein loading control since the overall abundance of the cleaved caspase-7 product was low compared to full length. We also assessed caspase-3 cleavage during *L. monocytogenes* infection by immunoblot (Fig A2). Although we detected cleavage of caspase-3 in response to infection, the cleavage of caspase-7 in response to infection was more robust, and we therefore decided to further investigate caspase-7. To determine the kinetics of caspase-7 activation during infection, we assayed cell lysates for cleavage at 2, 4, 6 and 8 h pi (Fig. 2.1D). Cleavage of caspase-7 was detected between 4 and 8 h pi, by which time the majority of *L. monocytogenes* are replicating in the cytosol. Taken together, these data indicate that caspase-7 is activated during *L. monocytogenes* infection, and requires LLO.

Caspase-7 was originally identified as an executioner caspase whose activity was associated with activation of the apoptotic cascade [31]. To determine whether caspase-7 cleavage was also associated with molecular markers of programmed cell death during *L. monocytogenes* infection, we first quantified the number of infected cells at 8 h pi by staining samples with anti-*Listeria* antibody, followed by immunofluorescence microscopy (Fig. 2.1B). We then prepared infected cell cultures for TUNEL staining to visualize DNA fragmentation. BMDM were exposed to *L. monocytogenes* at MOI1 or MOI5, and at 8 h pi cells were fixed and analyzed for DNA fragmentation by immunofluorescence microscopy. In agreement with previous findings [3], we found no significant increase in DNA fragmentation in cells infected at MOI1 compared to uninfected control cells (Fig. 2.2A). At MOI5, there was a statistically significant

Figure 2.2

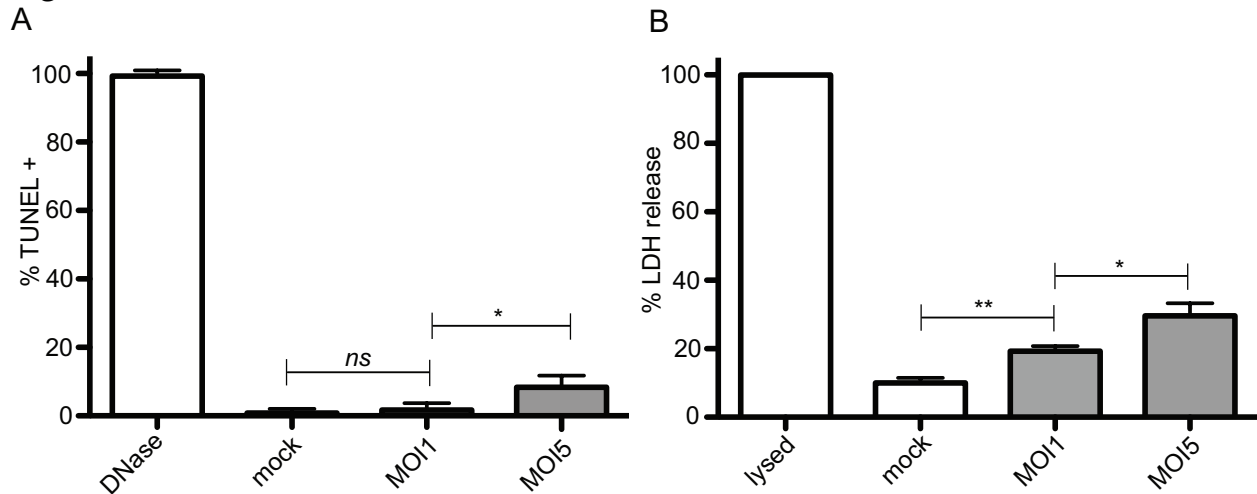


Figure 2.2. Caspase-7 activation during infection with *L. monocytogenes* induces minimal apoptosis. (A) BL/6 macrophages were infected and assessed for TUNEL staining as a marker of apoptosis 8 h pi. DNase treatment was used as a positive control for DNA fragmentation. P values were generated using unpaired t-tests of no less than 300 cells per condition. (B) Lactate dehydrogenase (LDH) release into cell culture supernatants was measured 8 h pi as a marker of cell integrity. The amount of LDH released as the result of detergent induced lysis was set to 100% and the signal from untreated cells was set as baseline. (A and B) are representative of no less than three independent experiments. * $P < 0.05$, ** $P < 0.01$ and *** $P < 0.001$, generated using unpaired t-tests. *ns* = not significant.

increase in the number of TUNEL positive cells compared to uninfected cells. However, comparing the overall number of TUNEL positive cells even in the MOI5 infection (~10-15%) to the number of cells infected (80-90%), we conclude that the majority of cells infected with *L. monocytogenes* do not display this characteristic hallmark of apoptosis by 8 h pi. We obtained similar results using Annexin V to measure phosphatidylserine exposure, an early event in apoptotic cell death (Fig. A3). We also measured lactate dehydrogenase (LDH) release at 8 h pi as an indicator of overall cell viability (Fig. 2.2B). *L. monocytogenes* infection induced a modest but notable increase in LDH release at 8 h pi compared to uninfected cells. This range is consistent with previously published reports [3], and indicates that at low MOI the majority of cells infected with *L. monocytogenes* retain LDH. We conclude from these results that *L. monocytogenes* infection stimulates caspase-7 cleavage, but is not predominantly associated with molecular markers of apoptotic cell death.

Key regulators of innate immune signaling are dispensable for caspase-7 activation during *L. monocytogenes* infection

L. monocytogenes infection triggers activation of caspase-1, and during some bacterial infections, caspase-7 can be a substrate of caspase-1 [28,29]. We therefore tested whether the activation of caspase-7 during *L. monocytogenes* infection was dependent on the presence of caspase-1 by infecting *csp1*^{-/-} BMDM and measuring DEVDase activity. We detected increased DEVDase activity upon infection of caspase-1 deficient BMDM (Fig. 2.3A). Analysis of caspase-7 protein by immunoblot of infected cell lysates definitively revealed cleavage of caspase-7 in *csp1*^{-/-} BMDM upon infection, and this cleavage was dependent on LLO (Fig. 2.3B). ASC is a key adaptor protein necessary for caspase-1 activation during inflammasome formation [32]. To determine if

Figure 2.3.

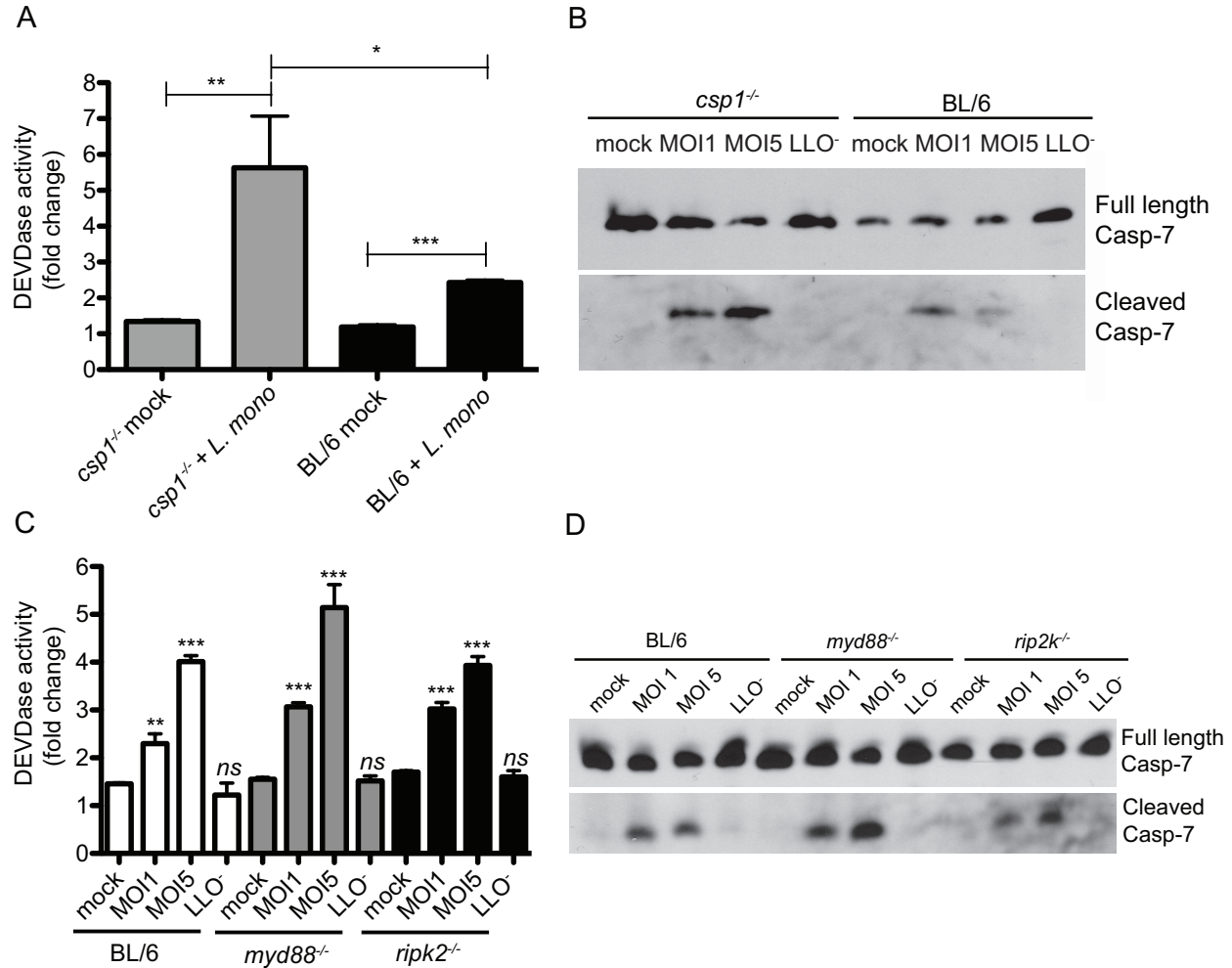


Figure 2.3. Caspase-1 and other key mediators of innate immunity are individually dispensable for caspase-7 cleavage. (A) Caspase-1 deficient and BL/6 BMDM were infected as indicated and lysed at 8 h pi. DEVDase activity in the lysates was measured by Caspase-Glo 3/7 assay. Signal from assay buffer alone was subtracted from all the sample values. (B) BMDM were infected as in (A) and cells were lysed at 8 h pi. Lysates were subjected to SDS-PAGE and immunoblotting with an anti-caspase-7 antibody that recognizes both full length and cleaved caspase-7 protein. (C) BL/6, MyD88- deficient and RIP2-deficient BMDM were infected as indicated and lysed at 8 h pi. DEVDase activity in the lysates was measured by Caspase-Glo 3/7 assay. Signal from assay buffer alone was subtracted from all the sample values. (D) BMDM were infected as in (A) and cells were lysed at 8 h pi. Lysates were subjected to SDS-PAGE and immunoblotting with the anti-caspase-7 antibody. Statistical significance was determined by Student's unpaired t-test; *p<0.05, **p<0.01 and ***p<0.001.

ASC was necessary for caspase-7 cleavage, we assayed caspase-7 cleavage in infected *Asc*^{-/-} BMDM and found that caspase-7 activation also did not require ASC during *L. monocytogenes* infection (data not shown). These data demonstrate that the mechanism of caspase-7 cleavage during *L. monocytogenes* infection does not require caspase-1, and thus appears to be distinct from mechanisms reported for other intracellular bacterial pathogens.

Extracellular (TLR2 and TLR5) and intracellular (Nod1 and Nod2) pattern recognition receptors are able to sense *L. monocytogenes* and direct transcription of cytokines and chemokines to promote inflammation and clearance [8-12]. To determine whether these bacterial recognition pathways contributed to caspase-7 activation upon infection, we evaluated *L. monocytogenes*-induced DEVDase activity and caspase-7 cleavage in BMDM from *myd88*^{-/-} and *rip2k*^{-/-} mice. MyD88 is a critical adaptor that mediates signaling for 9 of the 10 TLRs with known ligands. RIP2 is a protein kinase that mediates inflammatory signaling through Nod1 and Nod2. We observed infection-induced DEVDase activity and caspase-7 cleavage in *myd88*^{-/-} and *rip2k*^{-/-} BMDM at levels comparable to WT BMDM (Fig. 2.3C and 2.3D). We also detected caspase-7 cleavage in *nod1*^{-/-} and *nod2*^{-/-} macrophages comparable to WT (data not shown). From these results, we conclude that the innate immune signaling pathways regulated by MyD88-dependent TLRs, Nod1, Nod2, ASC, and caspase-1 are individually dispensable for caspase-7 activation during *L. monocytogenes* infection.

Caspase-7 deficient BMDM are permeable to small molecules during infection

Since caspase-7 was cleaved during infection with *L. monocytogenes*, we hypothesized that the activity of this enzyme could impact intracellular infection. We therefore measured *L. monocytogenes* replication in BL/6 and *csp7*^{-/-} BMDM in an antibiotic

protection assay where 50 μ g/ml of the cell impermeant antibiotic gentamicin was added 30 min pi to eliminate extracellular bacteria (Fig. 2.4A). We observed significant decline in the number of intracellular bacteria over time within the *csp7^{-/-}* BMDM compared to BL/6 cells. We considered the possibility that *csp7^{-/-}* cells were becoming permeable to gentamicin, allowing antibiotic influx into the intracellular space, killing intracellular bacteria. To test this idea, we performed a gentamicin washout, removing gentamicin from the medium 2 h pi, after which antibiotic-free medium was added and replaced every hour to limit extracellular bacterial growth (Fig. 2.4B). When gentamicin was removed from the extracellular space, there was no significant difference in bacterial replication between BL/6 and *csp7^{-/-}* macrophages. These data suggest increased plasma membrane permeability of *L. monocytogenes*-infected macrophages in the absence of caspase-7.

To more directly assess membrane integrity of *L. monocytogenes* infected BMDM, we evaluated their permeability to small fluorescent molecules during infection. At 8 h pi we exposed live infected cells to rhodamine-phalloidin (rho-phall), a small (1200 Da) cell impermeant compound that binds F-actin in the host cell. After a 15-minute exposure, the cells were fixed and counter-stained with DAPI. Permeability to rho-phall was compared between *csp7^{-/-}* and BL/6 BMDM using epifluorescence microscopy (Fig. 2.4CD). Untreated BMDM excluded rho-phall, while cells treated with Triton X-100 were fully permeable to rho-phall (Fig. 2.4C insets). Although rho-phall permeability was similar between genotypes in the absence of infection, during infection the overall number of cells stained with phalloidin was significantly greater in the *csp7^{-/-}* macrophages compared to wildtype BMDM. Notably, despite permeability to

Figure 2.4

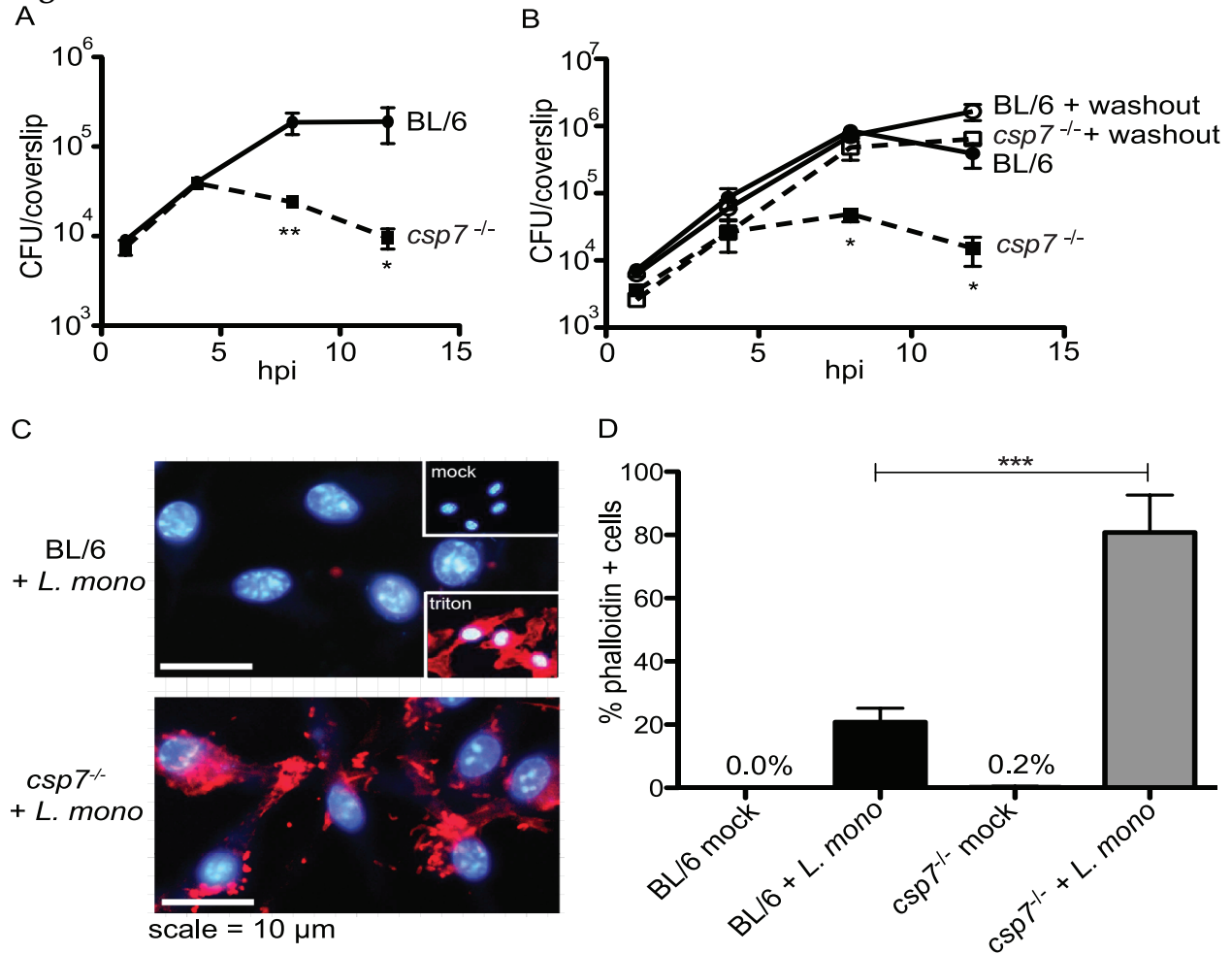


Figure 2.4. Caspase-7 deficient BMDM are permeable to small molecules during infection. (A) BMDM were infected with *L. monocytogenes* and gentamicin (480 Da) was added 30 min pi to abrogate extracellular bacterial growth. (B) Cells were infected as in (A), but beginning at 2 h pi, cells were washed with PBS and replenished with antibiotic free medium once an hour to limit extracellular bacterial growth. (C) BL/6 and *csp7*^{-/-} cells infected for 8 h with *L. monocytogenes* were incubated with rhodamine-phalloidin (rho-phall) (~1200 Da) for 15 min prior to fixation and DAPI counterstain. The insets show rho-phall staining of mock treated and Triton X-100 treated BL/6 macrophages. Samples were visualized by epifluorescence microscopy. (D) Cells were treated as in (C) and rho-phall influx was quantified by fluorescence microscopy (300 cells were counted per condition per experiment). Error bars represent standard deviation from the mean. All conditions were measured in triplicate, and all experiments were repeated ≥ 3 times. Statistics were calculated using the Student's unpaired t-test; * $p < 0.05$, ** $p < 0.01$ and *** $p < 0.001$.

small molecules, infected *csp7^{-/-}* cells displayed no significant increase in LDH release at 8 h pi compared to control cells (Fig. A4). These findings suggest that membrane damage occurring during *L. monocytogenes* infection may be transient, and is insufficient to allow efflux of the large LDH tetramer ($\approx 137,000$ Da) [33]. Taken together, these data indicate that caspase-7 promotes plasma membrane integrity during infection with *L. monocytogenes*.

Plasma membrane instability during *L. monocytogenes* infection requires LLO

Plasma membrane damage during *L. monocytogenes* infection could be the result of toxin-mediated pore formation. To determine whether bacterial protein synthesis was needed to induce host membrane instability, we treated infected cells with a bacteriostatic concentration of erythromycin (*erm*), a macrolide antibiotic that targets the bacterial 50S ribosomal subunit. Erythromycin was added to infected cells at 2 h pi, and at 8 h pi we found a significant reduction in the number of caspase-7-deficient phalloidin positive cells upon inhibition of bacterial protein synthesis (Fig. 2.5A). We then tested the requirement for LLO in driving the plasma membrane damage we observed in infected caspase-7 deficient macrophages. LLO is an oligomeric cytolysin that forms pores in cholesterol-containing membranes [34]. The oligomerization of LLO occurs optimally at acidic pH [5,35] but still maintains some pore-forming activity at neutral pH [36-38]. LLO is actively produced by cytosolic *L. monocytogenes* [39]. We hypothesized that LLO production by cytosolic bacteria could result in continual but transient membrane damage during infection, which was exacerbated in *csp7^{-/-}* cells. To test this hypothesis, we used a strain of *L. monocytogenes* with LLO expression controlled by an IPTG inducible promoter (iLLO) [40]. We transiently induced production of LLO during infection by the iLLO-expressing strain to permit escape

Figure 2.5

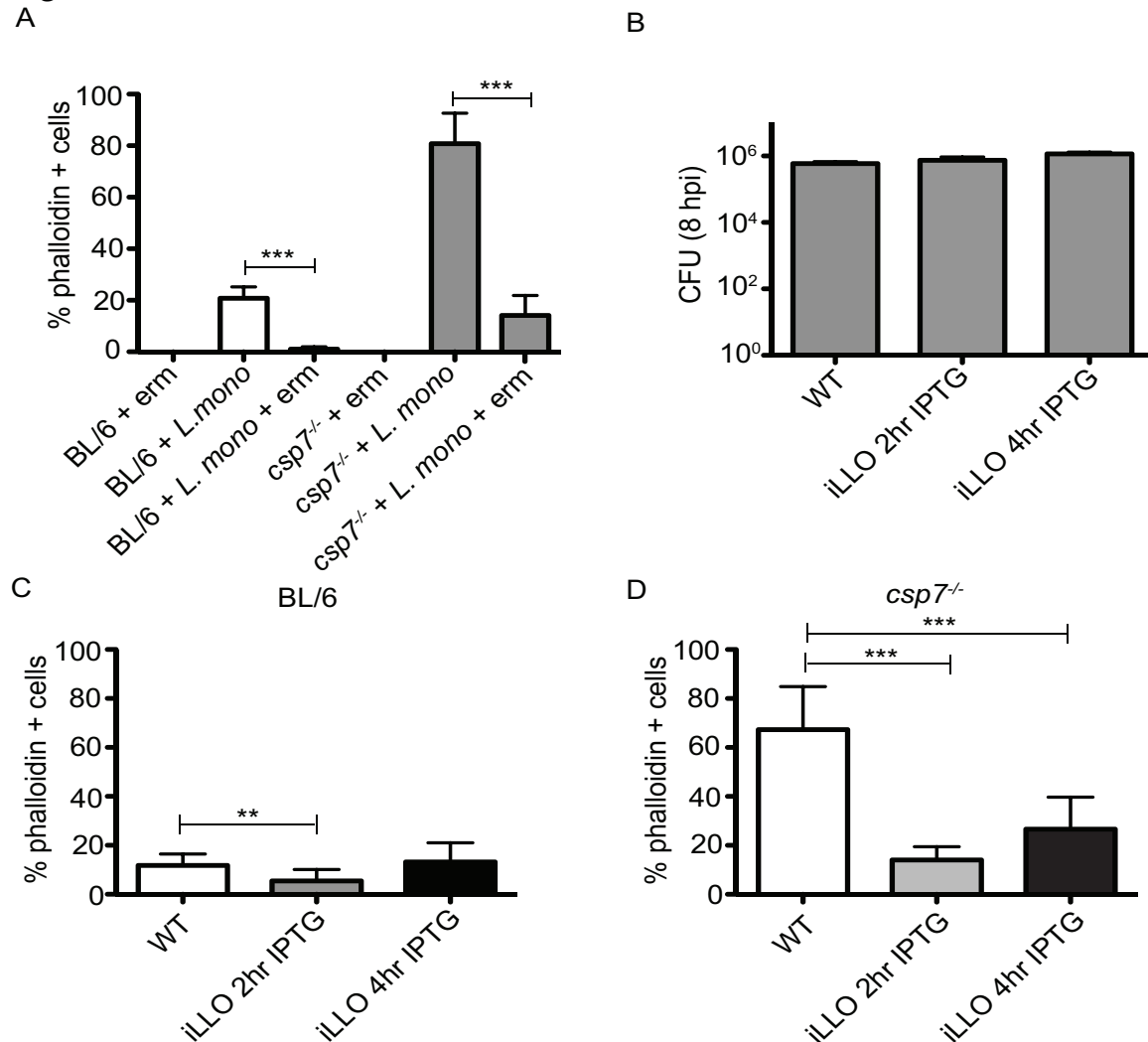


Figure 2.5. Caspase-7 enhances host resistance to LLO-mediated plasma membrane damage. (A) Caspase-7-deficient and BL/6 BMDM were infected with *L. monocytogenes*. At 4 h pi, 10mg/ml erythromycin (erm) was added to the medium to inhibit bacterial protein synthesis, and was maintained for the duration of the experiment. At 8 h pi, the cells were incubated with rho-phall and visualized by fluorescence microscopy as in Fig. 3CD to measure permeability. (B) BMDM were infected with WT *L. monocytogenes* or a bacterial strain expressing an inducible allele of LLO (iLLO). BMDM infected with the iLLO strain were incubated with 1mM IPTG as indicated. Intracellular colony forming units were measured at 8 h pi. (C) BL/6 BMDM were infected as in (B), and rho-phall influx was quantified at 8 h pi by epifluorescence microscopy. (D) Caspase-7-deficient BMDM were infected as in (B), and rho-phall permeability was quantified at 8 h pi by epifluorescence microscopy. Statistics were calculated using the Student's unpaired t-test; **p<0.01 and ***p<0.001.

from the phagosome, and then removed IPTG from the cell culture medium. Determination of endpoint CFU at 8 h pi in BL/6 macrophages infected with the WT and iLLO strains revealed no significant differences in the number of intracellular bacteria between strains (Fig. 2.5B). However, IPTG removal at 2 h pi resulted in significantly less phalloidin permeable BL/6 BMDM infected with the iLLO strain compared to cells infected with WT bacteria at 8 h pi (Fig. 2.5C). The reduction of permeability in *csp7^{-/-}* macrophages infected with the iLLO-expressing strain compared to the WT strain was even more pronounced, supporting a protective role for this protease against infection associated membrane damage (Fig. 2.5D). Increasing induction time from 2 to 4 hours increased the number of phalloidin positive cells in both genotypes. Therefore, we conclude that LLO is required to drive the membrane permeability defect in macrophages lacking caspase-7.

Pore formation by exogenous toxin is a trigger for caspase-7 cleavage

Bacterial production of LLO was required for permeability of caspase-7 deficient macrophages during infection (Fig. 2.5), leading us to question whether LLO was also the trigger that stimulated cleavage of caspase-7. To test this possibility, we infected BMDM with *L monocytogenes*, and then added 10 µg/ml erm at 2 h pi to inhibit bacterial protein synthesis and assayed for caspase-7 cleavage by immunoblot. We were unable to detect cleavage of caspase-7 when erm was added to infected cell cultures, demonstrating that bacterial protein synthesis was necessary to stimulate this response (Fig. 2.6A). We also infected BMDM with the IPTG-inducible LLO expressing strain, incubating with IPTG for 2h pi to promote vacuolar escape, followed by removal of IPTG from the medium to limit LLO production. Although the iLLO and WT strains

grew to equivalent intracellular CFU under these conditions (Fig. A5), we only observed caspase-7 cleavage in cells infected with the WT strain, not the iLLO strain (Fig. 2.6A). LLO is one of a large family of cholesterol dependent cytolysins (CDC) produced by Gram-positive bacterial pathogens. To determine whether activation of caspase-7 during bacterial infection was specific to LLO, or whether other CDC toxins behaved similarly, we infected wildtype and caspase-7^{-/-} BMDM with *L. monocytogenes* expressing the related CDC toxin perfringolysin O (PFO) instead of LLO [41]. *L. monocytogenes* expressing PFO also stimulated caspase-7 activation (Fig. 2.6B). Thus, we find that cytosolic bacterial replication per se is insufficient to stimulate caspase-7 cleavage, and that ongoing production of toxin is necessary for activation of the protease during *L. monocytogenes* infection.

We next asked if exogenous LLO could activate caspase-7 independent of infection. To this end, we first determined the sublytic concentration range of purified recombinant LLO (rLLO), using LDH release as a marker for loss of viability at 1 h post treatment (Fig. 2.6C). We then probed cell lysates incubated for 1 h with rLLO for caspase-7 cleavage by immunoblot. Concentrations of exogenous rLLO, i.e., 0.25µg/ml, that only induced a low level of LDH release (~5%) from BMDM up to 5 h pi (Fig. 2.6C and A6) were sufficient to stimulate caspase-7 cleavage (Fig. 2.6D). As we increased the concentration of exogenous LLO, we saw a concomitant increase in LDH release that correlated with more robust caspase-7 cleavage (Fig. 2.6CD). These data demonstrate that sublytic concentrations of LLO can activate caspase-7 in the absence of infection. To address whether LLO in its native conformation was necessary to stimulate caspase-7 cleavage, we heat-treated the protein for 10 minutes at 65°C (LLO*), and compared caspase-7 cleavage against cells intoxicated with the same concentration of native

Figure 2.6

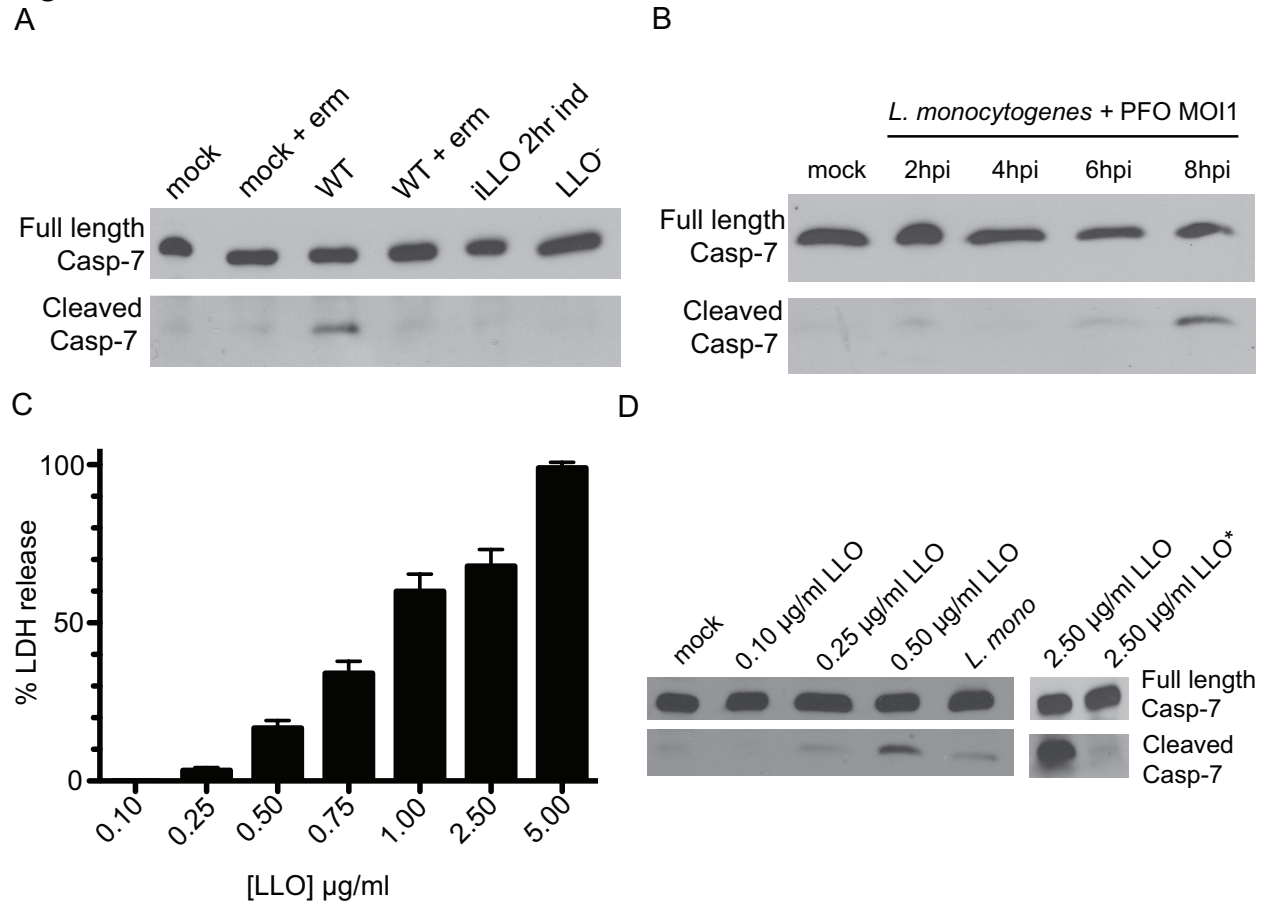


Figure 2.6. Caspase-7 is cleaved in response to membrane damage in the absence of infection. (A) BL/6 BMDM were infected with the indicated strains and lysed at 8 h pi. Lysates from uninfected (mock), mock infected cells treated with erythromycin (erm), WT infected, WT infected + erm 2h pi, iLLO infected + IPTG for 2h pi, and LLO⁻ infected were subjected to SDS-PAGE and immunoblot analysis with an anti-caspase-7 antibody that recognizes both the full length and cleaved protein. (B) BL/6 BMDMs were infected with a strain of *L. monocytogenes* expressing PFO in place of LLO and cell lysates were harvested at the given times post infection. Lysates were probed for caspase-7 protein using the anti-caspase-7 antibody. (C) BL/6 macrophages were incubated with the indicated concentrations of recombinant LLO protein for 1 h after which the media was assayed for lactate dehydrogenase activity. The amount of LDH release from detergent lysed cells was set to 100% and the LDH released from untreated cells was set to 0%. (D) BMDMs treated as in (C) were lysed at 1 h post treatment and assayed for caspase-7 cleavage by SDS-PAGE and immunoblot. The LLO* sample was heat treated for 10 minutes at 65 °C before addition to BMDMs to inactivate the toxin.

protein. When LLO was heat-inactivated, we observed significantly less caspase-7 cleavage compared to cells treated with active toxin (Fig. 2.6D). These data show that native LLO is necessary for induction of caspase-7 cleavage. One interpretation of these data could be that a native epitope of LLO stimulates caspase-7 cleavage through binding of a host receptor at the plasma membrane. However, since we observed LLO-dependent caspase-7 cleavage whether LLO was extracellular or in the cytosol, we propose instead that LLO triggers caspase-7 cleavage through pore formation.

Pore-forming toxins, but not detergents, stimulate caspase-7 cleavage

To address whether caspase-7 cleavage occurs as a general response to membrane damage, we assessed the ability of exogenous detergent treatment to activate the protease. Digitonin is a non-ionic glycoside detergent that can reversibly permeabilize the plasma membrane by forming complexes with cholesterol [42]. To determine if caspase-7 could be activated in response to detergent permeabilization, we treated BMDM with lytic and sublytic concentrations of digitonin and probed for caspase-7 cleavage 1 h post treatment by immunoblot. Although digitonin treatment induced plasma membrane damage, as assessed by measuring LDH release (Fig 2.7A), detergent treatment did not stimulate caspase-7 cleavage at any concentration tested (Fig. 2.7B). We obtained similar results using a sublytic to lytic range of the detergents Nonidet P-40, Triton-X100, Tween-20 and saponin (data not shown). These data indicate that plasma membrane damage alone is insufficient to stimulate caspase-7 activation.

We then asked if caspase-7 cleavage could be stimulated by other pore-forming toxins (PFT). *Staphylococcus aureus* α -hemolysin is a well studied PFT distinct from the CDC family of toxins. Treatment of BMDM with α -hemolysin resulted in little to no

Figure 2.7

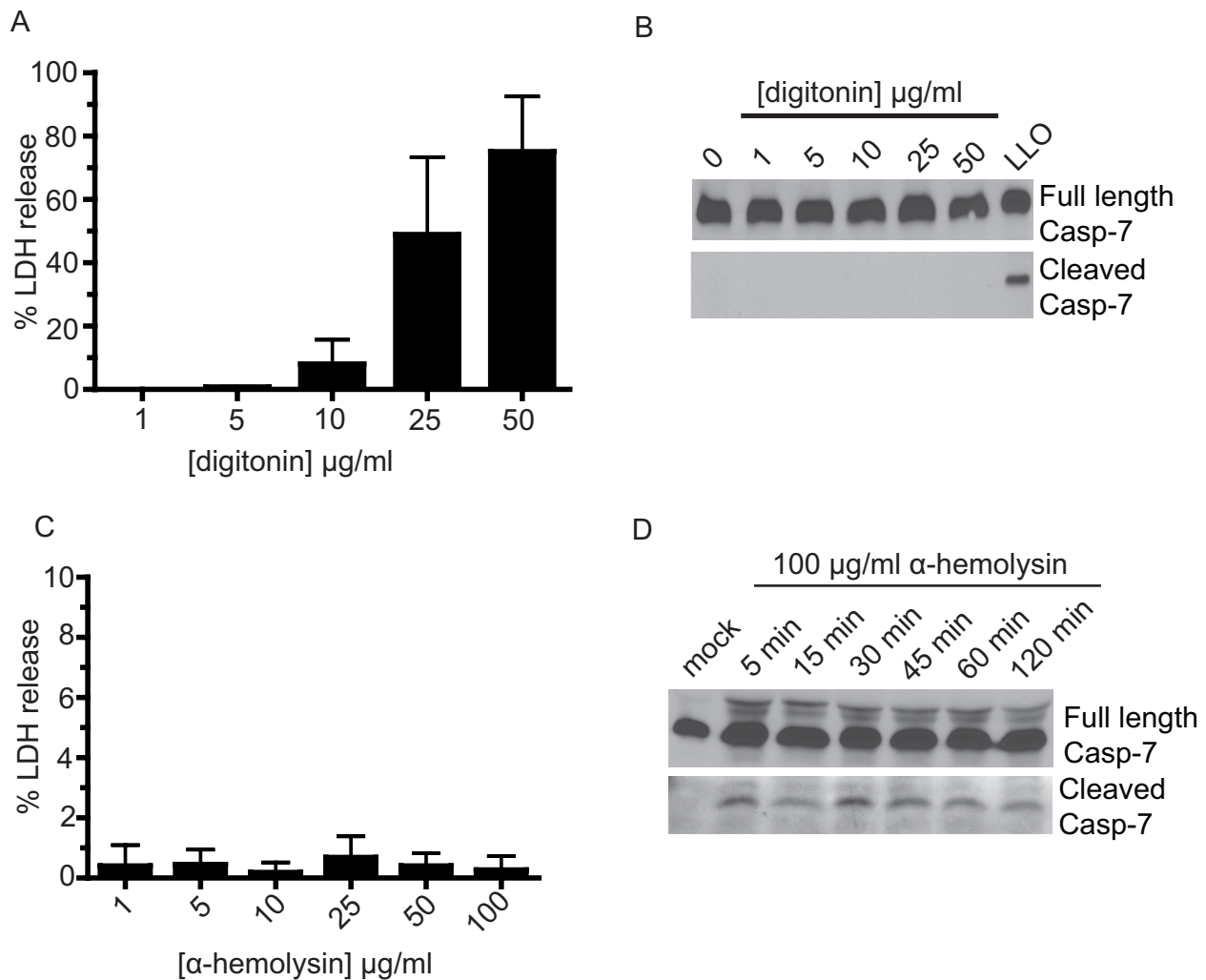


Figure 2.7. Damage caused by pore-forming toxins stimulates caspase-7 cleavage.

(A) BMDMs were treated with digitonin for 1 h after which the cell media was tested for lactate dehydrogenase activity. (B) BMDM treated as in (A) were lysed 1 h post treatment and assayed for caspase-7 cleavage by SDS-PAGE and immunoblot using an antibody that recognizes both the full length and cleaved protein. Treatment of BMDM with 0.75 µg/ml recombinant LLO was included as a control for caspase-7 cleavage. (C) BL/6 BMDM were treated with varying concentrations of α-hemolysin (Sigma-Aldrich) and cell media was tested for lactate dehydrogenase activity 1 h post treatment. The amount of LDH release from detergent lysed cells was set to 100% and the LDH released from untreated cells was set to 0%. (D) BMDM were treated with 100 µg/ml α-hemolysin and were lysed at the given times post treatment. Lysates were probed for caspase-7 cleavage by immunoblot.

LDH release up to 8 h post treatment (Fig 2.7C and A7), consistent with previous reports that nucleated cells can repair damage caused by this toxin [43-45]. To test the pore-forming ability of the toxin we confirmed it was lytic on red blood cells (data not shown). α -hemolysin did trigger caspase-7 activation as early as 5 min post treatment (Fig 2.7D). Some cells types activate the apoptotic cascade in response to treatment with low doses, but not high doses, of α -hemolysin [46,47]. However we observed no morphological hallmarks of apoptosis up to 8 h post toxin treatment (data not shown). These results suggest that caspase-7 activation is generally responsive to membrane damage by bacterial pore-forming toxins.

3. Discussion

Here we report that caspase-7 protects plasma membrane integrity during infection with *L. monocytogenes*. We found that the transient membrane damage observed during infection was dependent on the pore-forming toxin, LLO. We also showed that caspase-7 cleavage by *L. monocytogenes* infection did not individually require caspase-1, ASC, MyD88-dependent TLR, or Nod1 and Nod2 signaling. Instead, we found that sublytic membrane damage by recombinant LLO and α -hemolysin, even in the absence of infection, could stimulate caspase-7 activation. *L. monocytogenes* expressing PFO also stimulated caspase-7 activity. However, treatment of BMDM with sublytic concentrations of detergent did not trigger caspase-7 cleavage. These data suggest that general membrane damage or changes in ion gradients across the membrane are insufficient to stimulate caspase-7 and the subsequent cytoprotective response. Although these observations do not rule out a role for pattern recognition of specific microbial ligands in activation of caspase-7, our results suggest the possibility that caspase-7 participates in sensing and/or repair of PFT-induced membrane damage in the infected cell by a caspase-1 independent mechanism. Given the abundance and importance of PFTs for many pathogens, we propose a model whereby caspase-7 is induced by plasma membrane damage that occurs during microbial infection and initiates mechanisms of phagocyte membrane repair to protect the infected cell.

Caspases are well studied for their pivotal roles in apoptotic and inflammatory cell death cascades. However, there is a growing body of evidence that links caspase activation to additional cellular functions, independent from those leading to cell death. For instance, *in vitro* and *in vivo* studies indicate that caspase-7 cleaves and is regulated by sterol regulatory element binding proteins (SREBPs), transcription factors bound to

endoplasmic reticulum (ER) and nuclear membranes [48,49]. When cells are depleted of cholesterol, proteolytic cleavage of SREBPs results in their nuclear translocation and subsequent transcription of genes responsible for cholesterol biosynthesis and lipoprotein uptake [50]. Gurcel *et al* demonstrated that activation of SREBPs in response to the pore-forming toxin, aerolysin, promoted intoxicated cell survival in a caspase-1 dependent manner [22]. However, in our studies, activation of caspase-7 did not require caspase-1. Moreover, we observed no analogous upregulation of cholesterol biosynthesis genes (data not shown). Caspases can also regulate virulence determinants during intracellular infection. Caspase-3, a canonical “executioner” caspase highly related to caspase-7, was recently shown to cleave the *Salmonella* type III secreted effector protein SipA [51]. Processing of SipA was necessary for the generation of inflammation in mouse infection models, and inflammatory signaling is critical for *Salmonella* pathogenesis [52], suggesting co-evolution between host and pathogen to promote bacterial virulence in this context. Caspase-mediated cleavage of pathogen-derived proteins can also function to attenuate virulence. For instance, caspase-7 cleavage of ORF57, an early protein critical for viral replication during KSHV infection, inhibits the expression of viral lytic proteins, thereby limiting viral spread [53]. Taken together, these studies demonstrate that caspases play a complex role during microbial infection, and individual caspases may act in a manner that benefits the host and/or the pathogen.

The mechanisms by which the host cell defends itself from LLO-mediated toxicity or damage by other microbial virulence factors are not fully understood, although the concept of plasma membrane or phagosomal membrane damage as a signature of pathogenesis has been recognized [4,54]. Infection-associated signals, such as flagellin or membrane damage, may be sensed such that weak signals trigger a

protective response, whereas strong signals result in initiation of programmed cell death through pyroptosis or apoptosis. Sublytic levels of membrane damage by pore formation may send a “weak” signal, inducing adaptive mechanisms of membrane repair. Indeed, several groups have demonstrated that mammalian cells can tolerate sublytic concentrations of the related cytolysin, Streptolysin O, which causes transient membrane perforations that allows delivery of large macromolecules into live cells [55-57]. Repair of such membrane lesions can occur by the exocytosis of lysosomes to the site of injury, followed by endocytosis of the damaged section of membrane [55,58]. Previous studies indicate that LLO is actively produced by cytosolic *L. monocytogenes* [39] and therefore LLO could cause ongoing transient membrane damage throughout the infection that is kept in check by membrane repair. Investigating the pore forming toxin, BT toxin, from the invertebrate pathogen *Bacillus thuringiensis*, Bischof *et al* reported that intoxication of *C. elegans* and mammalian cells stimulated the unfolded protein response (UPR), a stress-related mechanism aimed at maintaining protein homeostasis in the ER, and that activation of this stress response was critical for nematode defense against the toxin [59]. Recent studies suggest the UPR is activated in response infection with *L. monocytogenes* [60]. Whether caspase-7 acts analogously or together with the UPR as a defense mechanism to protect host membrane integrity remains to be elucidated. Given that membrane-damaging virulence factors are virtually ubiquitous among bacterial pathogens, we propose that caspase-7 may represent a broad mechanism by which the host cell can sense this common insult and protect itself from ongoing damage.

4. Materials and Methods

Ethics Statement

Humane animal care at the University of Michigan is provided by the Unit for Lab Animal Medicine, which is accredited by the American Association for Accreditation of Laboratory Animal Care and the Department of Health and Human Services. This study was carried out in strict accordance with the recommendations in the Guide for the Care and Use of Laboratory Animals of the National Institutes of Health. The protocol was approved by the Committee on the Care and Use of Animals (UCUCA) of the University of Michigan (#A3114-01).

Bacterial Strains and Reagents

BMDM were infected with *Listeria monocytogenes* strain 10403S (WT), DP-L2161 (LLO) [41] which has an in-frame deletion of the *hly* gene, DH-616 (iLLO) [40] whose allele of the *hly* gene is controlled by an IPTG inducible promoter, and DPL-1875 [41], a *hly* deletion strain expressing *pfo* (perfringolysin O) using the *hly* promoter. The anti-caspase-7 antibody, which recognizes full length and cleaved caspase-7 (cat #9492) was purchased from Cell Signaling Technology. Rhodamine-phalloidin (cat #R415) was purchased from Molecular Probes. Digitonin and α -hemolysin were purchased from Sigma-Aldrich.

Cell Culture and Infection

Bone marrow derived macrophages (BMDM) were isolated from WT C57BL/6 mice, except where targeted mutations were indicated. All genetically deficient strains of mice used were constructed in this background. BL/6 and *csp7^{-/-}* mice were bred by the

G. Nuñez lab, the T-D Kanneganti lab, and Jackson Laboratories (Bar Harbor, Maine). Mice from the G. Nuñez lab were sacrificed and marrow was isolated immediately after necropsy. Mice from the T-D Kanneganti lab and Jackson Laboratories were sacrificed, their rear legs isolated and shipped overnight in media on ice to the O'Riordan lab, and marrow was isolated the next morning. Briefly, isolated BMDM were differentiated in DMEM with 20% heat-inactivated FBS (Hyclone Laboratories), 1% L-glutamine, 1% sodium pyruvate and 30% L929 fibroblast conditioned medium. Cells were cultured in non-TC treated plates, fed with fresh media on day 3 and harvested on day 6 for infection on day 7. Cultures were maintained in a humidified incubator at 37°C with 5% CO₂. Overnight cultures of *L. monocytogenes* in BHI broth were incubated statically at 30°C. Prior to infection, bacteria were pelleted and resuspended in PBS.

For experiments with the iLLO strain, cultures were grown overnight statically at 30°C in BHI + 1mM IPTG. Before infection, cultures were back diluted 1:10 in fresh BHI with 1mM IPTG and grown with shaking at 37°C until an OD₆₀₀ of 1.2 was achieved, at which point bacteria were pelleted and resuspended in PBS to be used for inoculation of cell cultures. All other strains was treated equivalently, but without IPTG. When iLLO was used to infect cells, 10mM IPTG was added to the cell culture media for the indicated times post infection. Cells were infected at MOI1 or MOI5 for most strains and MOI10 for iLLO to compensate for decreased phagosomal escape of the iLLO strain. When infected in this manner, the WT and iLLO strains grew with similar kinetics and cells supported equivalent intracellular growth at 4 (data not shown) and 8 h pi (Fig 2.5B).

Caspase-7 cleavage

Two million BMDM were plated in 60mm dishes 18 h prior to infection. Cells were infected at MOI5 for 30 minutes, after which the inoculum was removed, cells washed with PBS and replaced with media containing 10 µg/ml gentamicin. For samples infected at MOI1, cells were spun at 1200 rpm for 3 min to maximize the population of infected cells, after which the inoculum was removed, cells washed, and antibiotic-free media replaced. At 30 min pi, cells were washed again and 10 µg/ml gentamicin was added to inhibit extracellular bacterial replication. At 8 h pi cells were lysed in buffer containing 1% NP-40 on ice for 15 minutes and then spun at 13,000 rpm for 10 min to pellet the insoluble fraction. Soluble fractions were separated by SDS-PAGE, transferred to nitrocellulose membrane, and probed with anti-caspase-7 antibody. Membranes were incubated and treated according to the antibody manufacturer instructions. Membranes from individual gels were cut to optimize exposure times for the cleaved and full-length forms of the protein. Bands were visualized using West Femto chemiluminescent substrate (Thermo Scientific).

Enzyme Activity Assays

For DEVDase activity assays, 4 million BMDM were plated in a 96 well format and infected according to the protocol outlined for immunoblotting. At 8 h pi, cells were exposed to the DEVDase substrate per the manufacturer's instructions (Caspase-Glo 3/7 Assay; Promega) and enzyme activity was quantified by luminometer. For LDH assays, BMDM were seeded into 96-well plates at a density of 4 million cells per plate. Prior to infection, medium was replaced with DMEM lacking phenol red. All subsequent steps were performed in this medium. Cells were infected as described above and supernatants harvested at indicated times post infection. Lactate

dehydrogenase release was quantified using the Cyttox96 Assay Kit (Promega) according to the manufacturer's instruction and quantified by spectrophotometer.

Intracellular Growth Assays

L. monocytogenes growth curves were performed according to the following protocol. Sterile glass coverslips were placed in 24 wells, onto which 4×10^6 BMDM were seeded and allowed to adhere overnight. Bacteria were added to the BMDM at MOI1 and allowed to invade for 30 minutes. The inoculum was then removed, the cells were washed three times in PBS, and fresh BMDM media was added with 50 $\mu\text{g}/\text{ml}$ gentamicin to inhibit extracellular bacterial growth. For gentamicin washout experiments, the antibiotic was removed from the cultures 2h pi, and the media was replaced every hour to limit the contribution of extracellular bacteria to intracellular CFU counts. At the indicated time points, coverslips were removed and BMDM were osmotically lysed and serially diluted to enumerate CFU. CFU were counted using the aCOLyte SuperCount (Microbiology International, Fredrick, MD) plate reader and software.

Immunofluorescence and microscopy

For TUNEL staining, BMDM were plated in 6-well format at a density of 2×10^6 cells per dish and incubated overnight. The cells were then infected according to the protocol outlined for immunoblotting and stained for DNA fragmentation per the manufacturer's instructions (Roche). For host cell permeability assays, BMDM were seeded onto square coverslips in 6 well plates at a density of 5×10^5 per well the night before infection. The day of infection, host cells were infected with *L. monocytogenes* for

30 mins, after which the cells were washed 3 times with PBS and cell medium with 10 µg/ml gentamicin was added. Gentamicin was removed from the medium at 2h pi and cells were washed once per hour with fresh media. At 8 h pi, live cells were washed twice with HBSS + 30 mM HEPES, and then stained using 1:50 rhodamine-phalloidin (Invitrogen) in HBSS + 30 mM HEPES for 15 minutes. Coverslips were rinsed using HBSS + 30 mM HEPES and fixed in 4% paraformaldehyde. After fixation, coverslips were rinsed three times in TBS + 0.1% Triton-X 100 and counterstained with DAPI. Coverslips were mounted onto slides using Prolong Anti-Fade (Invitrogen), and imaged at the Center for Live Cell Imaging (CLCI) at the University of Michigan Medical School using an Olympus BX60 upright fluorescence microscope (Olympus; Center Valley PA). Images were collected using a DP70 CCD color camera (RGB, 12-bits/channel; Olympus America Inc., Center Valley PA) using DP70 controller/manager software v3.02. Automated image analysis was performed using MetaMorph software (Molecular Devices Sunnyvale, CA).

Listeriolysin O expression, purification, and quantification

For purification of recombinant LLO, 10mL LB cultures containing 50 µg/ml kanamycin (LB Kan50) sulfate were inoculated with single colonies of *E. coli* BL21(DE3) containing plasmid pET29 that encodes for a 6xHis-tagged copy of the *hly* gene encoding Listeriolysin O (LLO) from *L. monocytogenes* strain 10403S from freshly streaked LB agar plates and incubated overnight at 37°C with constant agitation. Cultures were then used to inoculate 100ml of LB Kan50 and incubated at 30°C with constant agitation for 30 minutes. IPTG was added to cultures at a final concentration of 1mM and incubation was resumed for an additional 18 h to induce LLO expression. Protein expression

cultures were pelleted at 4000 x g for 15 min at 4°C and supernatants were discarded. Pellets were resuspended in 1ml lysis buffer (50mM sodium phosphate dibasic, 300mM sodium chloride, 10mM imidazole; pH 8.0) containing 1 mg/ml lysozyme and incubated on ice for 30 minutes. Suspensions were then subjected to 4 x 30 sec sonication treatments separated by 15 sec incubation on ice with a Misonix Microson Ultrasonic Cell Disruptor XL set to intensity 4. Lysates were centrifuged for 30 minutes at 16,000 x g at 4°C. To purify 6xHis-tagged LLO, a NiNTA spin column (Qiagen, Cat. No. 31314) was loaded with 600µl wash buffer (50mM sodium phosphate dibasic, 300mM sodium chloride, 20mM imidazole; pH 8.0) and centrifuged at 700 x g for 2 minutes; flow-through was discarded. All subsequent NiNTA spin column centrifugation steps were carried out at 700 x g for 2 minutes. Lysate supernatants were passed through the column in 600µL increments. Columns were then washed sequentially with 600µl volumes of the following: wash buffer, 84% wash buffer / 16% glycerol v/v, and wash buffer containing 700mM NaCl. 6XHis-tagged LLO was then eluted from the column with two 200µl volumes of wash buffer containing 400mM imidazole. Combined elution volumes were then passed through an Amicon Ultra 3000 MWCO filter unit by centrifugation for 30 minutes at 16,000 x g at 4°C, after which 450µl HBSE (10mM HEPES, 140mM NaCl, 1mM EDTA; pH 8.4) buffer was added to the column, briefly agitated, and collected by flipping the column and centrifuging the solution into a microcentrifuge tube at 16,000 x g for 10 seconds. Protein solutions were then separated into 50µl aliquots and stored at - 80°C. Final protein concentration was measured by Bradford assay (Thermo Scientific) using a BSA standard curve.

Statistical analysis

All p values were generated between identified samples using unpaired two-tailed t-tests and represent analysis of ≥ 3 replicates per condition. * $P < 0.05$, ** $P < 0.01$ and *** $P < 0.001$.

5. References

1. Vázquez-Boland, J. A.; Kuhn, M.; Berche, P.; Chakraborty, T.; Domínguez-Bernal, G.; Goebel, W.; González-Zorn, B.; Wehland, J.; Kreft, J. *Listeria* pathogenesis and molecular virulence determinants. *Clin. Microbiol. Rev.* **2001**, *14*, 584–640.
2. Portnoy, D. A.; Jacks, P. S.; Hinrichs, D. J. Role of hemolysin for the intracellular growth of *Listeria monocytogenes*. *J. Exp. Med.* **1988**, *167*, 1459–1471.
3. Barsig, J.; Kaufmann, S. H. The mechanism of cell death in *Listeria monocytogenes*-infected murine macrophages is distinct from apoptosis. *Infect. Immun.* **1997**, *65*, 4075–4081.
4. Shaughnessy, L. M.; Hoppe, A. D.; Christensen, K. A.; Swanson, J. A. Membrane perforations inhibit lysosome fusion by altering pH and calcium in *Listeria monocytogenes* vacuoles. *Cell. Microbiol.* **2006**, *8*, 781–792.
5. Glomski, I. J.; Gedde, M. M.; Tsang, A. W.; Swanson, J. A.; Portnoy, D. A. The *Listeria monocytogenes* hemolysin has an acidic pH optimum to compartmentalize activity and prevent damage to infected host cells. *J. Cell Biol.* **2002**, *156*, 1029–1038.
6. Glomski, I. J.; Decatur, A. L.; Portnoy, D. A. *Listeria monocytogenes* mutants that fail to compartmentalize listeriolysin O activity are cytotoxic, avirulent, and unable to evade host extracellular defenses. *Infect. Immun.* **2003**, *71*, 6754–6765.
7. Schnupf, P.; Portnoy, D. A.; Decatur, A. L. Phosphorylation, ubiquitination and degradation of listeriolysin O in mammalian cells: role of the PEST-like sequence. *Cell. Microbiol.* **2006**, *8*, 353–364.
8. Torres, D.; Barrier, M.; Bihl, F.; Quesniaux, V. J. F.; Maillet, I.; Akira, S.; Ryffel, B.; Erard, F. Toll-like receptor 2 is required for optimal control of *Listeria monocytogenes* infection. *Infect. Immun.* **2004**, *72*, 2131–2139.
9. Park, J.-H.; Kim, Y.-G.; Shaw, M.; Kanneganti, T.-D.; Fujimoto, Y.; Fukase, K.; Inohara, N.; Núñez, G. Nod1/RICK and TLR signaling regulate chemokine and antimicrobial innate immune responses in mesothelial cells. *J. Immunol.* **2007**, *179*, 514–521.
10. Way, S. S.; Thompson, L. J.; Lopes, J. E.; Hajjar, A. M.; Kollmann, T. R.; Freitag, N. E.; Wilson, C. B. Characterization of flagellin expression and its role in *Listeria monocytogenes* infection and immunity. *Cell. Microbiol.* **2004**, *6*, 235–242.
11. Hayashi, F.; Smith, K. D.; Ozinsky, A.; Hawn, T. R.; Yi, E. C.; Goodlett, D. R.; Eng, J. K.; Akira, S.; Underhill, D. M.; Aderem, A. The innate immune response to bacterial flagellin is mediated by Toll-like receptor 5. *Nature* **2001**, *410*, 1099–1103.
12. Kim, Y.-G.; Park, J.-H.; Shaw, M. H.; Franchi, L.; Inohara, N.; Núñez, G. The cytosolic sensors Nod1 and Nod2 are critical for bacterial recognition and host defense after exposure to Toll-like receptor ligands. *Immunity* **2008**, *28*, 246–257.

13. Fink, S. L.; Cookson, B. T. Apoptosis, pyroptosis, and necrosis: mechanistic description of dead and dying eukaryotic cells. *Infect. Immun.* **2005**, *73*, 1907–1916.
14. Dinarello, C. A. Biologic basis for interleukin-1 in disease. *Blood* **1996**, *87*, 2095–2147.
15. Dinarello, C. A. IL-18: A TH1-inducing, proinflammatory cytokine and new member of the IL-1 family. *J. Allergy Clin. Immunol.* **1999**, *103*, 11–24.
16. Thornberry, N. A.; Bull, H. G.; Calaycay, J. R.; Chapman, K. T.; Howard, A. D.; Kostura, M. J.; Miller, D. K.; Molineaux, S. M.; Weidner, J. R.; Aunins, J. A novel heterodimeric cysteine protease is required for interleukin-1 beta processing in monocytes. *Nature* **1992**, *356*, 768–774.
17. Warren, S. E.; Mao, D. P.; Rodriguez, A. E.; Miao, E. A.; Aderem, A. Multiple Nod-like receptors activate caspase 1 during *Listeria monocytogenes* infection. *J. Immunol.* **2008**, *180*, 7558–7564.
18. Wu, J.; Fernandes-Alnemri, T.; Alnemri, E. S. Involvement of the AIM2, NLRC4, and NLRP3 Inflammasomes in Caspase-1 Activation by *Listeria monocytogenes*. *J Clin Immunol* **2010**, *30*, 693–702.
19. Rathinam, V. A. K.; Jiang, Z.; Waggoner, S. N.; Sharma, S.; Cole, L. E.; Waggoner, L.; Vanaja, S. K.; Monks, B. G.; Ganesan, S.; Latz, E.; Hornung, V.; Vogel, S. N.; Szomolanyi-Tsuda, E.; Fitzgerald, K. A. The AIM2 inflammasome is essential for host defense against cytosolic bacteria and DNA viruses. *Nat. Immunol.* **2010**, *11*, 395–402.
20. Sauer, J.-D.; Witte, C. E.; Zemansky, J.; Hanson, B.; Lauer, P.; Portnoy, D. A. *Listeria monocytogenes* triggers AIM2-mediated pyroptosis upon infrequent bacteriolysis in the macrophage cytosol. *Cell Host and Microbe* **2010**, *7*, 412–419.
21. Tsuji, N. M.; Tsutsui, H.; Seki, E.; Kuida, K.; Okamura, H.; Nakanishi, K.; Flavell, R. A. Roles of caspase-1 in *Listeria* infection in mice. *Int. Immunol.* **2004**, *16*, 335–343.
22. Gurcel, L.; Abrami, L.; Girardin, S.; Tschopp, J.; van der Goot, F. G. Caspase-1 activation of lipid metabolic pathways in response to bacterial pore-forming toxins promotes cell survival. *Cell* **2006**, *126*, 1135–1145.
23. Alnemri, E. S.; Livingston, D. J.; Nicholson, D. W.; Salvesen, G.; Thornberry, N. A.; Wong, W. W.; Yuan, J. Human ICE/CED-3 protease nomenclature. *Cell* **1996**, *87*, 171.
24. Denault, J.-B.; Salvesen, G. S. Human caspase-7 activity and regulation by its N-terminal peptide. *J. Biol. Chem.* **2003**, *278*, 34042–34050.
25. Lakhani, S. A.; Masud, A.; Kuida, K.; Porter, G. A.; Booth, C. J.; Mehal, W. Z.; Inayat, I.; Flavell, R. A. Caspases 3 and 7: key mediators of mitochondrial events of apoptosis. *Science* **2006**, *311*, 847–851.
26. Duan, H.; Chinnaiyan, A. M.; Hudson, P. L.; Wing, J. P.; He, W. W.; Dixit, V. M. ICE-LAP3, a novel mammalian homologue of the *Caenorhabditis elegans* cell death protein

Ced-3 is activated during Fas- and tumor necrosis factor-induced apoptosis. *J. Biol. Chem.* **1996**, *271*, 1621–1625.

27. Strasser, A.; Jost, P. J.; Nagata, S. The many roles of FAS receptor signaling in the immune system. *Immunity* **2009**, *30*, 180–192.

28. Lamkanfi, M.; Kanneganti, T.-D.; Van Damme, P.; Vanden Berghe, T.; Vanoverberghe, I.; Vandekerckhove, J.; Vandenabeele, P.; Gevaert, K.; Núñez, G. Targeted peptidecentric proteomics reveals caspase-7 as a substrate of the caspase-1 inflammasomes. *Mol. Cell Proteomics* **2008**, *7*, 2350–2363.

29. Akhter, A.; Gavrilin, M. A.; Frantz, L.; Washington, S.; Ditty, C.; Limoli, D.; Day, C.; Sarkar, A.; Newland, C.; Butchar, J.; Marsh, C. B.; Wewers, M. D.; Tridandapani, S.; Kanneganti, T.-D.; Amer, A. O. Caspase-7 activation by the Nlrc4/Ipafl inflammasome restricts *Legionella pneumophila* infection. *PLoS Pathog* **2009**, *5*, e1000361.

30. Demon, D.; Van Damme, P.; Vanden Berghe, T.; Deceuninck, A.; Van Durme, J.; Verspurten, J.; Helsens, K.; Impens, F.; Wejda, M.; Schymkowitz, J.; Rousseau, F.; Madder, A.; Vandekerckhove, J.; Declercq, W.; Gevaert, K.; Vandenabeele, P. Proteome-wide substrate analysis indicates substrate exclusion as a mechanism to generate caspase-7 versus caspase-3 specificity. *Mol. Cell Proteomics* **2009**, *8*, 2700–2714.

31. Boatright, K. M.; Salvesen, G. S. Mechanisms of caspase activation. *Curr. Opin. Cell Biol.* **2003**, *15*, 725–731.

32. Srinivasula, S. M.; Poyet, J.-L.; Razmara, M.; Datta, P.; Zhang, Z.; Alnemri, E. S. The PYRIN-CARD protein ASC is an activating adaptor for caspase-1. *J. Biol. Chem.* **2002**, *277*, 21119–21122.

33. Huston, J. S.; Fish, W. W.; Mann, K. G.; Tanford, C. Studies on the subunit molecular weight of beef heart lactate dehydrogenase. *Biochemistry* **1972**, *11*, 1609–1612.

34. Heuck, A. P.; Tweten, R. K.; Johnson, A. E. Assembly and topography of the prepore complex in cholesterol-dependent cytolysins. *J. Biol. Chem.* **2003**, *278*, 31218–31225.

35. Schuerch, D. W.; Wilson-Kubalek, E. M.; Tweten, R. K. Molecular basis of listeriolysin O pH dependence. *Proc. Natl. Acad. Sci. U.S.A.* **2005**, *102*, 12537–12542.

36. Schnupf, P.; Portnoy, D. A. Listeriolysin O: a phagosome-specific lysin. *Microbes and Infection* **2007**, *9*, 1176–1187.

37. Zwaferink, H.; Stockinger, S.; Hazemi, P.; Lemmens-Gruber, R.; Decker, T. IFN- β increases listeriolysin O-induced membrane permeabilization and death of macrophages. *J. Immunol.* **2008**, *180*, 4116–4123.

38. Bavek, A.; Gekara, N. O.; Priselac, D.; Gutiérrez Aguirre, I.; Darji, A.; Chakraborty, T.; Maček, P.; Lakey, J. H.; Weiss, S.; Anderluh, G. Sterol and pH interdependence in the binding, oligomerization, and pore formation of listeriolysin O. *Biochemistry* **2007**, *46*, 4425–4437.

39. Villanueva, M. S.; Sijts, A. J.; Pamer, E. G. Listeriolysin is processed efficiently into an MHC class I-associated epitope in *Listeria monocytogenes*-infected cells. *J. Immunol.* **1995**, *155*, 5227–5233.
40. Dancz, C. E.; Haraga, A.; Portnoy, D. A.; Higgins, D. E. Inducible control of virulence gene expression in *Listeria monocytogenes*: temporal requirement of listeriolysin O during intracellular infection. *J. Bacteriol.* **2002**, *184*, 5935–5945.
41. Jones, S.; Portnoy, D. A. Characterization of *Listeria monocytogenes* pathogenesis in a strain expressing perfringolysin O in place of listeriolysin O. *Infect. Immun.* **1994**, *62*, 5608–5613.
42. Girardin, S. E.; Boneca, I. G.; Carneiro, L. A. M.; Antignac, A.; Jéhanno, M.; Viala, J.; Tedin, K.; Taha, M.-K.; Labigne, A.; Zähringer, U.; Coyle, A. J.; DiStefano, P. S.; Bertin, J.; Sansonetti, P. J.; Philpott, D. J. Nod1 detects a unique muropeptide from gram-negative bacterial peptidoglycan. *Science* **2003**, *300*, 1584–1587.
43. Thelestam, M.; Möllby, R. Survival of cultured cells after functional and structural disorganization of plasma membrane by bacterial haemolysins and phospholipases. *Toxicon* **1983**, *21*, 805–815.
44. Walev, I.; Palmer, M.; Martin, E.; Jonas, D.; Weller, U.; Höhn-Bentz, H.; Husmann, M.; Bhakdi, S. Recovery of human fibroblasts from attack by the pore-forming alpha-toxin of *Staphylococcus aureus*. *Microb. Pathog.* **1994**, *17*, 187–201.
45. Valeva, A.; Walev, I.; Gerber, A.; Klein, J.; Palmer, M.; Bhakdi, S. Staphylococcal alpha-toxin: repair of a calcium-impermeable pore in the target cell membrane. *Mol. Microbiol.* **2000**, *36*, 467–476.
46. Haslinger, B.; Strangfeld, K.; Peters, G.; Schulze-Osthoff, K.; Sinha, B. *Staphylococcus aureus* alpha-toxin induces apoptosis in peripheral blood mononuclear cells: role of endogenous tumour necrosis factor-alpha and the mitochondrial death pathway. *Cell. Microbiol.* **2003**, *5*, 729–741.
47. Bantel, H.; Sinha, B.; Domschke, W.; Peters, G.; Schulze-Osthoff, K.; Jänicke, R. U. alpha-Toxin is a mediator of *Staphylococcus aureus*-induced cell death and activates caspases via the intrinsic death pathway independently of death receptor signaling. *J. Cell Biol.* **2001**, *155*, 637–648.
48. Pai, J. T.; Brown, M. S.; Goldstein, J. L. Purification and cDNA cloning of a second apoptosis-related cysteine protease that cleaves and activates sterol regulatory element binding proteins. *Proc. Natl. Acad. Sci. U.S.A.* **1996**, *93*, 5437–5442.
49. Gibot, L.; Follet, J.; Metges, J.-P.; Auvray, P.; Simon, B.; Corcos, L.; Le Jossic-Corcos, C. Human caspase 7 is positively controlled by SREBP-1 and SREBP-2. *Biochem. J.* **2009**, *420*, 473–483.
50. Wang, X.; Sato, R.; Brown, M. S.; Hua, X.; Goldstein, J. L. SREBP-1, a membrane-bound transcription factor released by sterol-regulated proteolysis. *Cell* **1994**, *77*, 53–62.

51. Srikanth, C. V.; Wall, D. M.; Maldonado-Contreras, A.; Shi, H. N.; Zhou, D.; Demma, Z.; Mummy, K. L.; McCormick, B. A. *Salmonella* pathogenesis and processing of secreted effectors by caspase-3. *Science* **2010**, *330*, 390–393.
52. Arpaia, N.; Godec, J.; Lau, L.; Sivick, K. E.; McLaughlin, L. M.; Jones, M. B.; Dracheva, T.; Peterson, S. N.; Monack, D. M.; Barton, G. M. TLR signaling is required for *Salmonella typhimurium* virulence. *Cell* **2011**, *144*, 675–688.
53. Majerciak, V.; Kruhlak, M.; Dagur, P. K.; McCoy, J. P.; Zheng, Z.-M. Caspase-7 cleavage of Kaposi sarcoma-associated herpesvirus ORF57 confers a cellular function against viral lytic gene expression. *J. Biol. Chem.* **2010**, *285*, 11297–11307.
54. Vance, R. E.; Isberg, R. R.; Portnoy, D. A. Patterns of Pathogenesis: Discrimination of Pathogenic and Nonpathogenic Microbes by the Innate Immune System. *Cell Host and Microbe* **2009**, *6*, 10–21.
55. Idone, V.; Tam, C.; Goss, J. W.; Toomre, D.; Pypaert, M.; Andrews, N. W. Repair of injured plasma membrane by rapid Ca²⁺-dependent endocytosis. *J. Cell Biol.* **2008**, *180*, 905–914.
56. Walev, I.; Bhakdi, S. C.; Hofmann, F.; Djonder, N.; Valeva, A.; Aktories, K.; Bhakdi, S. Delivery of proteins into living cells by reversible membrane permeabilization with streptolysin-O. *Proc. Natl. Acad. Sci. U.S.A.* **2001**, *98*, 3185–3190.
57. Broughton, C. M.; Spiller, D. G.; Pender, N.; Komorovskaya, M.; Grzybowski, J.; Giles, R. V.; Tidd, D. M.; Clark, R. E. Preclinical studies of streptolysin-O in enhancing antisense oligonucleotide uptake in harvests from chronic myeloid leukaemia patients. *Leukemia* **1997**, *11*, 1435–1441.
58. Reddy, A.; Caler, E. V.; Andrews, N. W. Plasma membrane repair is mediated by Ca²⁺-regulated exocytosis of lysosomes. *Cell* **2001**, *106*, 157–169.
59. Bischof, L. J.; Kao, C.-Y.; Los, F. C. O.; Gonzalez, M. R.; Shen, Z.; Briggs, S. P.; van der Goot, F. G.; Aroian, R. V. Activation of the unfolded protein response is required for defenses against bacterial pore-forming toxin *in vivo*. *PLoS Pathog* **2008**, *4*, e1000176.
60. Pillich, H.; Loose, M.; Zimmer, K.-P.; Chakraborty, T. Activation of the unfolded protein response by *Listeria monocytogenes*. *Cell. Microbiol.* **2012**, *14*, 949–964.

Chapter 3

Transient activation of caspase-7 promotes blebbing and survival in response to damage by pore-forming toxins (in collaboration with Marie-Ève Charbonneau)

Abstract: The plasma membrane of the mammalian cell is able to withstand damage caused by sub-lytic concentrations of pore-forming toxins, but how the membrane orchestrates damage control is incompletely understood. Recent work demonstrated that cells bleb and ectocytose (release or shedding of blebbed vesicles) damaged membrane to survive treatment with the cholesterol-dependent cytolysin (CDC) streptolysin O, but the molecular mechanisms that license toxin-induced blebbing were not identified. Here we report that macrophages treated with the related CDC, listeriolysin O, bleb via a mechanism that requires transient activation of the cysteine protease, caspase-7. Caspase-7 activation was protective during intoxication, as cells lacking this protease displayed altered blebbing, were more permeable to small dyes, and more likely to succumb after toxin treatment. Toxin-induced caspase-7 activity contributed to the cleavage of ROCK I, a Rho kinase that orchestrates the rearrangement of cytoskeletal actin. Inhibition of rho kinases or myosin II, an ATP-dependent motor protein activated by ROCK I that coordinates cell contractility, resulted in decreased blebbing in response to LLO, and increased susceptibility to intoxication. Therefore, our data support a model whereby transient caspase-7 activity orchestrates cytoskeletal remodeling

through Rho kinases and myosin II to promote membrane blebbing and increased survival in response to pore-forming damage.

1. Introduction

Membrane damage of host cells is a common hallmark of pathogenesis. Many viruses, intracellular bacteria, and parasites must breach the plasma membrane to gain access to the intracellular compartment, to egress from the infected cell, or both. Extracellular pathogens often secrete membrane-damaging agents, such as pore-forming toxins, that can elicit a broad range of outcomes for both infectious agent and host. The cholesterol-dependent cytolysins (CDCs) are a family of PFTs produced primarily by Gram-positive bacteria. CDC monomers oligomerize on target cells to form pores capable of allowing the influx of large molecules, such as antibodies, into the cytosol [1]. When intoxicated at low concentrations with CDCs, survival of host cells is well documented, although at higher concentrations intoxication can result in host cell lysis. CDCs have been used for selective permeabilization of cells, and wounds caused by CDCs can be rapidly resealed [1-3]. We previously discovered that a cysteine protease, caspase-7, was activated in response to PFT damage by various toxins and was important for promoting membrane fidelity after this insult [4]. However, the role of caspase-7 in promoting membrane integrity is not known. How damaged cells reseal the plasma membrane is an active area of investigation, and multiple mechanisms have been proposed to explain repair methods. One such mechanism of promoting barrier maintenance after PFT injury is through ectocytosis of damaged sections of membranes via the formation of membrane blebs.

Membrane blebbing was first characterized as a morphological feature of apoptosis [5]. Notably, blebbing is also critical for functions not associated with cell death, such as cytokinesis and cell motility [6]. Under resting conditions, the plasma membrane is attached to the actin cortical cytoskeleton, which provides rigidity and structure to the cell. Blebs are rounded protrusions that occur when the connection between the cortex

and the membrane is perturbed. The spherical shape of the bleb depends on cytosolic hydrostatic pressure and contraction of the actinomyosin cortex [7], and as such the formation of membrane blebs is a tightly regulated event. Much of the information on the molecular players that drive blebbing comes from studies on the execution phase of apoptosis and the cytoskeletal changes that occur during this process.

Blebbing can also promote cell healing and survival after treatment with PFTs. Cells blebbed when treated with the CDC, streptolysin O (SLO), and chemical inhibition of blebbing sensitized the cells to toxin-induced lysis [8]. By monitoring Ca^{2+} flux during PFT damage, Babiychuck *et al* suggested that blebbing protected CDC-treated cells by sequestering the damaged membrane, which was isolated from the cytoplasm via the formation of a plug composed of annexin A1, a membrane-binding Ca^{2+} -sensing protein, at the neck of the bleb [8]. SLO-mediated membrane damage also induced bleb shedding, or ectocytosis [9,10]. Ectosomes were enriched for SLO compared to the cell body [9], which suggests that blebbing and shedding may be a mechanism by which cells expel both toxin and damaged membrane. The molecular mechanisms that orchestrate blebbing and shedding in response to toxin damage were not determined. Based on our previous work which shows that caspase-7 promotes membrane integrity after pore-formation [4], we hypothesize that caspase-7 activity may regulate blebbing and shedding response to PFT treatment.

In this study we determine that intoxication of cells with the CDC listeriolysin O (LLO) results in transient activation of caspase-7, which correlates with the recovery of membrane integrity after pore-formation. Inhibition of rho-kinases and myosin II also decreased blebbing during intoxication and decreased survival rates of intoxicated cells. Thus, we have uncovered a mechanism where by the transient activation of an

“executioner caspase” directs a signaling cascade that promotes cell survival instead of programmed cell death. We speculate that this example of transient activation of caspase-7 reflects a broader paradigm of “signal strength”, whereby high levels of caspase-7 activity promote programmed cell death, but low-level activation triggers an adaptive response resulting in improved cell survival. Thus, the amount of signaling sensed provides context to tailor the appropriate cellular response.

2. Results

Caspase-7 is transiently activated and protective in response to damage by pore-forming toxins

We previously demonstrated that primary bone marrow-derived macrophages (BMDMs) activate caspase-7 in response to exogenous treatment with purified PFT toxin, listeriolysin O (LLO), in the absence of programmed cell death [4]. To address how caspase-7 activity could occur in the absence of apoptosis, we questioned whether PFT-induced caspase-7 activation was transient, which could explain why programmed cell death was not measured under these conditions. We treated RAW 264.7 cells (RAW cells) with a sub-lytic concentration (0.3 μ g/ml) of purified LLO for 1 h. The sub-lytic concentration of LLO is defined as the amount at which we measure approximately 10% LDH release after 1 h of treatment. After incubation with LLO, cell lysates were harvested and probed for the cleavage of caspase-7 via immunoblot using an antibody that recognizes both the full length protein and the larger cleavage product (Fig 3.1A). We observed cleavage of caspase-7 1 h after toxin treatment, and increased cleavage after 2 and 3 h of toxin treatment. To assess the fate of caspase-7 cleavage after toxin treatment, we pulsed RAW cells with toxin for 1 h, replaced with fresh media, and monitored the cleavage of caspase-7 at the indicated times post toxin pulse. We measured the percentage of cleaved caspase-7 in each sample against the total amount of signal from each lane of the immunoblot using ImageJ and combined the results from three separate experiments (Fig 3.1B). We found that the abundance of cleaved caspase-7 increased after 1 h of toxin treatment and that the amount of cleaved protease increased when RAW cells were exposed to LLO for longer periods of time (2 or 3 hours) (Fig 3.1A and B). Interestingly, when we incubated cells with LLO for 1 h, then

Figure 3.1

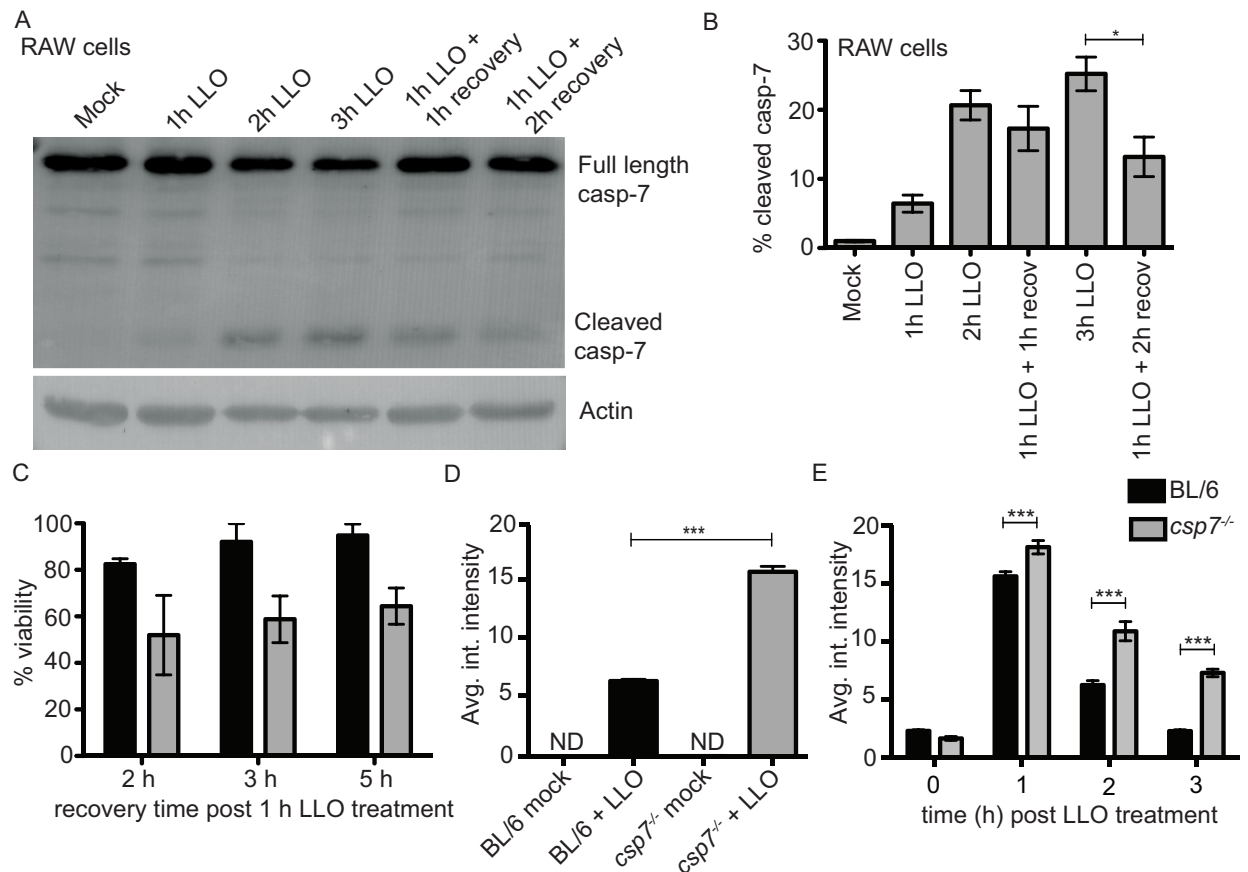


Figure 3.1 Transient caspase-7 activity promotes survival and membrane integrity in LLO-intoxicated cells. (A) RAW macrophages were incubated continuously with 0.3 $\mu\text{g}/\text{ml}$ LLO for 1, 2, or 3 h, or for 1 h, washed and allowed to recover in fresh media. Cells were then lysed and probed for caspase-7 cleavage and actin. (B) The percentage of cleaved caspase-7 in RAW cells using methods as in (A) was measured from the total signal in each lane using ImageJ. The graph includes the percentages calculated from three separate experiments. $P = 0.033$. (C) Viability of BMDMs, as measured by the metabolic marker WST-1, after 1 h intoxication with 0.25 $\mu\text{g}/\text{ml}$ LLO, and the noted recovery period. Data were combined from three independent experiments. * $P < 0.04$ and ** $P = 0.003$ using Student's t-test. (D) Average integrated intensity, as measured by Metamorph, of BL/6 and *csp7*^{-/-} BMDMs incubated with 0.5 $\mu\text{g}/\text{ml}$ LLO and rhodamine-phalloidin (rho-phall) for 15 min. ND = none detected, $N > 200$ cells, $P < 0.0001$ by Student's t-test. Error bars are SEM. (E) Rhodamine-phalloidin permeability after 1 h exposure to 0.25 $\mu\text{g}/\text{ml}$ LLO, and replacement with fresh media. $N < 130$ and $P < 0.0004$ for each condition by Students' t-test. (D, E) are representative of three independent experiments. (A-C and E) were performed and analyzed by MEC. the toxin removed and assessed cleavage of caspase-7 1 h later (1 h LLO + 1 h recovery),

we consistently saw an increase in signal over 1 h treatment alone that decreased 2 h after toxin removal (Fig 3.1A and B). Similarly, we saw transient caspase-7 activation when we pulsed BMDMs with sub-lytic LLO (0.25 μ g/ml) for 1 h and monitored the abundance of caspase-7 cleavage over time (Fig. A8). We considered the possibility that loss of cleaved caspase signal over time could be due to death of cells in which caspase-7 was activated. However, the amount of actin present in the cell lysates was equal over time, which is inconsistent with the hypothesis that cell loss was responsible for the loss of caspase-7 cleavage signal. Instead, these results suggest that caspase-7 is transiently activated in RAW cells and BMDMs in response to PFT treatment.

To determine if the activation of caspase-7 was promoting survival of intoxicated cells, we pulsed either BL/6 or *csp7^{-/-}* BMDMs with a sub-lytic concentration of LLO for 1 h, removed the toxin and replaced with fresh medium and monitored the viability of cells over time using the tetrazolium salt WST-1. WST-1 is reduced to a dye, formazan, by a mechanism that depends on the production of NAD(P)H in viable cells. Therefore, the amount of formazan dye formed from WST-1 directly correlates with the metabolic state of the cell culture. When compared to untreated cells, we measured a 15% decrease in formazan conversion in BL/6 cells 2 h after LLO was removed from the culture media (Fig 3.1C). However, at 3 and 5 h after toxin removal, formazan conversion was near untreated levels (mean of 92% and 95% respectively) (Fig 3.1C). Using our experimental conditions, BMDMs are not likely to divide significantly in the tested time period. Therefore, we hypothesize that cell division is not responsible for the increase in viability we see at 3 and 5 h compared to 2 h post intoxication. More likely, intoxication induces partial and transient metabolic quiescence, which has been documented for LLO intoxication by others [11]. When *csp7^{-/-}* cells were exposed to the

same concentration of LLO for 1 h, we observed a much sharper decrease (mean 52%) in metabolic activity 2 h after toxin removal (Fig 3.1C). LLO-treated *csp7^{-/-}* cells displayed significantly lower metabolic activity compared to BL/6 BMDMs at all times measured (Fig 3.1C). We measured no difference in the metabolic activity of untreated *csp7^{-/-}* and BL/6 cells. These data indicate that the *csp7^{-/-}* macrophages are more sensitive to LLO treatment, and less able to recover post-intoxication.

Previously we demonstrated that macrophages isolated from *csp7^{-/-}* mice were more permeable to small molecules during infection with *Listeria monocytogenes* compared to BL/6 macrophages [4]. However, whether *csp7^{-/-}* macrophages were more permeable during LLO intoxication was not determined. To address this, we treated BL/6 and *csp7^{-/-}* macrophages with LLO and assessed their permeability to the small fluorescent dye, rhodamine-phalloidin (rho-phall), for 15 minutes. Phalloidin is cell impermeant, but if the plasma membrane barrier is disrupted, it can diffuse into the cell and irreversibly bind to filamentous actin. We measured the amount of rho-phall that diffused into the cells during a 15 min treatment with LLO using quantitative Metamorph software analysis of fluorescent micrographs. We discovered that the *csp7^{-/-}* cells allowed more rho-phall into the cytosol during our 15 min toxin incubation compared to the BL/6 cells (Fig 3.1D). We also wanted to determine how long after toxin treatment these cells would remain sensitive to phalloidin influx. To test this, we treated cells with LLO for 1 h, removed the toxin and replaced with fresh media, and then stained with phalloidin at varying times after toxin removal. We found that the *csp7^{-/-}* allowed more phalloidin into the cytosol after 2 and 3 post intoxication compared to BL/6 cells (Fig 3.1E and Fig A9). This result, combined with Fig 3.1D, suggests that caspase-7 deficiency allows increased initial permeability in response to LLO treatment, and delays the ability of cells to become refractory to small molecule influx. Together,

these results suggest that transient activation of caspase-7 promotes cell integrity after PFT damage.

LLO damage stimulates rapid blebbing mediated by caspase-7

Our previous results suggested that caspase-7 plays a role in damage control in response to treatment with LLO. To determine if there exist differences in the way *csp7^{-/-}* and BL/6 BMDMs physically respond to treatment with exogenous LLO, we used live cell imaging to monitor the behavior of intoxicated cells over time. We included in the medium a cell impermeant fluorescent marker, SYTOX green, which upon binding nucleic acids increases in fluorescence >500 fold, as an indicator of when cells first experience membrane damage. We observed that BL/6 BMDMs treated with sub-lytic LLO rapidly blebbed (solid arrows) and ectocytosed (solid arrowhead) after becoming permeable, as measured by SYTOX green positivity (Fig 3.2A). These results are consistent with the results of others who have used a related CDC, SLO, to studying blebbing and ectocytosis in response to toxin-derived damage [8,9]. We observed that the blebs that formed on the membrane were highly dynamic; some blebs resolved quickly, while others continued to grow throughout the time course of the experiment (see the third and fourth panels of Fig 3.2A). Every BL/6 BMDM monitored using live cell imaging blebbed in response to toxin treatment. The amount of time between membrane breach (as measured by SYTOX positivity) and first bleb was consistent among cells (average ~180 sec) (Fig 3.2C). When we monitored the response to toxin in the *csp7^{-/-}* cells, however, we observed very different behavior. The *csp7^{-/-}* cells became initially permeable after the addition of toxin with similar kinetics to BL/6 cells. However, they were far less likely to bleb; only 40% *csp7^{-/-}* cells blebbed within 30

Figure 3.2

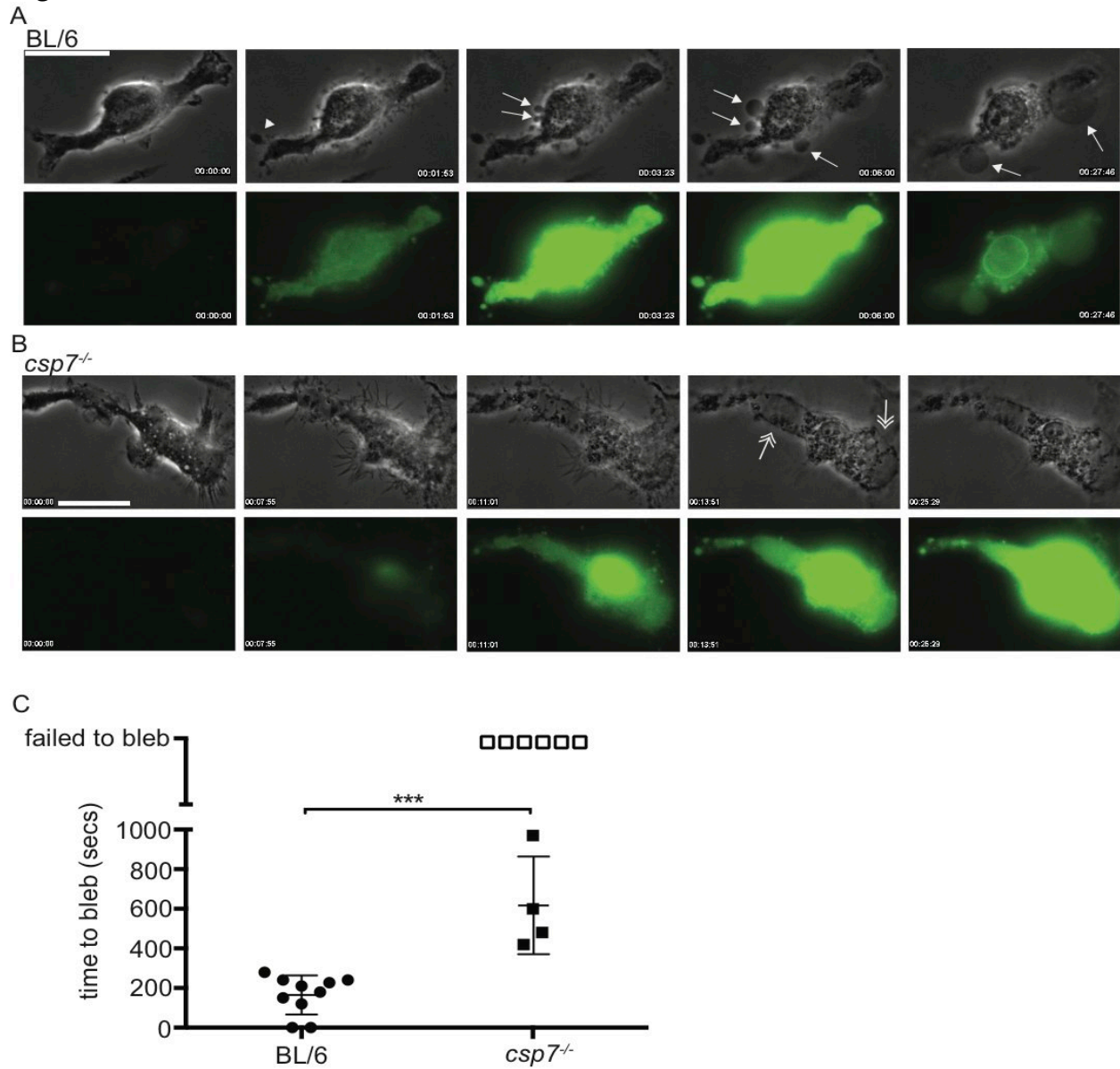


Figure 3.2. *Csp7^{-/-}* cells display altered blebbing compared to BL/6 cells in response to LLO treatment. (A) and (B) Micrographs were taken at time 0 before addition of LLO (far left panels). LLO was added at a working concentration of 0.1 μ g/ml and cells were monitored for 30 min after becoming SYTOX positive. Arrowheads denotes shedding, solid arrows denote blebbing, and double-headed arrows denote swelling. Scale bar = 10 μ m. (C) The amount for time between SYTOX positivity and first bleb. *Csp7^{-/-}* cells that failed to bleb within 30 min of becoming permeable are denoted on the graph in open squares and were not included in statistical analysis. All BL/6 cells blebbed in response to toxin. N=10 for BL/6 and N=10 for *csp7^{-/-}*, combining data from at least 5 separate live cell imaging experiments. *** P = 0.0003 using Students unpaired t-test. minutes of becoming SYTOX positive, whereas 100% BL/6 cells blebbed within this

time frame (Fig 3.2C). *Csp7^{-/-}* cells that did not bleb often swelled after becoming SYTOX positive (double-headed arrows), possibly indicative of unresolved membrane damage (Fig 3.2B). Of the *csp7^{-/-}* cells that did bleb in response to toxin, they did so with much slower kinetics than the BL/6 cells. The average time between permeability to blebbing of the 4 *csp7^{-/-}* cells that blebbed was an average of ~600 sec, three times longer than the BL/6 cells (Fig 3.2C). These results demonstrate that, upon PFT-mediated damage, caspase-7 deficiency perturbs blebbing, which correlates with decreased membrane integrity and cell survival post intoxication.

ROCK I is activated by PFT damage in a caspase-dependent manner

To determine the mechanism by which caspase-7 promotes blebbing during intoxication, we questioned whether toxin-induced blebbing and apoptotic blebbing could be controlled by similar mechanisms. During apoptosis, a rho-associated kinase, ROCK I, drives blebbing in a caspase-dependent manner [12,13]. Caspase-3 activity was required to cleave the kinase, an irreversible activation event. To determine if Rho-kinases were also important for blebbing in response to toxin damage, we monitored the cleavage of ROCK I in RAW cells via immunoblot after sub-lytic intoxication with LLO. Treatment with TNF α and cyclohexamide was used as a positive control for ROCK I cleavage. We were able to detect cleavage after 2 and 3 h of intoxication with LLO (Fig 3.3 top panel). To determine if ROCK I activation was mediated by caspases during PFT damage, we pre-treated RAW cells with a caspase-3/7 inhibitor, DEVD-fmk, which irreversibly binds the active form of these enzymes. Therefore, treatment with DEVD-fmk will not inhibit caspase-3/7 cleavage, but will inhibit their proteolytic

Figure 3.3

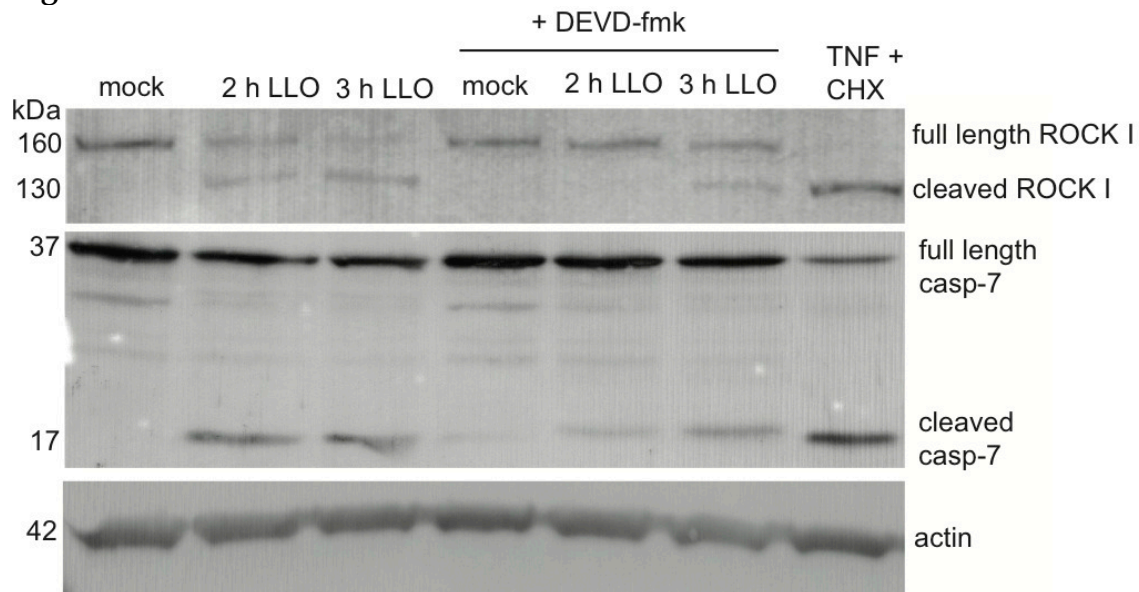


Figure 3.3. ROCK I is cleaved in a caspase-dependent manner in response to LLO damage. RAW cells were pre-incubated for 1 h with or without 100 μ M DEVD-fmk and then intoxicated for two or three hours with 0.3 μ g/ml LLO. Cells were lysed and probed for ROCK I, caspase-7, and actin via immunoblot. This blot is representative of three independent experiments, performed by MEC.

ability once cleaved. When DEVD-fmk was added to the cell media, ROCK I cleavage was no longer detected at 2h post intoxication (Fig 3.3), indicating that caspase-3/7 potentiate ROCK I cleavage in response to LLO treatment. We did, however, detect ROCK I cleavage at 3 h post intoxication, indicating that caspase-3/7 are not alone in their ability to activate ROCK I during intoxication, or that inhibition with DEVD-fmk is not complete (Fig 3.3). As expected, DEVD-fmk did not inhibit caspase-7 activation; instead a subtle size shift in the cleavage band compared to untreated lanes suggests the inhibitor did, in fact, bind the active caspase (Fig 3.3). This result demonstrates that ROCK I is cleaved in response to toxin and suggests that caspases are important in directing ROCK I cleavage.

ROCK I controls cytoskeletal contractility, and thus blebbing, through its regulation of myosin light chain (MLC). During apoptotic blebbing, Sebbagh *et al* demonstrated that caspase-3 cleavage of ROCK I was required for activation of MLC [12]. Therefore it is possible that caspase-7 directed ROCK I activation also activates MLC during toxin-induced blebbing.

Inhibition of Rho-kinases and MLC prevent blebbing in response to PFT damage

Since ROCK I activity is critical for blebbing in response to apoptotic stimuli, we tested whether Rho-kinase inhibition would limit blebbing in response to PFT damage. We pre-treated BMDMs with Y-27632 (Y27), a chemical inhibitor selective for both isoforms of ROCK (ROCK I and ROCK II) [14,15] and then monitored their ability to bleb after LLO intoxication using live cell imaging. We found that Rho-kinase inhibition significantly blunted BMDMs blebbing post intoxication (Fig 3.4A). Only 50% cells treated with Y27 blebbed after toxin treatment, and those that did blebbed with delayed kinetics after becoming permeable compared to mock treated BMDMs (Fig3.4C and D).

Figure 3.4

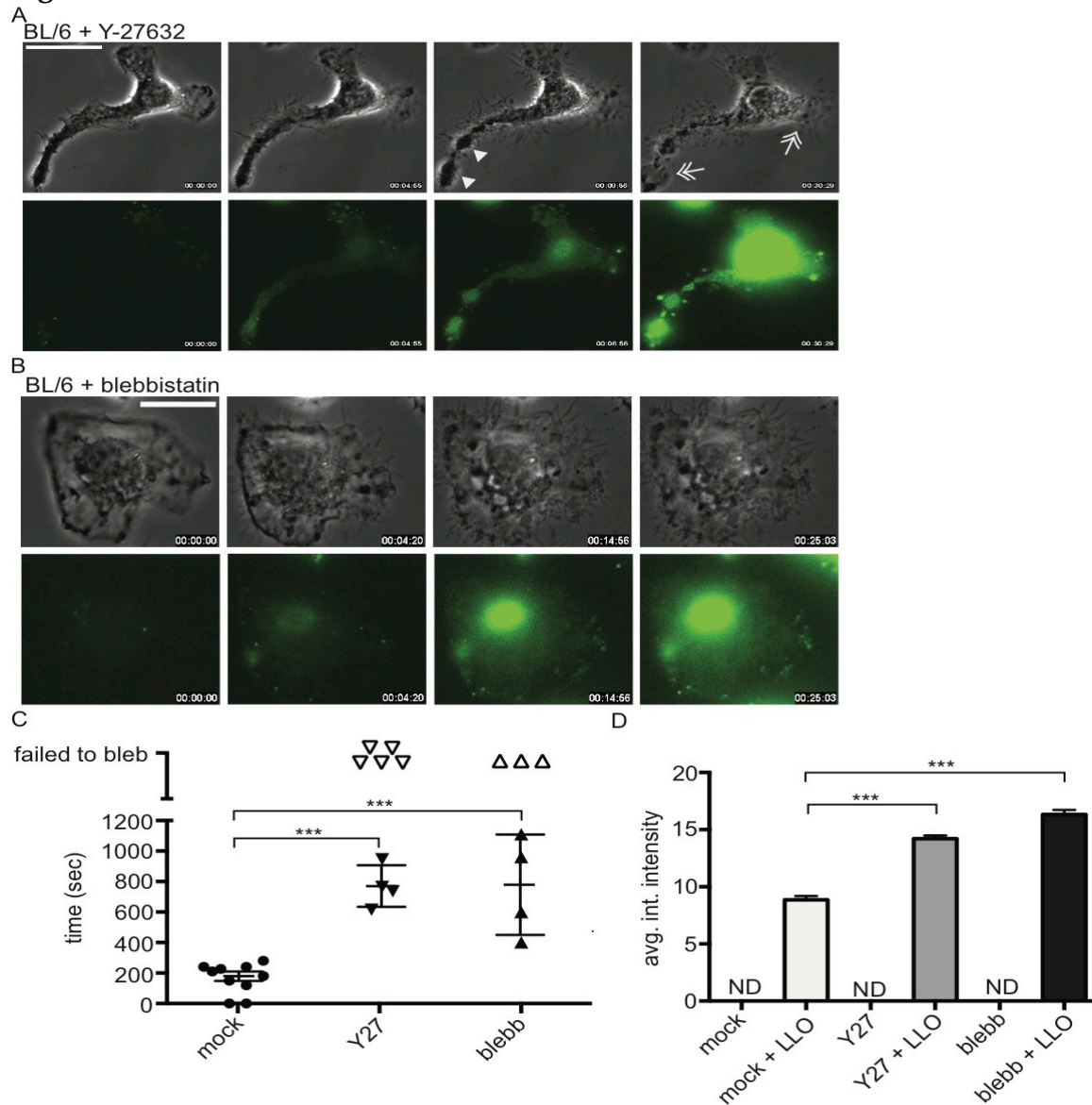


Figure 3.4. Inhibition of ROCK and myosin impedes toxin-induced blebbing. (A,B) Cells were treated with 10 μ M Y-27632 (Y27) for 2 hours (A) or 50 μ M blebbistatin (blebb) for 30 minutes (B) before visualization. Micrographs were taken at time 0 (far left) before addition of LLO at a working concentration of 0.1 μ g/ml. Cells were monitored for 30 min after becoming SYTOX positive. Solid arrowheads denote shedding and or unsuccessful blebbing, double-headed arrows denote swelling. Scale bar = 10 μ m. (C) The amount of time between SYTOX positivity and first bleb. Cells that failed to bleb within 30 min of becoming permeable are denoted on the graph in open symbols and were not included in statistical analysis. All BL/6 cells blebbed in response to toxin. N=10 for BL/6, N=9 for Y27-treated, and N=7 for blebb-treated, combining data from at least 4 separate live cell imaging experiments. (D) Permeability to rho-phall during 15 min 0.5 μ g/ml toxin treatment as assessed by Metamorph software. N>200 for each condition, representative of at least 3 independent experiments. (C,D) Error bars depict SD, $P \leq 0.0001$ for each condition compared to mock using Students' t-test.

These results suggest that Rho-kinases promote blebbing in response to PFT damage.

To determine if the proposed target of ROCK activity, myosin light chain (MLC), could also direct toxin-induced blebbing, we treated cells with a small molecule inhibitor specific for myosin II, blebbistatin [16,17], and assessed blebbing after toxin treatment using live cell imaging. Blebbistatin treatment significantly impaired the ability of cells to bleb and prolonged the time between membrane damage and blebbing, similarly to Y27 treatment and *csp7^{-/-}* deficiency (Fig 3.4B,C and D). Together these data suggest that Rho-kinases and myosin II contribute to the blebbing response after LLO-mediated damage.

To determine if inhibition of blebbing altered the ability of cells to withstand influx of small molecules during toxin damage, we pretreated cells with either Y27 or blebb and then incubated with LLO and rho-phall for 15 min. We quantified the intensity of rho-phall staining from fluorescent micrographs using Metamorph software. We found that inhibition of Rho-kinases and myosin II significantly increased the permeability of LLO intoxicated cells (Fig 3.4E). Inhibitors alone had no effect on permeability to rho-phall independent from toxin treatment (Fig 3.4E). Together, these results suggest that Rho-kinases and myosin II contribute to blebbing and membrane integrity in response to LLO-mediated damage.

Caspase-7 deficiency reduces annexin A1 aggregation in response to LLO

Blebbing in response to PFT damage has been proposed to promote the survival of intoxicated cells [8]. Babiychuk *et al* hypothesized that blebbing promoted survival by sequestering damaged membrane and separating the lesion from the cell body via the formation of a plug composed of the calcium-binding protein annexin A1 (anxA1) [8]. To determine whether the distribution of anxA1 was altered by absence of caspase-7 in

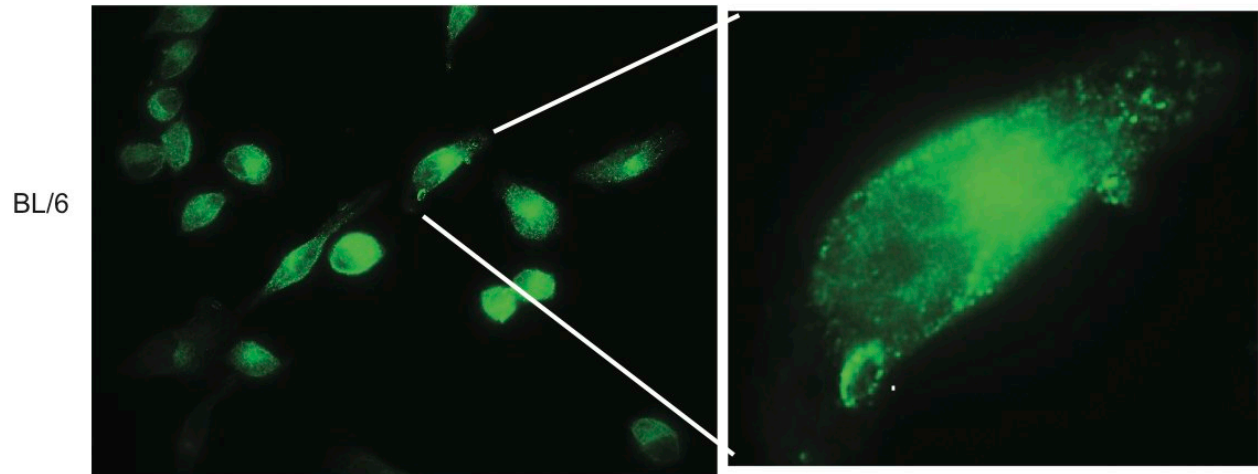
BMDMs in response to LLO, we intoxicated cells with 0.25 μ g/ml LLO for 1 h and then stained cells with a monoclonal antibody against anxA1. In un-intoxicated cells, we found the distribution of anxA1 staining was diffuse throughout the cytosol (Fig 3.5A). After 1 h of LLO treatment, most of the staining remained diffuse. However, we also noticed some aggregation of anxA1 into distinct ring-like structures in 12% of cells (Fig 3.5A and C). Given our data which suggest that most cells are permeable and bleb after this treatment with LLO (Fig 3.1 and Fig 3.2), we hypothesize that fixation and staining damages the relatively fragile blebs, and therefore, we are likely underscoring the incidence of AnxA1 aggregation due to experimental limitations. However, when we scored for the formation of anxA1 rings in the *csp7^{-/-}* cells, we counted significantly fewer rings (Fig3.5B and C), supporting our previous data that suggest *csp7^{-/-}* cells bleb less than BL/6 (Fig 3.2). Therefore, we conclude that anxA1 aggregation in response to LLO treatment is reduced in absence of caspase-7.

Rho-kinases and myosin II promote cell integrity during infection

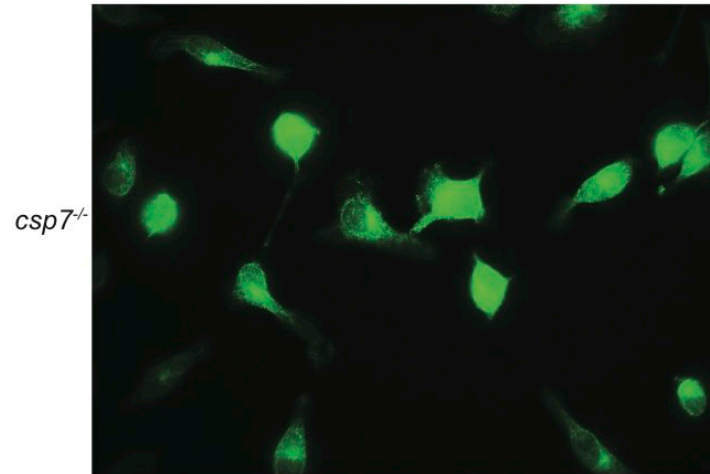
Our data establish a critical role for caspase-7, Rho-kinases, and myosin II in blebbing and survival upon damage by exogenous LLO. To assess whether this axis was important during infection with the bacterium that secretes LLO, *Listeria monocytogenes*, we infected BL/6 BMDMs at MOI 1 and allowed the infection to progress for 7.5 hours. We then added either Y27 or blebb to the cell media and incubated for an additional 30 min, after which we stained with rho-phall and scored the permeability of infected cells. Rho-kinase or myosin II inhibition significantly increased the permeability of infected cells to small molecules (Fig 3.6A). This suggests that Rho-kinases and myosin II promote cell integrity during infection with *L.*

Figure 3.5

A



B



C

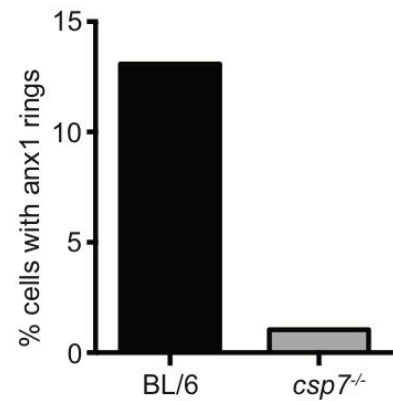


Figure 3.5. Annexin A1 aggregation is reduced in *csp7^{-/-}* BMDMs post intoxication. (A, B) BMDMs were incubated with 0.25ug/ml LLO for 1 h, after which the cells were fixed and probed with antibody specific for annexin A1 (anxA1) (Santa Cruz SC-1923-R). Cells were scored of the presence of anxA1 ring-like structures on their surface (see magnification of A). (C) Quantification of anxA1 ring like structures, N > 95 for both genotypes.

monocytogenes. To determine if ROCK I cleavage could be detected during *L. monocytogenes* infection, we infected RAW cells at an MOI 5 for 12 h and probed for both caspase-7 and ROCK I. We found that both proteins were activated under this condition (Fig 3.6B). However, infection with a strain of *L. monocytogenes* with a genetic deletion for *hly*, the gene that encodes LLO (LLO⁻), did not result in either caspase-7 or ROCK I cleavage (Fig 3.6B). To further implicate the importance of LLO in this cellular response, we infected with a strain of *L. monocytogenes* that expresses a mutant LLO protein previously reported to oligomerize with faster kinetics than endogenous LLO (L461T) [18,19]. We found that infection with this strain of bacteria increased the percentage of cleaved ROCK I compared to WT *L. monocytogenes* infection (Fig 3.6B) Taken together, these results suggest that cells activate caspase-7, ROCK I, and myosin II to promote cell integrity during infection with the pathogen, *L. monocytogenes*.

Figure 3.6

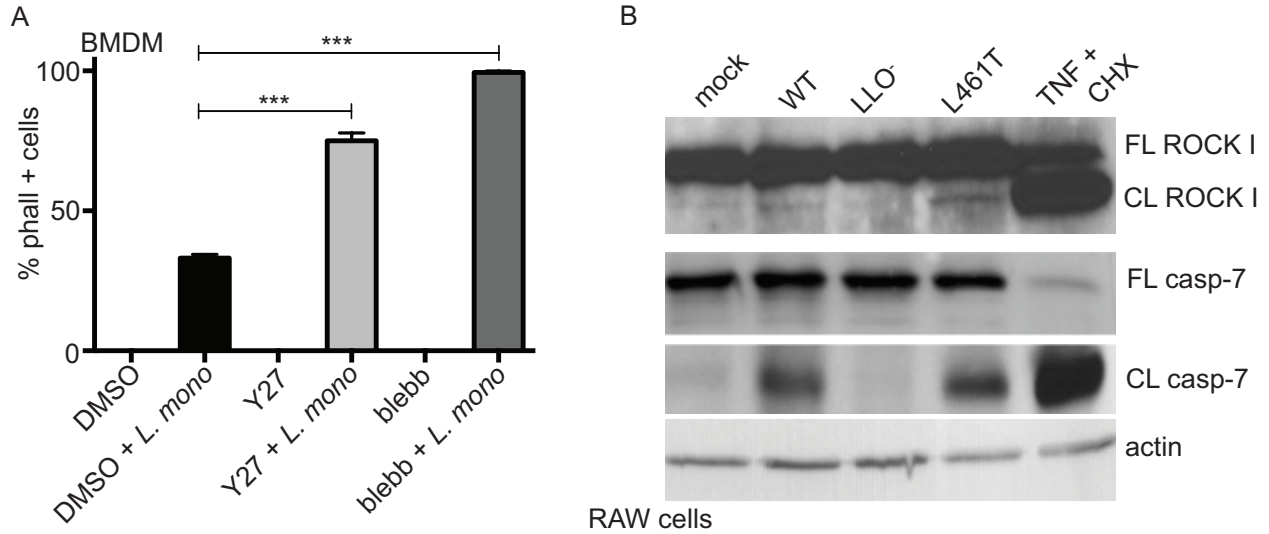


Figure 3.6. ROCK I and myosin II promote membrane fidelity during infection with *L. monocytogenes*. (A) BMDMs were infected at an MOI1 for 7.5 hours, after which 10 μ M Y-27632 or 50 μ M blebbistatin was added to the cell culture and incubated for an additional 30 min. At 8 h pi, cells were incubated with rho-phall and the total number of phall positive cells was assessed. Error bars represent SEM, N > 200 / condition, P < 0.0004 by Student's t-test, representative of two independent experiments. (B) RAW cells were infected at MOI5 with WT, LLO, or L461T *L. monocytogenes* for 12 h, after which lysates were collected for immunoblot and probed for ROCK I, caspase-7, and actin. (B) was performed by MEC.

3. Discussion

Here we find that treatment of cells with a PFT, LLO, induced blebbing in primary bone marrow derived macrophages and RAW 264.7 cells. Blebbing was mediated by caspase-7, which was transiently activated in response to LLO intoxication. Macrophages deficient in caspase-7 displayed profoundly altered blebbing: They blebbed less frequently, and blebbing was delayed compared to wild-type cells. Inability to properly bleb correlated with increased permeability to small molecules and decreased survival in response to toxin as measured by mitochondrial respiration. Macrophages from caspase-7 knock out mice were deficient in their ability to activate the rho kinase ROCK I in response to toxin treatment. Chemical inhibitors of Rho-kinases and myosin II displayed decreased toxin-induced blebbing and decreased survival post toxin treatment. These results suggest a model whereby PFT-induced damage transiently activates a caspase-7/Rho-kinase/myosin II axis to promote blebbing and survival of PFT-treated cells.

Members of the rho family of GTPases are signal transducing molecules and key regulators of the actin cytoskeleton [20]. A downstream effector activated by rho-GTPases is rho-associated kinase I, or ROCK I, which promotes cytoskeletal contractility through its regulation of myosin light chain (MLC). ROCK I activates MLC through at least two distinct mechanisms; direct phosphorylation [21], and through phosphorylation of MLC phosphatase, which promotes the constitutive activity of MLC [22,23]. ROCK I activation of MLC was necessary for the formation of blebs during the execution phase of apoptosis [12]. Notably, caspase-3 was responsible for the cleavage and irreversible activation of ROCK I under this condition, and chemical inhibition of caspase-3/7 or rho-kinases eliminated blebbing in response to apoptotic stimuli [12,13].

Thus, caspase-mediated signaling can direct the cytoskeletal rearrangement necessary to drive bleb formation during apoptosis.

Transient caspase activation can occur during cell differentiation. Transient caspase-3 activation was required for the differentiation of skeletal muscle myoblasts [24], and has been implied for other long-lived cell types, such as osteoblasts and neurons [25,26]. Caspase-3 is also necessary for the differentiation of embryonic stem cells [27] and hematopoietic cells [28]. However, the kinetics of caspase-3 inactivation was not addressed in these examples. To our knowledge, this is the first report of transient caspase-7 activation in differentiated cells.

Perhaps not surprisingly, the relative abundance of activated caspase-7 in response to sub-lytic LLO is low. The cleavage of caspase-7 increases with the amount of LLO introduced, as does the amount of LDH released (Chapter 2 and [4]), which suggests that the amount of cleaved caspase-7 may direct the fate of the affected cell. Low-level caspase-7 activation may promote cell survival by activating blebbing in response to toxin damage for example; but, increasing the amount of cleaved caspase-7 may shunt the cell into programmed cell death. An alternative hypothesis is that increased damage activates caspase-3, which then drives the cell into apoptosis.

Another method by which caspase-7 could control multiple and divergent cellular outcomes is through subcellular localization of the protease. Caspase-7 is a cytosolic protein [29], but there are published reports that link caspase-7 to particular subcellular compartments. For instance, caspase-7 may associate with the ER [30-33] (discussed in more detail below). Caspase-7 may also associate with the inflammasome [34,35]. Importantly, caspase-7 is found within TNF α multivesicular bodies [36], suggesting that some caspase-7 protein could be in close proximity to the plasma membrane. It is

attractive to speculate that the location of activated caspase-7 dictates the signal cascade activated. For instance, caspase-7 cleaved at the cell membrane could activate blebbing and survival in response to pore-formation. Localization would also allow for maximal proteolytic capacity from a relatively low abundance of active protein. We have not yet identified the subcellular location of caspase-7 activated by PFT damage. Additionally, it remains unclear how caspase-7 is activated in response to toxin.

Several reports link caspase-7 activation with the ER [30-33] and cellular calcium. Calpain, a Ca^{2+} sensing protease, can cleave and activate caspase-7 [37], and CDCs are well documented as causing Ca^{2+} flux in the cell [2,3,38,39]. Ca^{2+} sensing may be responsible for membrane blebbing and repair. We have preliminary results that suggest Ca^{2+} depletion inhibits blebbing and activates caspase-7 (data not shown), and others have shown that Ca^{2+} is necessary for repair [2,40]. Therefore, Ca^{2+} signaling is likely important for the activation of caspase-7 in this model, and may account for the caspase-7-dependent protective response after toxin damage.

Membrane damage is not confined to pathogenesis. For instance, cells that encounter mechanical stress, such as the gastrointestinal epithelium, display wounding and repair *in vivo* [41]. Membrane damage can also arise as an outcome of pathology. Amyloid proteins, which are involved in Alzheimer's disease, are known to perforate the plasma membrane [42-46]. The antinuclear antibodies generated as a result of autoimmunity are suggestive of chronic, irreparable membrane damage [47]. Indeed, mice deficient in lysosomal proteins responsible for resealing membrane lesions display autoimmune symptoms [48], highlighting the importance of quotidian barrier vigilance and fidelity.

The mammalian immune system also displays pore-forming capacity. For instance, cytotoxic T cells use a pore-forming protein, perforin, to introduce lethal granzyme into virus-infected and transformed cells [49]. Recent work suggests the pore produced by

perforin is rapidly resealed after granzyme delivery [50] similar to the rapid resealing of CDC pores [2,3], perhaps suggestive of shared repair mechanisms. This also suggests that cells may be able to withstand damage by physiological concentrations of perforin in the absence of proteolytic granzymes. Importantly, perforin and granulysin can activate caspase-7 and damage the ER [51]. Therefore, the mechanism that protects cells from bacterial PFTs may also protect from unintended perforin deposition in the absence of granzyme delivery.

We previously demonstrated that the caspase-7 is activated by membrane damage caused by PFTs, but not detergent [4], conferring specificity to the caspase-7-dependent cytoprotective response. Specificity may be achieved by the sensing of concentrated ion fluxes, such as a Ca^{2+} gradient, across the damaged membrane. Ca^{2+} sensing is the mechanism proposed by other groups for the recruitment of lysosomes and anxA1 to damaged membrane [8,40]. Detergents can selectively permeabilize host cells in the absence of overt cell death [52], which suggests that the cell uses different mechanisms to reseal the membrane in response to different types of membrane damage. Therefore, concentrated ion flux may be the mechanism by which cells can differentiate between acute and diffuse membrane damage, whereby acute damage may stimulate an adaptive repair mechanism. Given the ubiquity of membrane damage, we propose that cells activate a molecular signaling cascade in response to PFT damage that relies on signal strength to inform whether apoptosis or adaptive membrane repair should be executed.

4. Materials and Methods

Bacterial Strains and Reagents

BMDM and RAW 264.7 cells were infected with *Listeria monocytogenes* strain 10403S (WT), DP-L2161 (LLO⁻) [53] which has an in-frame deletion of the *hly* gene, and L461T [18] which has an in-frame deletion of the *hly* gene replaced with an allele that has an amino acid substitution at position 461. The anti-caspase-7 antibody, which recognizes full length and cleaved caspase-7 (cat #9492) was purchased from Cell Signaling Technology, anti-ROCK I (cat #611136) was purchased from BD Transduction Laboratories, anti-annexin A1 (cat #sc-1923-R) was purchased from Santa Cruz Biotechnology, Inc and anti-actin (cat #MS1295P1) was purchased from Fisher Scientific. Rhodamine-phalloidin (cat #R415) and SYTOX Green (cat #S7020) were purchased from Molecular Probes. WST-1 (cat #11644807001) was purchased from Roche Molecular Biochemicals. Y-27632 (cat #1254) was purchased from Tocris Bioscience and blebbistatin (cat #BML-EI15) was purchased from Enzo Life Sciences.

Cell Culture and Infection

Bone marrow derived macrophages (BMDM) were isolated from WT C57BL/6 mice and/or *csp7^{-/-}* mice in a C57BL/6 background. Mice were bred at Jackson Laboratories (Bar Harbor, ME) and sacrificed on-site. Leg bones were isolated and shipped overnight on ice to the University of Michigan, where the marrow was harvested the next morning. Briefly, isolated BMDM were differentiated in DMEM with 20% heat-inactivated FBS (Hyclone Laboratories or Gibco), 1% L-glutamine, 1% sodium pyruvate and 30% L929 fibroblast conditioned medium. Cells were cultured in non-TC treated plates, fed with fresh medium on day 3 and harvested on day 6 for infection on day 7.

Cultures were maintained in a humidified incubator at 37°C with 5% CO₂. Overnight cultures of *L. monocytogenes* in BHI broth were incubated statically at 30°C. Prior to infection, bacteria were pelleted and resuspended in PBS.

Immunoblots

Four million BMDM were plated in 6 well plates 18 h prior to infection. Cells were incubated with LLO or infected with bacteria for the stated time in complete cell medium. Cells were lysed in buffer containing 1% NP-40 on ice for 15 minutes and then spun at 13,000 rpm for 10 min to pellet the insoluble fraction. Soluble fractions were separated by SDS-PAGE, transferred to nitrocellulose membrane, and probed with antibody. Membranes were incubated and treated according to the antibody manufacturer instructions. For caspase-7 cleavage in BMDMs, membranes from individual gels were cut to optimize exposure times for the cleaved and full-length forms of the protein. Bands were visualized using either tetramethylbenzidine (TMB) (Sigma) or West Femto chemiluminescent substrate (Thermo Scientific).

Cell Viability Assay

Two and a half million BMDMs were plated in a 24-well format and intoxicated with a final concentration of LLO 0.25 µg/ml for 1 h. Toxin buffer alone was added to control wells. Cells were washed twice with PBS, and fresh medium was added. WST-1 reagent was diluted 1 in 10 in cell medium and added to wells at the given times post-intoxication. The OD_{440nm} was determined 90 minutes after addition of WST-1 and normalized to the buffer treated cells to obtain the percent viable cells in a given experimental condition.

Fixed cell microscopy

For host cell permeability assays in response to LLO treatment, BMDM or RAW cells were seeded onto square coverslips in 6 well plates at a density of 5×10^5 per well the night before infection. The day of infection, host cells were incubated with either 0.5 μ g/ml LLO and 1:50 rho-phall in cell medium for 15 minutes, or 0.25 μ g/ml for BMDM or 0.3 μ g/ml for RAW cells for 1 h, after which 1:50 rho-phall was added in cell medium for 15 min. Otherwise, cells were allowed to recover in cell medium for the given times and then incubated with 1:50 rho-phall for 15min. For host cell permeability during infection, cells were then washed 3 times with PBS and fixed in 4% paraformaldehyde. After fixation, coverslips were rinsed three times in TBS + 0.1% Triton-X 100 and counterstained with DAPI. For host cell permeability during infection, cells were infected with *L. monocytogenes* at MOI1 and spun for 3 min at 1200 rpm to maximize bacterial-host cell contact. After spinning the inoculum was removed and replaced with fresh medium. After 30 min, 10 μ g/ml gentamicin was added to kill any extracellular bacteria. Gentamicin was removed from the medium at 2h pi and cells were washed once per hour with fresh media. At 8 h pi, live cells were stained using 1:50 rho-phall for 15 minutes, rinsed with PBS, and fixed in 4% paraformaldehyde. For anxA1 staining, BMDMs were incubated in 0.25 μ g/ml for 1 h then fixed in 4% paraformaldehyde. After fixation cells were rinse in TBS + 0.1% Tx-100 (TBS-Tx) and blocked in 1% BSA for 10 min. Anti-AnxA1 was added at 1:500 for 1 h. For all fluorescence microscopy experiments, cells were counterstained with DAPI. Coverslips were mounted onto slides using Prolong Anti-Fade (Invitrogen), and imaged at the Center for Live Cell Imaging (CLCI) at the University of Michigan Medical School using an Olympus BX60 upright fluorescence microscope (Olympus; Center Valley PA).

Images were collected using a DP70 CCD color camera (RGB, 12-bits/channel; Olympus America Inc., Center Valley PA) using DP70 controller/manager software v3.02.

Micrographs of a minimum of 200 cells were analyzed per experiment and automated analysis of rho-phall intensity was quantified using Metamorph v7.7 software (Molecular Devices, Downingtown PA).

Live cell imaging

BMDMs were plated at a concentration of 1.5×10^5 onto 35mm glass bottom petri dishes (cat #P35G-0-10-C, Matek Corp.) and allowed to adhere overnight. Before visualization the overnight medium was removed and replaced with LCI medium (DMEM lacking phenol red, + 25mM HEPES + 500nM SYTOX Green). Microscopy experiments were performed in the Center for Live Cell Imaging (CLCI) at the University of Michigan Medical School using an Olympus IX70 inverted microscope (Olympus; Center Valley PA). Illumination was provided from a 100W halogen lamp for phase-contrast microscopy and by an X-Cite 120 metal halide light source (EXFO; Mississauga, ON, Canada) for fluorescent microscopy using a 100X (oil immersion; UPlan FI, NA=1.30) objective. Images were collected using a CoolSNAP HQ2 14-bit CCD camera (Photometrics; Tucson AZ). All devices were controlled through Metamorph Premier v6.3 software (Molecular Devices, Downingtown PA). Analysis of the imaging data, including the preparation of image overlays, montages and movies, was performed using Metamorph v7.7 software. Micrographs for phase contrast and SYTOX (excitation 492nm/BP18, emission 535nm/BP40) were taken before the addition of LLO at a working concentration 0.1 μ g/ml, after which micrographs were taken every 30

secs. Cells were monitored for SYTOX positivity, after which micrographs were collected for an additional 30 min.

Listeriolysin O expression, purification, and quantification

For purification of recombinant LLO, 10mL LB cultures containing 50µg/ml kanamycin (LB Kan50) sulfate were inoculated with single colonies of *E. coli* BL21(DE3) containing plasmid pET29 that encodes for a 6xHis-tagged copy of the *hly* gene encoding Listeriolysin O (LLO) from *L. monocytogenes* strain 10403S from freshly streaked LB agar plates and incubated overnight at 37°C with constant agitation. Cultures were then used to inoculate 125 ml of LB Kan50 and incubated at 30°C with constant agitation for 2 h. IPTG was added to cultures at a final concentration of 1mM and incubation was resumed for an additional 5 h to induce LLO expression. Protein expression cultures were pelleted at 4000 x g for 15 min at 4°C and supernatants were discarded. Pellets were then stored at -80°C overnight. The next morning, pellets were resuspended in 1.3ml Buffer A (50mM sodium phosphate buffer pH 8.0, 1M sodium chloride, 5mM mercaptoethanol, 10mM imidazole, and 1 mini-complete protease inhibitor tablet (Roche)) containing 1mg/ml lysozyme and 0.75mg/ml DNase1. Suspensions were then subjected to 4 x 30 sec sonication treatments separated by 15 sec incubation on ice with a Misonix Microson Ultrasonic Cell Disruptor XL set to intensity 4. Lysates were centrifuged for 30 min at 16,000 x g at 4°C. To purify 6xHis-tagged LLO, a NiNTA spin column (Qiagen, Cat. No. 31314) was loaded with 600µl Buffer A and centrifuged at 700 x g for 2 minutes; flow-through was discarded. Lysate supernatants were passed through the column in 600µL increments and spun at 1600 rpms for 5 min. All subsequent NiNTA spin column centrifugation steps were carried out at 700 x g for 2

min. Columns were washed sequentially with 600µl volumes of the following: 3 times with Buffer B (50mM sodium phosphate buffer pH 8.0, 1M sodium chloride, 5mM mercaptoethanol, 20mM imidazole) and 2 times with Buffer C (50mM sodium phosphate buffer pH 6.0, 1M sodium chloride, 5mM mercaptoethanol, 20mM imidazole, 0.1% Tween-20, 10% glycerol). 6XHis-tagged LLO was then eluted from the column with 200µl elution buffer (50mM sodium phosphate buffer pH 6.0, 1M sodium chloride, 5mM mercaptoethanol, 500mM imidazole). Eluted samples were then dialyzed overnight in 1L dialysis buffer (50mM sodium phosphate buffer pH 6.0, 500mM sodium chloride, 1mM EDTA, 170µM TCEP) using Tube-O-DIALYZERS with a MW cutoff of 15,000 Da (cat #786-618 GBiosciences). The next morning, samples were washed with 1L fresh dialysis buffer for an additional 4 h at 4°C. Protein solutions were then separated into 10µl aliquots and stored at – 80°C. Final protein concentration was measured by Bradford assay (Thermo Scientific) using a BSA standard curve and activity was measured by hemolysis of sheep red blood cells.

Statistical analysis

All p values were generated between identified samples using unpaired two-tailed t-tests. * P < 0.05, ** P < 0.01 and *** P < 0.001.

5. References

1. Bhakdi, S.; Weller, U.; Walev, I.; Martin, E.; Jonas, D.; Palmer, M. A guide to the use of pore-forming toxins for controlled permeabilization of cell membranes. *Med. Microbiol. Immunol.* **1993**, *182*, 167–175.
2. Walev, I.; Bhakdi, S. C.; Hofmann, F.; Djonder, N.; Valeva, A.; Aktories, K.; Bhakdi, S. Delivery of proteins into living cells by reversible membrane permeabilization with streptolysin-O. *Proc. Natl. Acad. Sci. U.S.A.* **2001**, *98*, 3185–3190.
3. Gonzalez, M. R.; Bischofberger, M.; Frêche, B.; Ho, S.; Parton, R. G.; van der Goot, F. G. Pore-forming toxins induce multiple cellular responses promoting survival. *Cell. Microbiol.* **2011**, *13*, 1026–1043.
4. Cassidy, S. K. B.; Hagar, J. A.; Kanneganti, T.-D.; Franchi, L.; Núñez, G.; O’Riordan, M. X. D. Membrane damage during *Listeria monocytogenes* infection triggers a caspase-7 dependent cytoprotective response. *PLoS Pathog* **2012**, *8*, e1002628.
5. Kerr, J. F.; Wyllie, A. H.; Currie, A. R. Apoptosis: a basic biological phenomenon with wide-ranging implications in tissue kinetics. *Br. J. Cancer* **1972**, *26*, 239–257.
6. Charras, G.; Paluch, E. Blebs lead the way: how to migrate without lamellipodia. *Nat. Rev. Mol. Cell Biol.* **2008**, *9*, 730–736.
7. Tinevez, J.-Y.; Schulze, U.; Salbreux, G.; Roensch, J.; Joanny, J.-F.; Paluch, E. Role of cortical tension in bleb growth. *Proc. Natl. Acad. Sci. U.S.A.* **2009**, *106*, 18581–18586.
8. Babiychuk, E. B.; Monastyrskaya, K.; Potez, S.; Draeger, A. Blebbing confers resistance against cell lysis. *Cell Death Differ* **2011**, *18*, 80–89.
9. Keyel, P. A.; Loultcheva, L.; Roth, R.; Salter, R. D.; Watkins, S. C.; Yokoyama, W. M.; Heuser, J. E. Streptolysin O clearance through sequestration into blebs that bud passively from the plasma membrane. *Journal of Cell Science* **2011**, *124*, 2414–2423.
10. Keyel, P. A.; Heid, M. E.; Salter, R. D. Macrophage responses to bacterial toxins: a balance between activation and suppression. *Immunol. Res.* **2011**, *50*, 118–123.
11. Stavru, F.; Bouillaud, F.; Sartori, A.; Ricquier, D.; Cossart, P. *Listeria monocytogenes* transiently alters mitochondrial dynamics during infection. *Proc. Natl. Acad. Sci. U.S.A.* **2011**, *108*, 3612–3617.
12. Sebbagh, M.; Renvoizé, C.; Hamelin, J.; Riché, N.; Bertoglio, J.; Bréard, J. Caspase-3-mediated cleavage of ROCK I induces MLC phosphorylation and apoptotic membrane blebbing. *Nat. Cell Biol.* **2001**, *3*, 346–352.
13. Coleman, M. L.; Sahai, E. A.; Yeo, M.; Bosch, M.; Dewar, A.; Olson, M. F. Membrane blebbing during apoptosis results from caspase-mediated activation of ROCK I. *Nat. Cell Biol.* **2001**, *3*, 339–345.

14. Uehata, M.; Ishizaki, T.; Satoh, H.; Ono, T.; Kawahara, T.; Morishita, T.; Tamakawa, H.; Yamagami, K.; Inui, J.; Maekawa, M.; Narumiya, S. Calcium sensitization of smooth muscle mediated by a Rho-associated protein kinase in hypertension. *Nature* **1997**, *389*, 990–994.
15. Davies, S. P.; Reddy, H.; Caivano, M.; Cohen, P. Specificity and mechanism of action of some commonly used protein kinase inhibitors. *Biochem. J.* **2000**, *351*, 95–105.
16. Straight, A. F.; Cheung, A.; Limouze, J.; Chen, I.; Westwood, N. J.; Sellers, J. R.; Mitchison, T. J. Dissecting temporal and spatial control of cytokinesis with a myosin II Inhibitor. *Science* **2003**, *299*, 1743–1747.
17. Limouze, J.; Straight, A. F.; Mitchison, T.; Sellers, J. R. Specificity of blebbistatin, an inhibitor of myosin II. *J. Muscle Res. Cell. Motil.* **2004**, *25*, 337–341.
18. Glomski, I. J.; Gedde, M. M.; Tsang, A. W.; Swanson, J. A.; Portnoy, D. A. The *Listeria monocytogenes* hemolysin has an acidic pH optimum to compartmentalize activity and prevent damage to infected host cells. *J. Cell Biol.* **2002**, *156*, 1029–1038.
19. Glomski, I. J.; Decatur, A. L.; Portnoy, D. A. *Listeria monocytogenes* mutants that fail to compartmentalize listeriolysin O activity are cytotoxic, avirulent, and unable to evade host extracellular defenses. *Infection and Immunity* **2003**, *71*, 6754–6765.
20. Hall, A. Rho GTPases and the actin cytoskeleton. *Science* **1998**, *279*, 509–514.
21. Amano, M.; Ito, M.; Kimura, K.; Fukata, Y.; Chihara, K.; Nakano, T.; Matsuura, Y.; Kaibuchi, K. Phosphorylation and activation of myosin by Rho-associated kinase (Rho-kinase). *J. Biol. Chem.* **1996**, *271*, 20246–20249.
22. Kimura, K.; Ito, M.; Amano, M.; Chihara, K.; Fukata, Y.; Nakafuku, M.; Yamamori, B.; Feng, J. H.; Nakano, T.; Okawa, K.; Iwamatsu, A.; Kaibuchi, K. Regulation of myosin phosphatase by Rho and Rho-Associated kinase (Rho-kinase). *Science* **1996**, *273*, 245–248.
23. Kawano, Y.; Fukuta, Y.; Oshiro, N.; Amano, M.; Nakamura, T.; Ito, M.; Matsumura, F.; Inagaki, M.; Kaibuchi, K. Phosphorylation of myosin-binding subunit (MBS) of myosin phosphatase by Rho-kinase in vivo. *J. Cell Biol.* **1999**, *147*, 1023–1037.
24. Fernando, P.; Kelly, J. F.; Balazsi, K.; Slack, R. S.; Megeney, L. A. Caspase 3 activity is required for skeletal muscle differentiation. *Proc. Natl. Acad. Sci. U.S.A.* **2002**, *99*, 11025–11030.
25. Miura, M.; Chen, X.-D.; Allen, M. R.; Bi, Y.; Gronthos, S.; Seo, B.-M.; Lakhani, S.; Flavell, R. A.; Feng, X.-H.; Robey, P. G.; Young, M.; Shi, S. A crucial role of caspase-3 in osteogenic differentiation of bone marrow stromal stem cells. *J Clin Invest* **2004**, *114*, 1704–1713.
26. D'Amelio, M.; Cavallucci, V.; Cecconi, F. Neuronal caspase-3 signaling: not only cell death. *Cell Death Differ* **2010**, *17*, 1104–1114.

27. Fujita, J.; Crane, A. M.; Souza, M. K.; Dejosez, M.; Kyba, M.; Flavell, R. A.; Thomson, J. A.; Zwaka, T. P. Caspase activity mediates the differentiation of embryonic stem cells. *Cell Stem Cell* **2008**, *2*, 595–601.
28. Janzen, V.; Fleming, H. E.; Riedt, T.; Karlsson, G.; Riese, M. J.; Celso, Lo, C.; Reynolds, G.; Milne, C. D.; Paige, C. J.; Karlsson, S.; Woo, M.; Scadden, D. T. Hematopoietic stem cell responsiveness to exogenous signals is limited by Caspase-3. *Cell Stem Cell* **2008**, *2*, 584–594.
29. Denault, J.-B.; Salvesen, G. S. Human caspase-7 activity and regulation by its N-terminal peptide. *J. Biol. Chem.* **2003**, *278*, 34042–34050.
30. Pai, J. T.; Brown, M. S.; Goldstein, J. L. Purification and cDNA cloning of a second apoptosis-related cysteine protease that cleaves and activates sterol regulatory element binding proteins. *Proc. Natl. Acad. Sci. U.S.A.* **1996**, *93*, 5437–5442.
31. Chandler, J. M.; Cohen, G. M.; MacFarlane, M. Different subcellular distribution of caspase-3 and caspase-7 following Fas-induced apoptosis in mouse liver. *J. Biol. Chem.* **1998**, *273*, 10815–10818.
32. Nakagawa, T.; Zhu, H.; Morishima, N.; Li, E.; Xu, J.; Yankner, B. A.; Yuan, J. Y. Caspase-12 mediates endoplasmic-reticulum-specific apoptosis and cytotoxicity by amyloid-beta. *Nature* **2000**, *403*, 98–103.
33. Rao, R. V. Coupling Endoplasmic Reticulum Stress to the Cell Death Program. MECHANISM OF CASPASE ACTIVATION. *Journal of Biological Chemistry* **2001**, *276*, 33869–33874.
34. Akhter, A.; Gavrilin, M. A.; Frantz, L.; Washington, S.; Ditty, C.; Limoli, D.; Day, C.; Sarkar, A.; Newland, C.; Butchar, J.; Marsh, C. B.; Wewers, M. D.; Tridandapani, S.; Kanneganti, T.-D.; Amer, A. O. Caspase-7 activation by the Nlrc4/Ipafl inflammasome restricts *Legionella pneumophila* infection. *PLoS Pathog* **2009**, *5*, e1000361.
35. Lamkanfi, M.; Kanneganti, T.-D.; Van Damme, P.; Vanden Berghe, T.; Vanoverberghe, I.; Vandekerckhove, J.; Vandenabeele, P.; Gevaert, K.; Núñez, G. Targeted peptide-centric proteomics reveals caspase-7 as a substrate of the caspase-1 inflammasomes. *Mol. Cell Proteomics* **2008**, *7*, 2350–2363.
36. Edelmann, B.; Bertsch, U.; Tchikov, V.; Winoto-Morbach, S.; Perrotta, C.; Jakob, M.; Adam-Klages, S.; Kabelitz, D.; Schütze, S. Caspase-8 and caspase-7 sequentially mediate proteolytic activation of acid sphingomyelinase in TNF-R1 receptosomes. *EMBO J.* **2011**, *30*, 379–394.
37. Gafni, J.; Cong, X.; Chen, S. F.; Gibson, B. W.; Ellerby, L. M. Calpain-1 Cleaves and Activates Caspase-7. *Journal of Biological Chemistry* **2009**, *284*, 25441–25449.
38. Hamon, M. A.; Cossart, P. K⁺ efflux is required for histone H3 dephosphorylation by *Listeria monocytogenes* listeriolysin O and other pore-forming toxins. *Infection and Immunity* **2011**, *79*, 2839–2846.

39. Gekara, N. O.; Westphal, K.; Ma, B.; Rohde, M.; Groebe, L.; Weiss, S. The multiple mechanisms of Ca²⁺ signalling by listeriolysin O, the cholesterol-dependent cytolysin of *Listeria monocytogenes*. *Cell. Microbiol.* **2007**, *9*, 2008–2021.
40. Reddy, A.; Caler, E. V.; Andrews, N. W. Plasma membrane repair is mediated by Ca(2+)-regulated exocytosis of lysosomes. *Cell* **2001**, *106*, 157–169.
41. McNeil, P. L.; Ito, S. Gastrointestinal cell plasma-membrane wounding and resealing *in vivo*. *Gastroenterology* **1989**, *96*, 1238–1248.
42. Diociaiuti, M.; Polzi, L. Z.; Valvo, L.; Malchiodi-Albedi, F.; Bombelli, C.; Gaudiano, M. C. Calcitonin forms oligomeric pore-like structures in lipid membranes. *Biophys. J.* **2006**, *91*, 2275–2281.
43. Lashuel, H. A.; Lansbury, P. T. Are amyloid diseases caused by protein aggregates that mimic bacterial pore-forming toxins? *Q. Rev. Biophys.* **2006**, *39*, 167–201.
44. Connelly, L.; Jang, H.; Arce, F. T.; Capone, R.; Kotler, S. A.; Ramachandran, S.; Kagan, B. L.; Nussinov, R.; Lal, R. Atomic force microscopy and MD simulations reveal pore-like structures of all-D-enantiomer of Alzheimer's β -amyloid peptide: relevance to the ion channel mechanism of AD pathology. *J Phys Chem B* **2012**, *116*, 1728–1735.
45. Sepulveda, F. J.; Parodi, J.; Peoples, R. W.; Opazo, C.; Aguayo, L. G. Synaptotoxicity of Alzheimer beta amyloid can be explained by its membrane perforating property. *PLoS ONE* **2010**, *5*, e11820.
46. Milanesi, L.; Sheynis, T.; Xue, W.-F.; Orlova, E. V.; Hellewell, A. L.; Jelinek, R.; Hewitt, E. W.; Radford, S. E.; Saibil, H. R. Direct three-dimensional visualization of membrane disruption by amyloid fibrils. *Proc. Natl. Acad. Sci. U.S.A.* **2012**, *109*, 20455–20460.
47. Tan, E. M. Autoantibodies, autoimmune disease, and the birth of immune diagnostics. *J Clin Invest* **2012**, *122*, 3835–3836.
48. Chakrabarti, S.; Kobayashi, K. S.; Flavell, R. A.; Marks, C. B.; Miyake, K.; Liston, D. R.; Fowler, K. T.; Gorelick, F. S.; Andrews, N. W. Impaired membrane resealing and autoimmune myositis in synaptotagmin VII-deficient mice. *J. Cell Biol.* **2003**, *162*, 543–549.
49. Anthony, D. A.; Andrews, D. M.; Watt, S. V.; Trapani, J. A.; Smyth, M. J. Functional dissection of the granzyme family: cell death and inflammation. *Immunol. Rev.* **2010**, *235*, 73–92.
50. Lopez, J. A.; Susanto, O.; Jenkins, M. R.; Lukoyanova, N.; Sutton, V. R.; Law, R. H. P.; Johnston, A.; Bird, C. H.; Bird, P. I.; Whisstock, J. C.; Trapani, J. A.; Saibil, H. R.; Voskoboinik, I. Perforin forms transient pores on the target cell plasma membrane to facilitate rapid access of granzymes during killer cell attack. *Blood* **2013**.

51. Saini, R. V.; Wilson, C.; Finn, M. W.; Wang, T.; Krensky, A. M.; Clayberger, C. Granulysin delivered by cytotoxic cells damages endoplasmic reticulum and activates caspase-7 in target cells. *J. Immunol.* **2011**, *186*, 3497–3504.
52. Girardin, S. E.; Boneca, I. G.; Carneiro, L. A. M.; Antignac, A.; Jéhanno, M.; Viala, J.; Tedin, K.; Taha, M.-K.; Labigne, A.; Zähringer, U.; Coyle, A. J.; DiStefano, P. S.; Bertin, J.; Sansonetti, P. J.; Philpott, D. J. Nod1 detects a unique muropeptide from gram-negative bacterial peptidoglycan. *Science* **2003**, *300*, 1584–1587.
53. Jones, S.; Portnoy, D. A. Characterization of *Listeria monocytogenes* pathogenesis in a strain expressing perfringolysin O in place of listeriolysin O. *Infection and Immunity* **1994**, *62*, 5608–5613.

Chapter 4

The contribution of cellular processes to membrane repair after LLO damage

1. Introduction

We successfully identified some molecular constituents responsible for driving blebbing and promoting membrane integrity in response to LLO-mediated membrane damage. However the cell may employ multiple mechanisms to ameliorate membrane injury. For instance, we hypothesize that damaged sections of membrane are sequestered into blebs and then shed as vesicles from the cell body. This implies that the damaged and shed membrane must be replaced to maintain cellular shape and homeostasis. Cell surface area may be maintained after injury by co-opting internal sources of membrane to patch the plasma membrane. This method of membrane repair has been reported in the context of PFT-derived, infection-associated, and scratch wound damage [1-3]. Another method by which membrane maintenance can be achieved after injury is by the generation of new membrane *de novo*. Lipid synthesis was shown to ameliorate membrane damage by chemical and electrical injury, as well as PFT injury [4-6]. This chapter will discuss some experiments which aim to identify whether cells recruit internal membrane to the surface to patch PFT-damaged lesions and whether the cell upregulates lipid synthesis to make new membrane. Some of experiments outlined here will also attempt to tie in data from previous chapters identifying causes for defective repair in the context of caspase and blebbing deficiencies.

2. Results

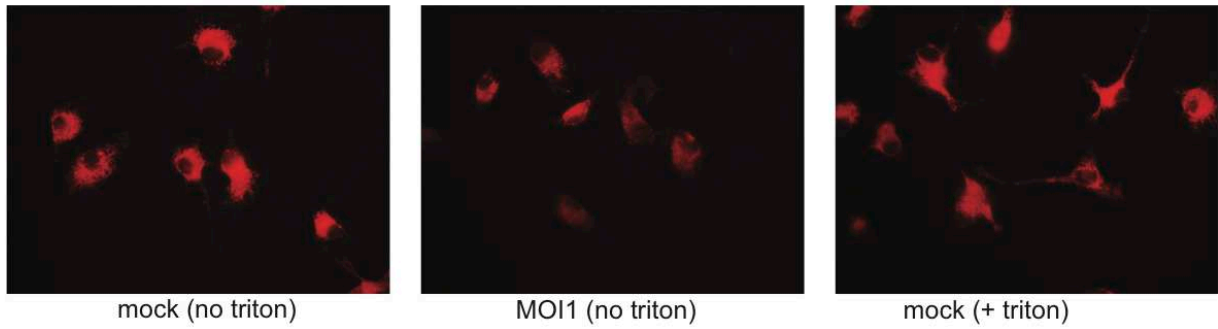
Lysosomal exocytosis as a possible repair mechanism for LLO-mediated damage

Research in Norma Andrews' lab has elegantly described a mechanism of membrane healing that requires the exocytosis of lysosomes to the cell surface in response to scratch wounds and the PFT streptolysin O. One of the seminal papers describing this repair mechanism shows relocation of a lysosomal surface protein, LAMP-1, to the plasma membrane after injury [1]. To test whether this repair mechanism might also occur during infection with *L. monocytogenes*, we infected BMDMs at MOI 1 for 8 h and then incubated the cells with an anti-LAMP-1 antibody, in the absence of permeabilization. We then looked for LAMP-1 staining by fluorescence microscopy. We were surprised to find that uninfected, resting macrophages expressed LAMP-1 on their surface (Fig 4.1A), which was inconsistent with published reports using other cell types such as fibroblasts, myoblasts and epithelial cells [1]. Others have also observed plasma membrane staining of LAMP-1 in resting macrophages (B. Byrne, M. Swanson lab, personal communication). There was no obvious visual increase in surface staining upon infection (Fig 4.1A). Thus, we concluded that infection with *L. monocytogenes* does not result in a detectable increase in LAMP-1 staining on the surface to BMDMs.

However, we reasoned that if lysosomes were being recruited to a damaged plasma membrane, LAMP-1 might be degraded after fusion at the plasma membrane, which may result in the depletion of LAMP-1 from the intracellular compartment over time. Therefore, we performed the same infection protocol and permeabilized the cells with triton-X100 before staining with the anti-LAMP-1 antibody. We calculated the average intensity of LAMP-1 signal from fluorescence micrographs using Metamorph software and compared these values between infected and uninfected BMDMs. We

Figure 4.1

A



B

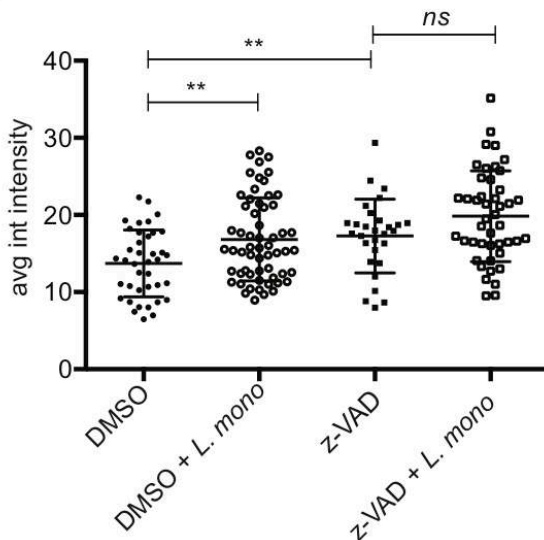


Figure 4.1. LAMP-1 staining of BMDMs in response to infection. (A) BMDMs were incubated with 1:50 anti-LAMP-1 antibody (1D4B, cat #sc-19992, Santa Cruz) with or without triton treatment or *L. monocytogenes*. (B) Quantification of cells permeabilized with triton and then stained with anti-LAMP-1 antibody 8 h post infection. BMDMs were pretreated for 1 h with 100 μ M z-VAD-fmk (Enzo) and z-VAD remained constant throughout the course of the experiment. ** $P < 0.004$ by Student's t-test.

measured the opposite of what was predicted. Infection for 8 h increased the overall intensity of LAMP-1 staining (Fig 4.1C). This suggests that infection upregulates LAMP-1 expression, and by proxy, lysosomes. To determine whether caspases play a role in LAMP-1 expression or distribution during infection, we pretreated cells with 100 μ M z-VAD-fmk, a pan-caspase inhibitor, for 1 h before infection. This concentration of z-VAD was maintained in the cell medium for the duration of the experiment. We discovered that z-VAD-treated, resting cells displayed an increase in LAMP-1 intensity compared to caspase-sufficient cells, but no difference was observed between infected and uninfected z-VAD treated cell populations (Fig 4.1C). From these methods, we concluded that LAMP-1 staining increases upon infection with *L. monocytogenes*, but not at the cell surface, and chemical inhibition of caspases does not alter the amount of LAMP-1 present in infected BMDMs.

Another way to test for the importance of lysosomal exocytosis during the caspase-7 protective response to LLO damage is to assess whether a lysosomal enzyme, acid sphingomyelinase (ASM), contributes to repair. The Andrews lab determined that, during wound-induced lysosomal exocytosis, plasma membrane-fused lysosomes release enzymes into the extracellular space, including ASM, which converts sphingomyelin to ceramide. Ceramide-rich microdomains generated during lysosomal exocytosis are critical for the invagination of damaged sections of membrane [2]. Importantly, during TNF α receptor ligation, caspase-7 activates ASM [7]. Therefore, we hypothesized that the membrane integrity defect detected in *csp7^{-/-}* cells might be due to a deficiency in the processing of ASM. We predicted if ASM deficiency is the source of the increased *csp7^{-/-}* permeability, we should restore membrane integrity and measure less phalloidin influx during infection with the addition of exogenous ASM. Exogenous

addition of the enzyme was successfully used by Fernandes *et al* to restore *T. cruzi* invasion after ASM transcriptional silencing [8]. To test this hypothesis, we infected BL/6 and *csp7^{-/-}* cells with *L. monocytogenes*. At 7 h pi, we added sphingomyelinase from *Bacillus cereus* to the cell medium. At 8 h pi we stained for phalloidin and assessed phalloidin influx using fluorescence microscopy. We tried several different infection conditions and concentrations of ASM, however we never saw consistent changes in phalloidin influx after ASM addition (Fig. 4.2A and B). Therefore, we conclude that ASM does not contribute to caspase-7-mediated membrane integrity. Combining results from figures 4.1 and 4.2, we conclude that lysosomal exocytosis does not contribute to caspase-7-mediated cytoprotectivity.

Cholesterol biosynthesis during *L. monocytogenes* infection

Caspase-7 may regulate cholesterol biosynthesis. Caspase-7 was first identified as a protease capable of cleaving sterol regulatory element binding proteins (SREBPs) [9]. SREBPs are transcription factors bound to the ER membrane and nuclear envelope. When cells are depleted of cholesterol, proteolytic cleavage releases the bound transcription factor, which enters the nucleus to activate proteins involved in cholesterol biosynthesis and lipoprotein uptake [10]. Additionally, the Van der Goot lab demonstrated that caspase-1 activated SREBPs after PFT damage to promote survival of the intoxicated cell [6]. Although we had previously ruled out the contribution of caspase-1 in the caspase-7 protective phenotype in response to LLO damage (Chapter 2), we reasoned it was possible that multiple caspases could regulate similar pathways. Thus, we hypothesized the *csp7^{-/-}* cells display increased permeability after LLO-mediated damage due to an inability to activate SREBPs, which would otherwise

Figure 4.2

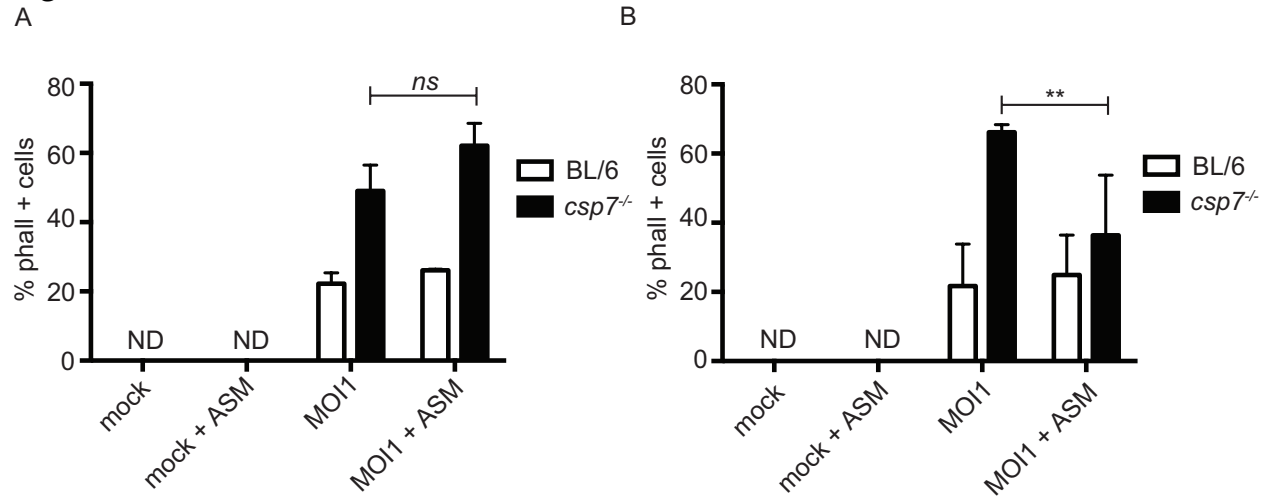


Figure 4.2. ASM treatment of *L. monocytogenes* infected BMDMs. (A and B) BMDMs were infected at an MOI1 with *L. monocytogenes* for 7 h, after which 20mU/ml sphingomyelinase derived from *Bacillus cereus* (Sigma) was added to the cell medium. Cells were then incubated with 1:50 rho-phalloidin for 15 min and the percentage of phalloidin positive cells was determined from fluorescent micrographs. N > 200 cells per condition. A and B were performed 6 d apart, with cells derived from the same mouse, and treated with the same stock of sphingomyelinase. ** P < 0.001 by Student's t-test and ns = not significant.

upregulate cholesterol biosynthesis and maintain membrane homeostasis after PFT injury.

To test this hypothesis, we first needed to determine if SREBPs were activated during infection with *L. monocytogenes*. We assayed for SREBP2 cleavage in BL/6 cells by immunoblot using different infection conditions. As a control, we incubated cells in DMEM without FBS for 1 h, and then added methyl- β -cyclodextrin for 30 min to deplete cellular cholesterol. We discovered that SREBP2 is not cleaved during any of the infection conditions tested (Fig 4.3A). Antibodies for other SREBPs were less reliable, so we shifted our focus to test whether we could measure transcription upregulation of cholesterol biosynthetic genes by qRT-PCR during infection. For these experiments we measured the transcription of two genes necessary for cholesterol biosynthesis, fatty acid synthase (FAS) and HMG-CoA-reductase (HMGCR), during infection at MOI5 and harvested samples for RNA extraction at various times post infection. We used the starvation condition for SREBP2 activation as a positive control. Using the cholesterol starvation condition that activated SREBP2, we measured a slight decrease in FAS transcript and no change in HMGCR (Fig 4.3B). It is possible that under our experimental control condition, we did not incubate long enough (1.5 h) to measure an increase in transcription of these genes by activated SREBP2. The cholesterol depletion protocol used induced morphological changes in the BMDMs, and we were careful to harvest the cells before we monitored significant cell death. However, it is striking that we measure a substantial decrease in the transcription of both FAS and HMGCR during the course of the infection, a result we replicated twice in independent experiments (Fig 4.3B). This result cannot be explained by cell loss due to infection over time, as all samples were normalized to the level of actin transcript at each time point. Therefore, *L.*

Figure 4.3

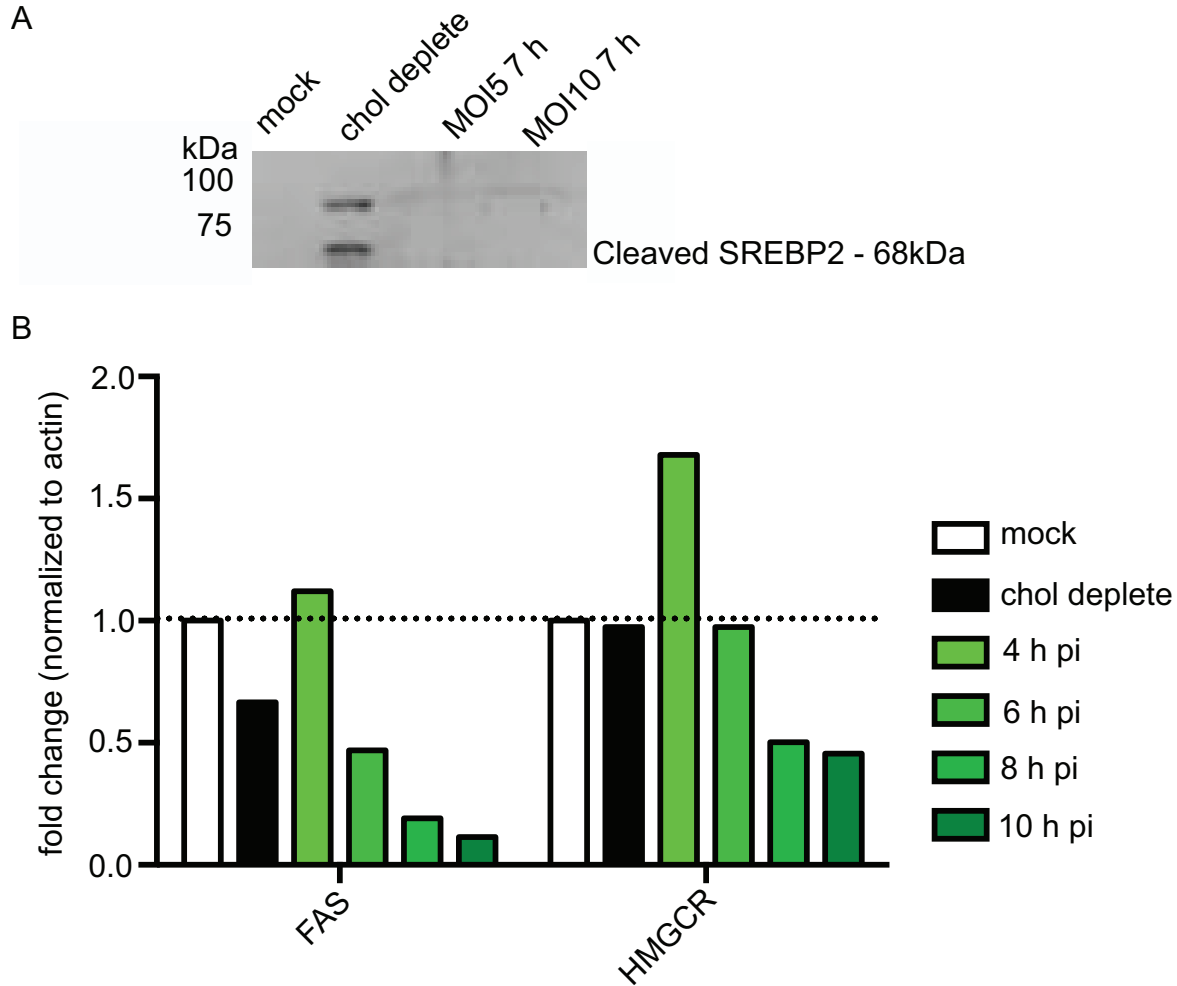


Figure 4.3. Cholesterol biosynthesis regulation during *L. monocytogenes* infection. (A) Samples from mock treated, cholesterol depleted and *L. monocytogenes* infected cell lysates were probed for the cleavage of SREBP2 by immunoblot. The predicted cleavage product migrates at 68 kDa; the source of the 90 kDa fragment is unknown, but was consistently present in cholesterol depleted samples in 3 separate experiments. (B) Fold change by qRT-PCR in transcript levels of either fatty acid synthase or HMG-CoA-reductase compared to actin transcripts during cholesterol depletion or infection with *L. monocytogenes* at MOI5. This graph is representative of two independent experiments.

monocytogenes infection induces a decrease in cholesterol biosynthetic transcript levels.

A possible explanation for this result is that the interferon response to *L. monocytogenes* infection is responsible for the decrease in cholesterol biosynthetic transcripts. *L. monocytogenes* has been long known to stimulate IFN production [11], and interferons are key regulators of lipid metabolism [12]. Additionally, interferon-induced lipid metabolic alterations have been described during *L. monocytogenes* infection [13]. Therefore, it is possible that the transcriptional program activated by interferon signaling supercedes any potential cholesterol requirements at the membrane due to PFT damage. It is also possible that, instead of activating cholesterol biosynthesis to heal damaged membrane, the host cell co-opts internal stores of membrane and repurposes those to patch holes. We did not observe the lysosomal compartment being used in this manner (Fig 4.1 and 4.2), however, there are many other sources of membrane in the intracellular compartment, perhaps the most abundant of which is the ER.

ER stress and membrane integrity during *L. monocytogenes* infection

The ER is an interconnected network of membrane vesicles that act as the site of protein folding and posttranslational modification within the cell. Perturbations in proper protein synthesis can induce ER stress. Also known as the unfolded protein response (UPR), this signal transduction pathway increases the biosynthetic capacity and decreases the biosynthetic burden of the ER to maintain homeostasis. Infection with a variety of pathogens can also stimulate the UPR and inform the innate immune response [14]. Activation of the UPR stimulates increased vesicular traffic between the ER and Golgi [15]. Importantly, infection with *L. monocytogenes* activates the UPR in an LLO-dependent manner [16]. Since caspase-7 can interact with ER membrane proteins

[9], we hypothesized that ER stress activation in response to *Listeria* infection or LLO may increase ER-derived vesicular traffic to the PFT damaged plasma membrane, and that this process may be perturbed in *csp7^{-/-}* cells.

Since there are many arms to the UPR, and many pathogens and perturbations selectively activate some arms but not others, one of the first experiments we performed was a visual analysis of ER stress in response to LLO treatment. We hypothesized that treatment with an ER stress-inducing agent may stimulate morphological changes in the ER compartment, similar to morphological changes during mitochondrial stress [17], which could be monitored using fluorescence microscopy and an antibody to an ER luminal protein, protein disulfide isomerase (PDI). We treated RAW cells with 0.5 $\mu\text{g}/\text{ml}$ LLO for 1 h and then stained for PDI. We used tunicamycin treatment, which activates all three arms of the UPR, as a positive control. We saw small differences between untreated, tunicamycin treated, and infected cells; the most obvious was increased punctate staining in the tunicamycin treated group (fig 4.4A). However, because these differences were difficult to quantify, we instead focused on molecular techniques to determine if LLO treatment caused UPR activation.

Work in the Ragahavan lab demonstrated that, during thapsigargin-induced UPR activation, dendritic cells secrete some ER resident proteins, one of which is PDI [18]. Therefore we wanted to determine whether PDI was secreted from BMDMs during intoxication with LLO. We treated cells with 0.25 or 0.5 $\mu\text{g}/\text{ml}$ LLO for 3 or 6 h, and then harvested supernatants to probe for PDI secretion by immunoblot. We used supernatants from thapsigargin treated cells as a positive control. We were able to visualize the secretion of PDI once (Fig 4.4B) but never again (Fig 4.4C). It is possible that we were at the limit of detection for the antibody, and immunoprecipitation or

Figure 4.4

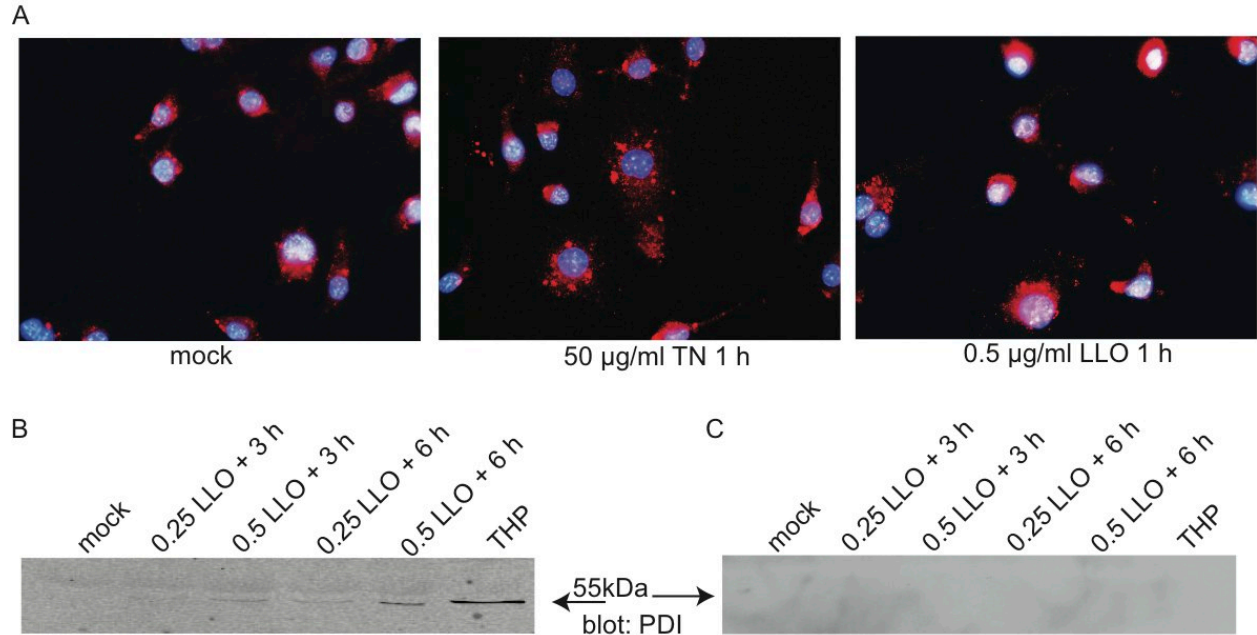


Figure 4.4. Monitoring PDI as a marker of ER stress in response to PFT damage. (A) RAW cells were stained using an anti-PDI antibody (Cell Signaling cat #3501) to monitor visual changes in the ER in response to chemical induction (tunicamycin treatment – TN) and LLO treatment. (B and C) Secretion of PDI into the cell supernatant after chemical induction (thapsigargin – THP) or LLO treatment as assessed by immunoblot using the same antibody as in (A). LLO concentrations are in µg/ml. Cells were treated with 25µM THP for 6 h.

trichloroacetic acid precipitation of protein would improve the regularity of PDI signal on my immunoblots, especially considering we inconsistently saw PDI secretion in the positive control lysates. However, there are many ways to detect ER stress, so we decided to try another technique.

There are three ER stress sensors that, upon activation, drive the physiological response to the UPR. These sensors, IRE1 α , PERK, and ATF6, can be preferentially activated to induce cellular processes not related to protein folding, such as innate immunity and metabolism [19]. Infection with intracellular pathogens can activate some, but not necessarily all, of the UPR sensors [16,20,21]. Therefore, we tested whether any of the UPR sensors were activated during infection with *L. monocytogenes* or after treatment with LLO.

IRE1 α is an ER-anchored kinase and ribonuclease that functions to post-transcriptionally modify *xbp1* RNA. Xbp1 is a transcription factor whose activity is greatly increased by IRE1 α splicing [14]. There is a strong connection in the literature between IRE1 α and intracellular infection [21]. Therefore, we first tested whether chemical inhibition of this sensor would result in increased permeability during infection with *L. monocytogenes*. We hypothesized that if IRE1 α signaling was needed to increase vesicular traffic to injured membrane during infection, then chemical inhibition of IRE1 α would increase permeability over time, similar to the permeability phenotype seen in the *csp7^{-/-}* BMDMs (Fig 2.4). To test this, we pre-treated RAW cells for 1 h with the IRE1 α inhibitor, irestatin, and then infected at MOI5. After a 30 min incubation, cell medium was removed and 50 μ g/ml gentamicin was added to kill any extracellular bacteria. In control groups, gentamicin was removed 2 h pi and replaced with media containing no antibiotic. Cells were lysed at various time points post infection and

assessed for intracellular CFU. We found the irestatin treatment did have an effect on the intracellular growth of *L. monocytogenes* (Fig 4.5A). However, this inhibitor affected the entry and escape of *L. monocytogenes*, as fewer bacteria were inside host cells after 1 h. This defect was overcome over time as the slope of intracellular growth sharply increased between 4h and 8 h pi (Fig 4.5A). Because the presence of gentamicin in the extracellular space did not inhibit the growth of *L. monocytogenes* inside irestatin treated cells over time, unlike *csp7⁻* cells (Fig 2.4), this indicates irestatin treatment does not result in increased permeability during infection. Therefore, we concluded that IRE1 α is important during *L. monocytogenes* infection, but does not correlate with increased permeability to small molecules as a result of increased PFT damage.

Pillich *et al* reported that extracellular *L. monocytogenes* were capable of activating IRE1 α using *xbp1* splicing as a read out, and attributed that activation to LLO secretion [16]. We hypothesized that pleiotropic effects of IRE1 α inhibition during *L. monocytogenes* infection could be masking the importance of this sensor in response to PFT damage. Therefore, we assayed the ability of exogenous LLO treatment to stimulate *xbp1* splicing in BMDMs. The unspliced *xbp1* mRNA contains a Pst1 digestion site, however IRE1 α splicing removes this sequence. Therefore Pst1 treatment of DNA made from *xbp1* RNA can be used to differentiate spliced from unspliced transcript. We treated cells with a range of concentrations of LLO and harvested for RNA at 1, 3 and 6 h post-intoxication. We used thapsigargin treatment as a positive control. We saw no *xbp1* splicing in any experimental condition tested, even at lytic concentrations (0.75 and 1.0 $\mu\text{g/ml}$) of toxin (Fig 4.5B). *Xbp1* splicing is regarded as the most sensitive method of detection for IRE1 α activation. Therefore, we conclude that PFT damage by LLO does

Figure 4.5

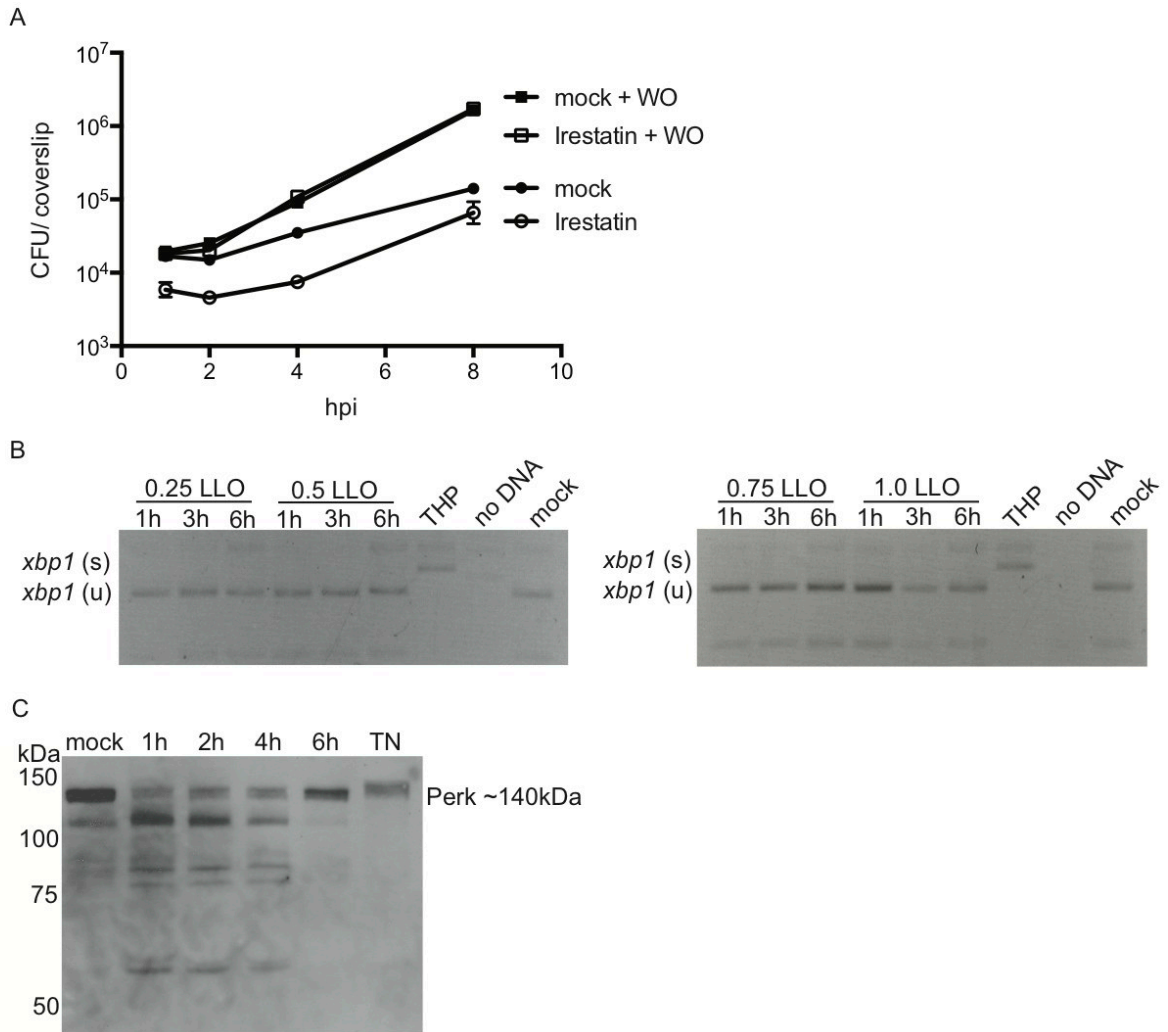


Figure 4.5. Activation of the UPR in response to LLO damage. (A) RAW cells pre-incubated with 25 μ g/ml irestatin for 1 h; this concentration was maintained throughout the experiment. Cells were infected at MOI5 for 30 min, after which the inoculum was removed and media containing 50 μ g/ml gentamycin. For WO conditions, gentamycin was removed from the media 2 h pi. RAW cells were lysed and CFU were enumerated using serial dilution of lysates onto agar plates. (B) *xbp1* splicing was assessed under various LLO treatment conditions (concentrations of LLO are μ g/ml), using Pst1 digestion. Spliced transcripts are resistant to Pst1 digestion and therefore migrate higher than unspliced transcripts. (C) immunoblot for PERK protein (Cell Signaling, cat #5683) phosphorylation in response to LLO damage. LLO concentration is in μ g/ml.

not stimulate this arm of the UPR.

ATF6 is another sensor of ER stress that resides in the ER membrane. Activation induces ATF6 to translocate to the Golgi where it is proteolytically processed to an isoform capable of activating the transcription of a variety of degradative proteins [19]. Therefore, the activation of ATF6 can be monitored by immunoblot using an antibody that can detect the cleaved fragment. We probed for the activation of ATF6 and a downstream effector, CHOP, in BMDMs intoxicated with LLO but were unable to detect cleavage of either protein (data not shown). Others in our laboratory have success using these antibodies (personal communication). Therefore, we conclude that ATF6 is not likely to be activated by LLO treatment.

A third ER stress sensor is PERK, a kinase that undergoes oligomerization and autophosphorylation upon activation. This leads to the translational activation of the transcription factor ATF4 and causes attenuation of global mRNA translation by phosphorylating the α -subunit of the regulating initiator of the translation machinery, eIF2 [14]. The most common ways to assay for PERK activation are using immunoblot and probing for either the phosphorylation of PERK or eIF2. When we assayed for PERK phosphorylation we saw a curious result. Tunicamycin (TN) treatment resulted in a slight size shift compared to mock treated cells, consistent with slower migration resulting from the phosphorylation modification (Fig 4.5C). However, treatment with 0.25 $\mu\text{g}/\text{ml}$ LLO for 1, 2, or 4 h produced a banding pattern on the immunoblot not seen in mock or tunicamycin treatment (Fig 4.5C). This result suggested that PERK might be degraded in response to LLO treatment. We were able to replicate this result using the same lot of antibody, however, when we purchased more of the same antibody (but from a different lot) and different antibodies from other companies, we never again saw

the banding pattern, nor did we ever see the phosphorylation size shift seen in the positive control sample. A possible interpretation of the banding pattern is that proteins were degraded during the lysate harvest. However, all samples were treated equivalently using the same lysis buffer with protease inhibitors, and therefore, it is unlikely that some samples would experience degradation and not others. We were unable to find any evidence in the literature of PERK degradation, which suggests that PERK degradation in response to LLO-treatment may be a novel phenomenon. We were unable to detect eIF2 phosphorylation in response to LLO treatment. Therefore, we hypothesize that the ER stress sensor PERK may be proteolytically degraded in response to LLO treatment, but different tools need to be used to assess this more directly.

Although the results of the ER stress experiments are inconsistent, it is likely that LLO damage does not classically activate any of the three known UPR sensors in BMDMs. This conclusion conflicts with results published by Pillich *et al*, which suggest that exogenous LLO damage stimulates the UPR [16]. It is possible that differences in cellular responses between cell types account for this conflict; they used P388D1 cells, which are a human macrophage cell line, and we use RAW cells and BMDMs, both of murine origin. This does not rule out ER contribution, in some way, to the response to PFT damage. Work in the Weiss lab demonstrated in mast cells that the ER rapidly releases Ca^{2+} in response to LLO-mediated damage [22]. Additionally, our laboratory has data suggesting that chemical induction of ER stress activates caspase-7 (data not shown). More studies need to be done to determine whether the ER contributes to PFT-damaged membrane repair, and whether this accounts for the defect seen in *csp7^{-/-}* BMDMs.

Autophagy and membrane repair after PFT treatment

Autophagy is a process by which cells can balance catabolic requirements during times of stress, remove misfolded or aggregated proteins, and clear damaged organelles. Autophagy can also aid the clearance of intracellular pathogens, such as *Shigella* and *Legionella* [23,24]. Infection with *L. monocytogenes* stimulates autophagy as a result of LLO-mediated phagosomal lysis; however, the role of autophagy in promoting the clearance of *L. monocytogenes* is controversial [25,26]. Liposomes loaded with purified LLO are sufficient to stimulate autophagy, indicating that internal membrane damage, independent of infection, is a trigger for this response [25]. It is possible that exogenous treatment with LLO could also activate autophagy. Thus, autophagosomes represent a possible source of membrane that could be co-opted to patch plasma membrane after LLO-mediated damage.

To determine whether exogenous LLO treatment stimulates autophagy, we performed live cell imaging on macrophages isolated from mice expressing GFP-labeled LC3, which is a marker for autophagosomes (a gift from M. Swanson) [27]. We used the same protocol for live cell imaging outline in Chapter 3. We measured no LC3-positive punctae in resting cells, however intoxication with LLO resulted in punctae formation in 60% of cells monitored (Fig 4.6), with an average of 3 punctae per cell. From this result, we conclude that autophagy is activated by exogenous treatment with LLO.

Using this method of investigation however, it was not clear whether autophagic vesicles were being recruited to the cell surface, which would indicate that autophagy may contribute to membrane healing after PFT damage. Using fixed-cell microscopy, the M. Swanson lab measured no increase in LC3 positivity on the plasma membrane of LLO-treated cells compared to un-intoxicated controls (personal communication). However, they did measure an increase in intracellular LC3-punctae similar to what we

Figure 4.6

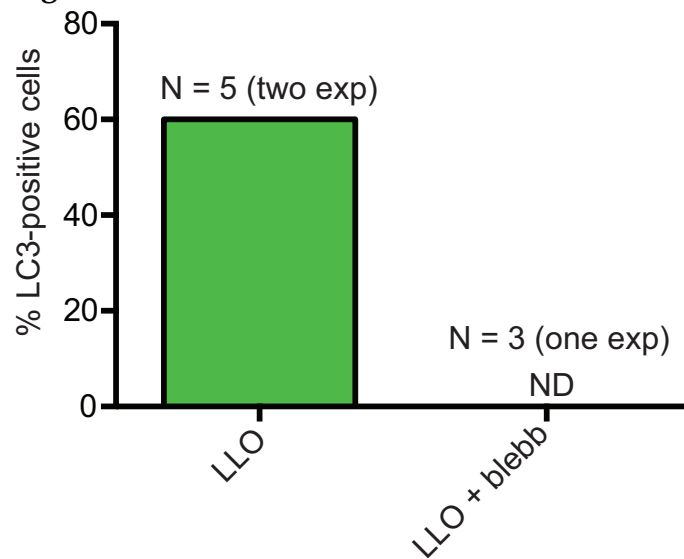


Figure 4.6 Autophagy is activated by exogenous LLO treatment and is reduced by myosin II inhibition. Macrophages isolated from mice expressing GFP-tagged LC3 were plated for live cell imaging at a concentration of 1.5×10^5 /plate. Just before imaging, LCI media was added to the cells (see Chapt. 3 for details). Micrographs in phase and the FITC filter were captured before the addition of LLO. LLO was added to the plates at a final working concentration of $0.1 \mu\text{g}/\text{ml}$. For blebbistatin treatment, cells were incubated for 30 min in $50 \mu\text{g}/\text{ml}$ blebbistatin before the addition of LCI media + $50 \mu\text{g}/\text{ml}$ blebbistatin. Cells were monitored for 30 min after the addition of toxin.

observed using live cell imaging. Although these experiments require more replicates, the preliminary data suggest that while autophagy is activated by LLO-treatment, LC3 positive vesicles are not being recruited to the cell surface to patch damaged membrane.

Interestingly, treatment of cells with the myosin II inhibitor, blebbistatin, resulted in a decrease in LC3-positive cells in live cell imaging (Fig 4.6), which suggests that myosin motor proteins may play a role in autophagy. These results are preliminary and need to be repeated to determine if a role exists for myosin in the generation of autophagosomes, and whether autophagic membrane is recruited to the cell surface after PFT damage.

3. Discussion

These experiments contain some hints that internal membrane that could be used to patch plasma membrane lesions caused PFT damage. However, more thorough research needs to be done to determine whether membrane is repurposed to ameliorate plasma membrane damage. Additionally, some sources of internal membrane were not researched. For instance, membrane originating for the Golgi was shown to be important in healing cells infected with *Mycobacterium tuberculosis* [3]. Also, it has been reported that the architecture of the mitochondrial network undergoes rapid, transient changes after treatment with LLO [17], and perhaps mitochondrial membrane could plug plasma membrane damage after pore-formation. More experiments need to be performed before ruling out a role for internal membrane in the resolution of PFT damage at the plasma membrane.

A confounding issue of detection might be the rapid turnover of markers used to label different intracellular compartments. This is not reported to be the case for the lysosomal marker LAMP-1 [1], however, turnover kinetics may differ between intracellular compartments and in different cell types. One method of investigation that could alleviate the issue of marker turnover would be to label intracellular compartments directly, and monitor their behavior after the addition of LLO using live cell imaging. We used this method to label Golgi with Bodipy-C5-ceramide, which preferentially accumulates in this organelle [28]. We did not notice obvious changes in staining after treatment with LLO (data not shown), however it is possible that another intracellular compartment may provide membrane to the site of PFT injury that we have yet to label in this manner. We hypothesize repurposed internal stores of membrane for plasma membrane repair after PFT damage remains a viable hypothesis

supported by the literature [1,3], and improved techniques may illuminate which compartments contribute to repair.

It is also possible that new membrane is made *de novo* in response to PFT damage. qRT-PCR of cholesterol biosynthetic genes during *L. monocytogenes* infection did not support this hypothesis, however, pleiotropic effects of interferon signaling during infection may have confounded analysis. Additionally, other genes may be responsible for lipid biogenesis in this context. We believe there is still value in looking at whether lipid synthesis is upregulated in response to LLO treatment, but using exogenous toxin instead of infection would be ideal for experimentation moving forward. We and others have shown that LLO treated cells undergo transient metabolic quiescence after LLO treatment (Chapter 3 and [17]), and this data should inform the likely timing of when transcriptional activity can be measured. It is also possible that lipid synthesis could be stimulated without gene transcription, for instance by the stimulation of lipid catabolic pathways repressed under resting conditions. Therefore, a more thorough analysis of lipid synthesis may illuminate whether membrane is made in response to LLO-mediated damage.

It is also possible that membrane is repaired without the aid of alternative membrane sources or *de novo* synthesis. This could be the case if PFTs were, for instance, proteolytically degraded at the plasma membrane. The resulting PFT fragments could be taken up into autophagic compartments for further processing. Then, as the PFT is degraded, membrane lesions would resolve due to hydrophobic bilayer re-fusion. Utilizing the concepts presented in Chapter 3, this would suggest that proteolytic proteins must be present inside membrane blebs after PFT damage. In order to get to the site of damage, it is possible that the proteolytic degradation machinery is endogenously present at the bilayer, perhaps through interaction with the cortical

cytoskeleton, or that it is rapidly recruited to damage sites, for instance via the sensing of ion flux. To test this, we could isolate resting membrane and toxin-induced blebs by ultracentrifugation and/or sucrose gradation and then assay for what is present inside the blebs or at the membrane. Current efforts in the lab are focused on isolation of blebs from intoxicated cells.

The experiments carried out through the course of this dissertation have identified molecular players involved in membrane maintenance after LLO intoxication. However, more work is needed to identify the physical mechanism by which the membrane is healed after pore-forming toxin damage.

4. References

1. Reddy, A.; Caler, E. V.; Andrews, N. W. Plasma membrane repair is mediated by Ca(2+)-regulated exocytosis of lysosomes. *Cell* **2001**, *106*, 157–169.
2. Tam, C.; Idone, V.; Devlin, C.; Fernandes, M. C.; Flannery, A.; He, X.; Schuchman, E.; Tabas, I.; Andrews, N. W. Exocytosis of acid sphingomyelinase by wounded cells promotes endocytosis and plasma membrane repair. *J. Cell Biol.* **2010**, *189*, 1027–1038.
3. Divangahi, M.; Chen, M.; Gan, H.; Desjardins, D.; Hickman, T. T.; Lee, D. M.; Fortune, S.; Behar, S. M.; Remold, H. G. *Mycobacterium tuberculosis* evades macrophage defenses by inhibiting plasma membrane repair. *Nat. Immunol.* **2009**, *10*, 899–906.
4. Ballas, S. K.; Burka, E. R. Stimulation of lipid synthesis in reticulocytes as a response to membrane damage. *Blood* **1974**, *44*, 263–273.
5. García, D.; Mañas, P.; Gómez, N.; Raso, J.; Pagán, R. Biosynthetic requirements for the repair of sublethal membrane damage in *Escherichia coli* cells after pulsed electric fields. *J. Appl. Microbiol.* **2006**, *100*, 428–435.
6. Gurcel, L.; Abrami, L.; Girardin, S.; Tschopp, J.; van der Goot, F. G. Caspase-1 activation of lipid metabolic pathways in response to bacterial pore-forming toxins promotes cell survival. *Cell* **2006**, *126*, 1135–1145.
7. Edelmann, B.; Bertsch, U.; Tchikov, V.; Winoto-Morbach, S.; Perrotta, C.; Jakob, M.; Adam-Klages, S.; Kabelitz, D.; Schütze, S. Caspase-8 and caspase-7 sequentially mediate proteolytic activation of acid sphingomyelinase in TNF-R1 receptosomes. *EMBO J.* **2011**, *30*, 379–394.
8. Fernandes, M. C.; Cortez, M.; Flannery, A. R.; Tam, C.; Mortara, R. A.; Andrews, N. W. *Trypanosoma cruzi* subverts the sphingomyelinase-mediated plasma membrane repair pathway for cell invasion. *J. Exp. Med.* **2011**, *208*, 909–921.
9. Pai, J. T.; Brown, M. S.; Goldstein, J. L. Purification and cDNA cloning of a second apoptosis-related cysteine protease that cleaves and activates sterol regulatory element binding proteins. *Proc. Natl. Acad. Sci. U.S.A.* **1996**, *93*, 5437–5442.
10. Brown, M. S.; Goldstein, J. L. Sterol regulatory element binding proteins (SREBPs): controllers of lipid synthesis and cellular uptake. *Nutr. Rev.* **1998**, *56*, S1–3– discussion S54–75.
11. Kaufmann, S. H.; Hahn, H.; Berger, R.; Kirchner, H. Interferon-gamma production by *Listeria monocytogenes*-specific T cells active in cellular antibacterial immunity. *Eur. J. Immunol.* **1983**, *13*, 265–268.
12. Grunfeld, C.; Feingold, K. R. Regulation of lipid metabolism by cytokines during host defense. *Nutrition* **1996**, *12*, S24–S26.
13. Zou, T.; Garifulin, O.; Berland, R.; Boyartchuk, V. L. *Listeria monocytogenes* infection

- induces prosurvival metabolic signaling in macrophages. *Infection and Immunity* **2011**, *79*, 1526–1535.
14. Martinon, F.; Glimcher, L. H. Regulation of innate immunity by signaling pathways emerging from the endoplasmic reticulum. *Curr. Opin. Immunol.* **2011**, *23*, 35–40.
 15. Chen, X.; Shen, J.; Prywes, R. The luminal domain of ATF6 senses endoplasmic reticulum (ER) stress and causes translocation of ATF6 from the ER to the Golgi. *J. Biol. Chem.* **2002**, *277*, 13045–13052.
 16. Pillich, H.; Loose, M.; Zimmer, K.-P.; Chakraborty, T. Activation of the unfolded protein response by *Listeria monocytogenes*. *Cell. Microbiol.* **2012**, *14*, 949–964.
 17. Stavru, F.; Bouillaud, F.; Sartori, A.; Ricquier, D.; Cossart, P. *Listeria monocytogenes* transiently alters mitochondrial dynamics during infection. *Proc. Natl. Acad. Sci. U.S.A.* **2011**, *108*, 3612–3617.
 18. Peters, L. R.; Raghavan, M. Endoplasmic reticulum calcium depletion impacts chaperone secretion, innate immunity, and phagocytic uptake of cells. *J. Immunol.* **2011**, *187*, 919–931.
 19. Hetz, C. The unfolded protein response: controlling cell fate decisions under ER stress and beyond. *Nat. Rev. Mol. Cell Biol.* **2012**, *13*, 89–102.
 20. Ambrose, R. L.; Mackenzie, J. M. ATF6 signaling is required for efficient West Nile virus replication by promoting cell survival and inhibition of innate immune responses. *J. Virol.* **2013**, *87*, 2206–2214.
 21. Martinon, F.; Chen, X.; Lee, A.-H.; Glimcher, L. H. TLR activation of the transcription factor XBP1 regulates innate immune responses in macrophages. *Nat. Immunol.* **2010**, *11*, 411–418.
 22. Gekara, N. O.; Westphal, K.; Ma, B.; Rohde, M.; Groebe, L.; Weiss, S. The multiple mechanisms of Ca²⁺ signalling by listeriolysin O, the cholesterol-dependent cytolysin of *Listeria monocytogenes*. *Cell. Microbiol.* **2007**, *9*, 2008–2021.
 23. Huang, J.; Brumell, J. H. Autophagy in immunity against intracellular bacteria. *Curr. Top. Microbiol. Immunol.* **2009**, *335*, 189–215.
 24. Amer, A. O.; Swanson, M. S. Autophagy is an immediate macrophage response to *Legionella pneumophila*. *Cell. Microbiol.* **2005**, *7*, 765–778.
 25. Meyer-Morse, N.; Robbins, J. R.; Rae, C. S.; Mochegova, S. N.; Swanson, M. S.; Zhao, Z.; Virgin, H. W.; Portnoy, D. Listeriolysin O is necessary and sufficient to induce autophagy during *Listeria monocytogenes* infection. *PLoS ONE* **2010**, *5*, e8610.
 26. Birmingham, C. L.; Canadien, V.; Gouin, E.; Troy, E. B.; Yoshimori, T.; Cossart, P.; Higgins, D. E.; Brumell, J. H. *Listeria monocytogenes* evades killing by autophagy during colonization of host cells. *Autophagy* **2007**, *3*, 442–451.

27. Shpilka, T.; Weidberg, H.; Pietrokovski, S.; Elazar, Z. Atg8: an autophagy-related ubiquitin-like protein family. *Genome Biol.* **2011**, *12*, 226.

28. Terasaki, M.; Loew, L.; Lippincott-Schwartz, J.; Zaal, K. Fluorescent staining of subcellular organelles: ER, Golgi complex, and mitochondria. *Curr Protoc Cell Biol* **2001**, Chapter 4, Unit 4.4.

Chapter 5

Perspectives

Caspase-7 is the middle of the story

Unknown are the signals and/or upstream factors that stimulate caspase-7 after PFT treatment. To our knowledge there are no instances in the literature where caspase-7 undergoes autocatalysis. The best studied pathways that activate caspase-7 are the intrinsic and extrinsic mechanisms of apoptosis, both of which rely on initiator caspases -8/-10 or -9 for caspase-7 cleavage [1]. Our laboratory has preliminary data suggesting caspase-9 is activated by LLO treatment with similar kinetics to caspase-7 (data not shown), which would suggest the involvement of mitochondria in the toxin response. The Cossart group published data suggesting that the mitochondrial network undergoes dramatic but transient rearrangement after treatment with LLO [2]. Whether caspase-9 is activating caspase-7 after PFT damage has not yet been determined, but it is interesting to speculate that transient mitochondrial dysregulation stimulates components of the intrinsic apoptotic pathway to promote membrane repair after treatment with LLO.

As previously mentioned in Chapter 4, ER stress has been associated with caspase-7 activation, namely through proteolysis by caspase-12, although this connection is controversial [3-5]. We were unable to detect ER stress in response to LLO, therefore, caspase-12 is not the most likely candidate for PFT induced caspase-7 activation, but this has yet to be tested. However, Ca^{2+} sensing represents a viable mechanism by

which caspase-7 directed repair may be initiated, and it is possible that a non-caspase protease is responsible for caspase-7 cleavage. In chapter 4, we discussed the importance of Ca^{2+} signaling in repair and blebbing and others have shown that calpain-1, a Ca^{2+} -dependent cysteine protease, can activate caspase-7 [6]. We have yet to determine if calpain-1 cleaves caspase-7 during intoxication. But, given the known role for Ca^{2+} during intoxication and repair [7-9], we speculate that Ca^{2+} -dependent signaling is critical for the execution of the caspase-7 cytoprotective response.

Also unknown is how cleaved caspase-7 is turned over in response to PFT treatment. Transient activation of caspase-3 has been implied for the differentiation of a variety of cell types [10,11], but resolution of caspase-3 cleavage has only been demonstrated in the transition from myoblasts to skeletal muscle cells [12]. The mechanism by which active caspases are turned over during cell differentiation was not addressed in these papers, however there are some hints in the literature about how this might be achieved. Inhibitor of apoptosis proteins (IAPs), as their name suggests, are a large family of proteins that function to suppress programmed cell death in host cells [13]. Of particular interest are the c-IAPs, which contain a caspase recruitment domain (CARD) in addition to the standard baculovirus IAP repeat (BIR) and RING domain typified by this family. Work by Choi *et al* has demonstrated that cIAP1 binds to the active form of caspase-7 [14]. The RING domain of cIAP1 ubiquitinated the larger active subunit of caspase-7 to promote its degradation by the proteasome [14]. Therefore, we hypothesize that toxin-induced, activated caspase-7 may be turned over in the same manner. Whether active caspase-7 is bound by c-IAP1 and/or ubiquitinated after PFT-induced activation is currently being investigated.

Mechanisms of caspase activation and implications for partial activation

Caspases are resident in the cytosol of cells as zymogens often called pro-caspases. In a resting state, proteolytic activity is constrained by the structural conformation of these proteins. For the initiator caspases, pro-caspase monomers are recruited to polymeric activation platforms, and the subsequent dimerization of pro-caspases induces an activating rearrangement called the induced proximity model of activation [15,16]. Auto-processing after dimerization of the initiator caspases -8 and -2 promotes stability and protease activity [16-18]. However, inter-domain cleavage after dimerization of the initiator caspase-9 attenuates its activity [16,19]. Thus the initiator caspases can be controlled by cleavage with divergent outcomes for their proteolytic capacity.

In contrast, the executioner pro-caspases -3 and -7 exist as dimers in the cytosol and generally require cleavage by an external protease to promote their activity [20-22]. Cleavage results in two antiparallel heterodimers, each composed of a p20 and p10 subunit. Each exposed p20 subunit contains the catalytically active site, whereas the p10 subunit forms the substrate-binding pocket [23,24]. Therefore, the intramolecular rearrangement resulting from activating cleavage helps define the active site of caspases -3 and -7. It is interesting to speculate that cleavage may represent a mechanism by which caspase activity can be finely tuned. In this case, the canonical cleavage site may form a substrate-binding pocket selective for apoptotic substrates. However, if caspase activity is needed to drive a survival response, alternative cleavage could form an active site specific for a defined subset of proteins whose cleavage supports an adaptive response.

The kinetics and mechanism of activation may explain how specificity of the caspase-7 cytoprotectivity is achieved. Recent work elegantly described the structural changes that occur during the transition from pro-form to active form for both caspases -3 and -7. The authors found that caspase-3 activation is “all or nothing”: The pro-form is

catalytically inactive and both heterodimers mature concurrently at maximal activity [25]. However, pro-caspase-7 maturation is significantly different. Pro-caspase-7 has latent, albeit weak, catalytic activity [25], which suggests that alterations in structure, in the absence of direct cleavage, are sufficient to expose the caspase-7 catalytic site (Fig 5.1). It is possible that protein-protein interaction could provide the context for the caspase-7 cytoprotective response, whereby off-site binding could deform pro-caspase-7 sufficiently to expose to the active site. This may also help to explain the relatively low cleavage of caspase-7 in response to PFT damage, despite that striking phenotype in *csp7^{-/-}* cells. Thus, we may be overestimating the importance of cleavage to the activity of caspase-7. Additionally, the uncleaved, but active, enzyme would have a different substrate-binding pocket than the cleaved form, and could have preference for substrates involved in the adaptive survival response as opposed to substrates responsible for the execution of apoptosis.

Caspase-7 can exist in a partial activation state, where one heterodimer is immature and one is cleaved [25,26] (Fig 5.1). Partial activation may help to temper the catalytic capacity of caspase-7. We have demonstrated the activation of proteins important in apoptosis, such as ROCKs, in a caspase-7 dependent manner after intoxication, in the relative absence of cell death. It is possible that partial maturation of caspase-7 is insufficient to stimulate an apoptotic cascade within the cell. Indeed, research suggest that caspase-3 is the predominate caspase responsible for the execution of apoptosis [27]. Our data suggests that caspase-3 is very weakly activated by infection (Fig. A2), which may also explain why *Listeria* infected cells are not apoptotic.

During apoptosis, caspases -3 and -7 display overlapping substrate specificity. However, careful studies have identified proteolytic targets unique to each enzyme both *in vitro* and *in vivo* [27,28]. Additionally, proteomics and synthetic chemistry have

Figure 5.1

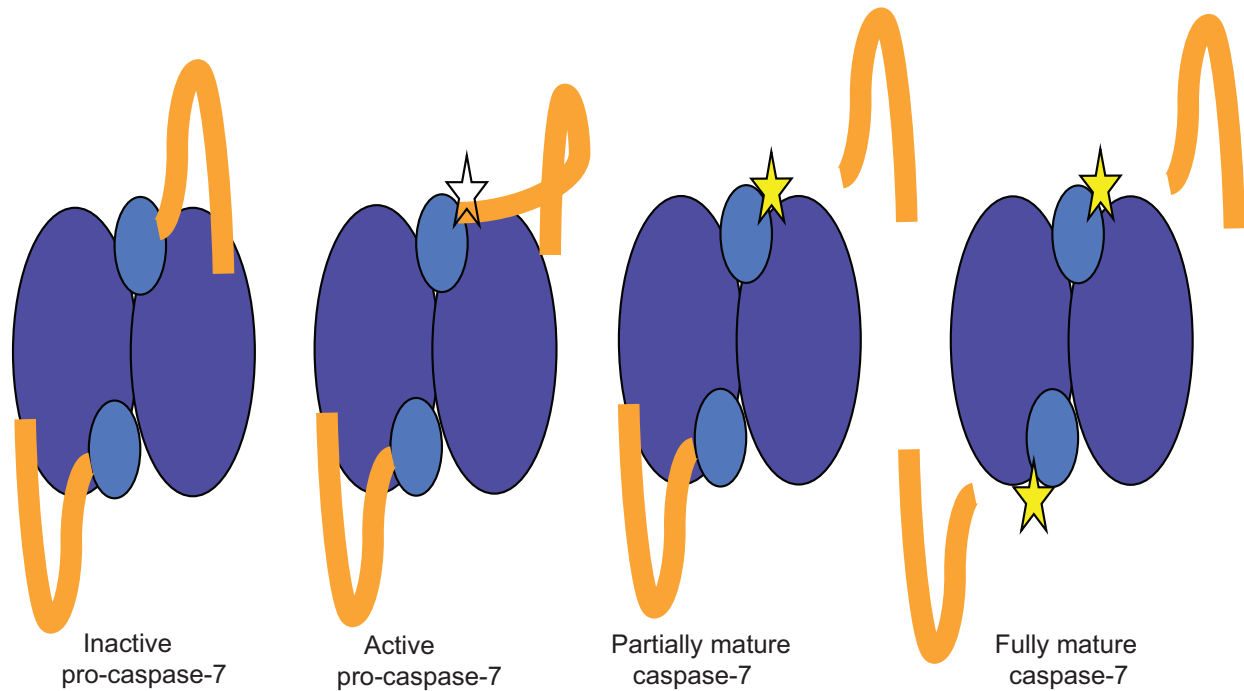


Figure 5.1 Models of caspase-7 activation. Pro-caspase-7 exists in the cytosol as a dimer with an anti-parallel conformation. Unlike pro-caspase-3, pro-caspase-7 can have proteolytic activity in the absence of cleavage [25]. Caspase-7 can also exist in a partially mature state, where the linker region occluding one active site is cleaved [25,26]. Finally, the fully mature caspase-7 has two fully exposed active site.

identified peptides cleaved by one but not the other caspase [28], indicating these two enzymes are not functionally redundant. However, there is little evidence in the literature of selective activation of these two proteases. As such, the question arises as to how caspase-activating specificity is achieved during infection. It is possible that subcellular location shapes the resulting response. Caspase-7 is reported to associate with plasma membrane-proximal structures [29], and thus could be in close proximity to the signaling cascade resulting from PFT-derived membrane damage.

A role for caspase-3 during intoxication?

In this body of work, we have demonstrated a role for caspase-7 in promoting membrane integrity after damage by the pore-forming toxin (PFT) listeriolysin O, LLO. Given that caspase-7 and caspase-3 are both activated during apoptosis and cleave many of the same substrates, the question arises as to whether caspase-3 may also play a role in membrane protection after PFT damage. In chapter 2, we demonstrated that caspase-3 is not activated as strongly as caspase-7 in the context of infection (Fig. A2) [30]. This result is recapitulated in the context of toxin treatment as well. At sub-lytic concentrations of LLO (0.25 μ g/ml), we can detect caspase-7 activation as early as 30 min post toxin treatment in the absence of caspase-3 cleavage (Fig. 5.2). We also detect no caspase-3 cleavage after 1 h of toxin treatment, however, if we allow the cells to incubate with toxin for longer periods of time, caspase-3 does eventually become activated in BL/6 and *csp7^{-/-}* cells (Fig 5.2). Recent reports suggest the threshold of activation of caspase-7 is lower than caspase-3 [25], which may represent a mechanism by which the cell diverts adaptive caspase signaling from apoptotic caspase signaling. Importantly, this experiment also demonstrates that there is no compensatory

upregulation of caspase-3 activity in the absence of caspase-7, unlike what has been observed under other experimental conditions [31,32] (Fig 5.2). In fact the opposite seems true; there is less caspase-3 activation in the *csp7^{-/-}* cells compared to BL/6. It is unlikely that caspase-7 is activating caspase-3 as this does not occur *in vitro* [33]. Therefore, this suggests caspase-7 plays a non-redundant role in protecting the membrane after PFT damage.

I speculate that the appearance of caspase-3 activation after longer periods of intoxication may indeed be a bellwether of apoptosis. During initial PFT damage, caspase-7 is activated to stimulate the repair of damaged membrane, but in the absence of adequate repair, or during continuous and unresolved damage by LLO, programmed cell death is invoked by caspase-3. It is also possible that, during unresolved damage, caspase-3 is activated to aid the repair process. Since inducers of apoptosis tend to activate both proteases equivalently, sequential activation could act as a hallmark to shunt the cell into repair and not death. If caspase-3 does promote repair, we hypothesize that the *csp3^{-/-}* cells should behave similarly to the *csp7^{-/-}* cells when damaged by PFTs. The role of caspase-3 activation during LLO treatment has yet to be tested. However, based on the delayed kinetics of caspase-3 activation in response to toxin treatment, we favor a model whereby caspase-7 is the principal caspase orchestrating membrane repair after PFT injury.

Although caspase-3 and -7 have considerable overlapping substrate specificity, there are reports highlighting the differences between these proteases. For instance, several reports indicate that caspase-3 is the more proteolytically active caspase on a variety of substrates [33-36]. Higher proteolytic activity of caspase-3 may represent another reason why the cell would preferentially activate caspase-7 over caspase-3 when repairing

Figure 5.2

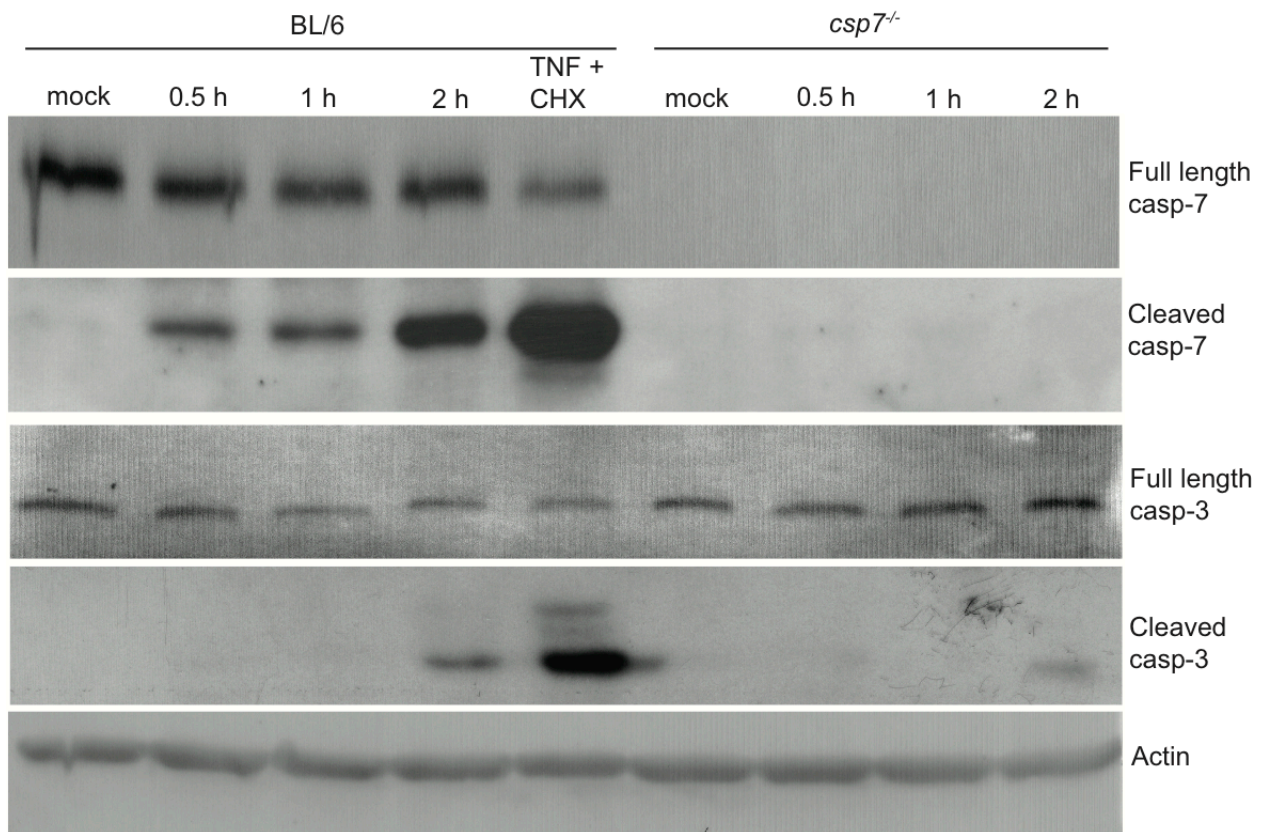


Figure 5.2. Caspase-3 is activated with slower kinetics than caspase-7 in response to toxin treatment. BMDMs were intoxicated with 0.25 μ g/ml LLO for the indicated times, after which the cells were lysed and probed for caspase-7 and caspase-3 cleavage (Cell Signaling cat #9492 and #9665 respectively) and actin. Treatment with TNF α and cyclohexamide (TNF α + CHX) was used as positive control for cleavage of both caspases. This experiment was performed by MEC.

damage rather than inducing apoptosis. Others have reported that caspase-3 directly cleaves ROCK I during programmed cell death to promote membrane blebbing [37,38]. We currently have no evidence that caspase-7 cleaves ROCK I directly during PFT damage, but it is possible, given the large number of shared targets between these two proteases that ROCK I is cleaved by caspase-7 to orchestrate blebbing after LLO treatment. It is also possible that caspase-7 does not directly cleave ROCK I, but promotes the activity of the kinase in other ways discussed below. In this example, the lower proteolytic activity of caspase-7 may be beneficial to the cell. ROCK I can be activated by several mechanisms including cleavage, phosphorylation, and dimerization [39-41]. Cleavage is an irreversible activation which increases the activity of this protein 8-fold [38], and we have yet to find in the literature a mechanism by which cleaved ROCK I is turned over. Therefore, cleavage of a large proportion of ROCK I may not represent the most efficient mechanism to achieve transient or acute activation. The lower proteolytic activity of caspase-7 may help to regulate the amount of ROCK I activated, which could in turn regulate unmitigated signaling resulting in apoptosis. Additionally, caspase-7 activity may indirectly activate the rho-kinases, through promoting their phosphorylation for example. ROCK I activated in this manner could then be deactivated by a phosphatase when membrane damage is resolved. Thus, the specificity of the blebbing response to toxin, employing proteins with known roles in apoptosis, may be conferred and controlled by the strength of signal received.

Live to fight another day

For macrophages, there are many potential benefits to withstanding damage by PFTs. Macrophages are among the first responders to an infection, and as such encounter a variety of membrane-damaging agents. Their ability to aid in the clearance

of infection likely depends on their ability to survive such insults. Similarly, macrophages that survive such damage promote inflammation by cytokine secretion and adaptive immunity through antigen presentation. Thus, having mechanisms in place to protect macrophages from infectious membrane damage is beneficial to many arms of the immune system. However, the ability of macrophages to heal from PFT damage may also be a consequence of their lifestyle. As mentioned previously, some cell types use blebbing as a form of motility [42], and because macrophages are motile cells, they likely encounter membrane stress traveling to different locations in the host. Therefore, it is also possible that macrophages have adapted to repair acute membrane damage independent of infection, but this ability fortuitously improves immunity by extending the life span of macrophages under attack.

However, in the case of intracellular pathogens such as *L. monocytogenes*, extending the life of macrophages greatly benefits the invader as well. This is exemplified by infection with *L. monocytogenes* that produces a hyperactive allele of LLO, or a copy of LLO deficient in translational repression. These bacteria are attenuated in mouse models of infection, presumably because misregulated LLO overtakes the cells ability to repair PFT damage resulting in cell lysis and exposing *L. monocytogenes* to neutrophils, against which they have little defense [43-45]. Thus, the bacterium must tune the production of LLO in the macrophage to a balance that promotes both its escape from the cytosol and the resolution of collateral damage at the plasma membrane.

The importance of this work

The contribution of this dissertation research to the advancement of science lies in two broad concepts: duality and signal strength. Caspase-7, Rho-kinases, and myosin II, proteins with defined roles in the execution of apoptosis, are also needed to stimulate

membrane repair and survival in the context of LLO-mediated membrane damage. As previously discussed, I speculate the low-level activation of caspase-7 is the key to defining the downstream response, in this case, the difference between survival and programmed cell death. Figure 5.3 illustrates this idea as a graphic. This idea is not new to science, but I feel the work outlined in this dissertation provide strong evidence for the importance of this concept. When I first presented this research, it was suggested that the DEVDase activity (a marker of caspase3/7 activity) in infected cells was very weak compared to staurosporine (an inducer of apoptosis) treatment, and that the small increase in activity over baseline was not significant. I was fortunate to have genetic data supporting a role of caspase-7 during infection, but I use this anecdote as an example of our internal bias as scientists that more is better.

I propose that a large part of the dichotomous role of caspase-7 lies not only in the amount of caspase-7 activated, but also its rapid turn over once membrane integrity has been reestablished. In RAW cells we detect decreases in cleaved caspase-7 as early as 2 h after toxin removal, which correlates well with decreased permeability to small fluorescent molecules (Fig 3.1). Thus, caspase-7 is degraded when the signaling it generates is no longer needed, reducing the likelihood of unintended apoptotic activation. The concept of signal strength is gaining support in the literature thanks in part to more sensitive detection methods that have uncovered low-level, but physiologically relevant, changes after cell stimulation. Understanding the underlying signals that promote cellular homeostasis and survival are integral to our understanding of host-pathogen interaction and cellular biology.

Figure 5.3

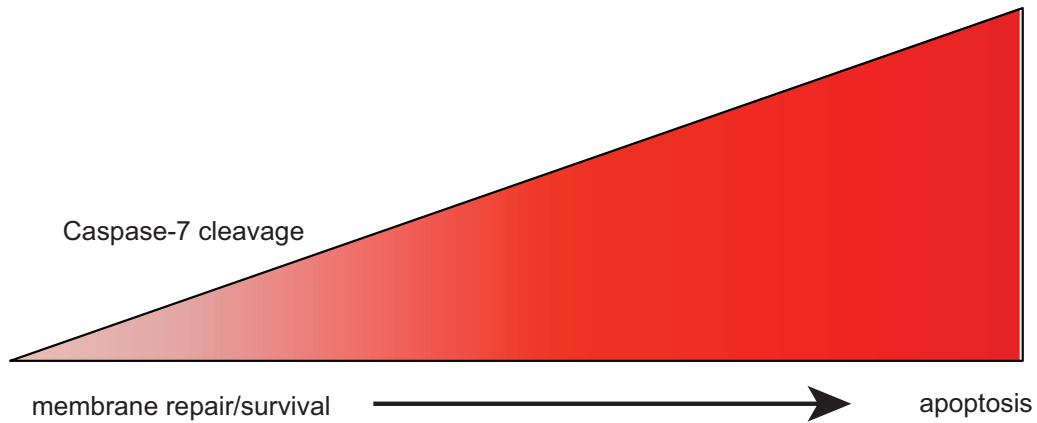


Figure 5.3. A schematic of the dichotomous roles of activated caspase-7. When a small proportion of caspase-7 is activated by LLO-mediated membrane damage, the resulting response favors membrane integrity and cell survival. When a larger proportion of total caspase-7 is activated, the cell executes apoptosis.

References

1. Riedl, S. J.; Salvesen, G. S. The apoptosome: signalling platform of cell death. *Nat. Rev. Mol. Cell Biol.* **2007**, *8*, 405–413.
2. Stavru, F.; Bouillaud, F.; Sartori, A.; Ricquier, D.; Cossart, P. *Listeria monocytogenes* transiently alters mitochondrial dynamics during infection. *Proc. Natl. Acad. Sci. U.S.A.* **2011**, *108*, 3612–3617.
3. Nakagawa, T.; Zhu, H.; Morishima, N.; Li, E.; Xu, J.; Yankner, B. A.; Yuan, J. Y. Caspase-12 mediates endoplasmic-reticulum-specific apoptosis and cytotoxicity by amyloid-beta. *Nature* **2000**, *403*, 98–103.
4. Shiraiishi, H.; Okamoto, H.; Yoshimura, A.; Yoshida, H. ER stress-induced apoptosis and caspase-12 activation occurs downstream of mitochondrial apoptosis involving Apaf-1. *Journal of Cell Science* **2006**, *119*, 3958–3966.
5. Shibata, M.; Hattori, H.; Sasaki, T.; Gotoh, J.; Hamada, J.; Fukuuchi, Y. Activation of caspase-12 by endoplasmic reticulum stress induced by transient middle cerebral artery occlusion in mice. *Neuroscience* **2003**, *118*, 491–499.
6. Gafni, J.; Cong, X.; Chen, S. F.; Gibson, B. W.; Ellerby, L. M. Calpain-1 Cleaves and Activates Caspase-7. *Journal of Biological Chemistry* **2009**, *284*, 25441–25449.
7. Walev, I.; Bhakdi, S. C.; Hofmann, F.; Djonder, N.; Valeva, A.; Aktories, K.; Bhakdi, S. Delivery of proteins into living cells by reversible membrane permeabilization with streptolysin-O. *Proc. Natl. Acad. Sci. U.S.A.* **2001**, *98*, 3185–3190.
8. Gonzalez, M. R.; Bischofberger, M.; Frêche, B.; Ho, S.; Parton, R. G.; van der Goot, F. G. Pore-forming toxins induce multiple cellular responses promoting survival. *Cell. Microbiol.* **2011**, *13*, 1026–1043.
9. Reddy, R.; Mao, C.; Baumeister, P.; Austin, R.; Kaufman, R.; Lee, A. Endoplasmic reticulum chaperone protein GRP78 protects cells from apoptosis induced by topoisomerase inhibitors - Role of ATP binding site in suppression of caspase-7 activation. *J. Biol. Chem.* **2003**, *278*, 20915–20924.
10. Miura, M.; Chen, X.-D.; Allen, M. R.; Bi, Y.; Gronthos, S.; Seo, B.-M.; Lakhani, S.; Flavell, R. A.; Feng, X.-H.; Robey, P. G.; Young, M.; Shi, S. A crucial role of caspase-3 in osteogenic differentiation of bone marrow stromal stem cells. *J Clin Invest* **2004**, *114*, 1704–1713.
11. D'Amelio, M.; Cavallucci, V.; Cecconi, F. Neuronal caspase-3 signaling: not only cell death. *Cell Death Differ* **2010**, *17*, 1104–1114.
12. Fernando, P.; Kelly, J. F.; Balazsi, K.; Slack, R. S.; Megeney, L. A. Caspase 3 activity is required for skeletal muscle differentiation. *Proc. Natl. Acad. Sci. U.S.A.* **2002**, *99*, 11025–11030.
13. Deveraux, Q. L.; Reed, J. C. IAP family proteins--suppressors of apoptosis. *Genes*

Dev. **1999**, *13*, 239–252.

14. Choi, Y. E.; Butterworth, M.; Malladi, S.; Duckett, C. S.; Cohen, G. M.; Bratton, S. B. The E3 ubiquitin ligase cIAP1 binds and ubiquitinates caspase-3 and -7 via unique mechanisms at distinct steps in their processing. *J. Biol. Chem.* **2009**, *284*, 12772–12782.
15. Muzio, M.; Stockwell, B. R.; Stennicke, H. R.; Salvesen, G. S.; Dixit, V. M. An induced proximity model for caspase-8 activation. *J. Biol. Chem.* **1998**, *273*, 2926–2930.
16. Pop, C.; Timmer, J.; Sperandio, S.; Salvesen, G. S. The apoptosome activates caspase-9 by dimerization. *Mol. Cell* **2006**, *22*, 269–275.
17. Boatright, K. M.; Renatus, M.; Scott, F. L.; Sperandio, S.; Shin, H.; Pedersen, I. M.; Ricci, J. E.; Edris, W. A.; Sutherlin, D. P.; Green, D. R.; Salvesen, G. S. A unified model for apical caspase activation. *Mol. Cell* **2003**, *11*, 529–541.
18. Baliga, B. C.; Read, S. H.; Kumar, S. The biochemical mechanism of caspase-2 activation. *Cell Death Differ* **2004**, *11*, 1234–1241.
19. Malladi, S.; Challa-Malladi, M.; Fearnhead, H. O.; Bratton, S. B. The Apaf-1*procaspase-9 apoptosome complex functions as a proteolytic-based molecular timer. *EMBO J.* **2009**, *28*, 1916–1925.
20. Riedl, S. J.; Fuentes-Prior, P.; Renatus, M.; Kairies, N.; Krapp, S.; Huber, R.; Salvesen, G. S.; Bode, W. Structural basis for the activation of human procaspase-7. *Proc. Natl. Acad. Sci. U.S.A.* **2001**, *98*, 14790–14795.
21. Chai, J.; Wu, Q.; Shiozaki, E.; Srinivasula, S. M.; Alnemri, E. S.; Shi, Y. Crystal structure of a procaspase-7 zymogen: mechanisms of activation and substrate binding. *Cell* **2001**, *107*, 399–407.
22. Boatright, K. M.; Salvesen, G. S. Mechanisms of caspase activation. *Curr. Opin. Cell Biol.* **2003**, *15*, 725–731.
23. Rotonda, J.; Nicholson, D. W.; Fazil, K. M.; Gallant, M.; Gareau, Y.; Labelle, M.; Peterson, E. P.; Rasper, D. M.; Ruel, R.; Vaillancourt, J. P.; Thornberry, N. A.; Becker, J. W. The three-dimensional structure of apopain/CPP32, a key mediator of apoptosis. *Nat. Struct. Biol.* **1996**, *3*, 619–625.
24. Wei, Y.; Fox, T.; Chambers, S. P.; Sintchak, J.; Coll, J. T.; Golec, J. M.; Swenson, L.; Wilson, K. P.; Charifson, P. S. The structures of caspases-1, -3, -7 and -8 reveal the basis for substrate and inhibitor selectivity. *Chem. Biol.* **2000**, *7*, 423–432.
25. Thomsen, N. D.; Koerber, J. T.; Wells, J. A. Structural snapshots reveal distinct mechanisms of procaspase-3 and -7 activation. *Proc. Natl. Acad. Sci. U.S.A.* **2013**, *110*, 8477–8482.
26. Berger, A. B.; Witte, M. D.; Denault, J.-B.; Sadaghiani, A. M.; Sexton, K. M. B.; Salvesen, G. S.; Bogoy, M. Identification of early intermediates of caspase activation using selective inhibitors and activity-based probes. *Mol. Cell* **2006**, *23*, 509–521.

27. Walsh, J. G.; Cullen, S. P.; Sheridan, C.; Lüthi, A. U.; Gerner, C.; Martin, S. J. Executioner caspase-3 and caspase-7 are functionally distinct proteases. *Proc. Natl. Acad. Sci. U.S.A.* **2008**, *105*, 12815–12819.
28. Demon, D.; Van Damme, P.; Vanden Berghe, T.; Deceuninck, A.; Van Durme, J.; Verspurten, J.; Helsens, K.; Impens, F.; Wejda, M.; Schymkowitz, J.; Rousseau, F.; Madder, A.; Vandekerckhove, J.; Declercq, W.; Gevaert, K.; Vandenabeele, P. Proteome-wide substrate analysis indicates substrate exclusion as a mechanism to generate caspase-7 versus caspase-3 specificity. *Mol. Cell Proteomics* **2009**, *8*, 2700–2714.
29. Edelmann, B.; Bertsch, U.; Tchikov, V.; Winoto-Morbach, S.; Perrotta, C.; Jakob, M.; Adam-Klages, S.; Kabelitz, D.; Schütze, S. Caspase-8 and caspase-7 sequentially mediate proteolytic activation of acid sphingomyelinase in TNF-R1 receptosomes. *EMBO J.* **2011**, *30*, 379–394.
30. Cassidy, S. K. B.; Hagar, J. A.; Kanneganti, T.-D.; Franchi, L.; Núñez, G.; O’Riordan, M. X. D. Membrane damage during *Listeria monocytogenes* infection triggers a caspase-7 dependent cytoprotective response. *PLoS Pathog* **2012**, *8*, e1002628.
31. Woo, M.; Hakem, R.; Soengas, M. S.; Duncan, G. S.; Shahinian, A.; Kägi, D.; Hakem, A.; McCurrach, M.; Khoo, W.; Kaufman, S. A.; Senaldi, G.; Howard, T.; Lowe, S. W.; Mak, T. W. Essential contribution of caspase 3/ CPP32 to apoptosis and its associated nuclear changes. *Genes Dev.* **1998**, *12*, 806–819.
32. Sung, Y. H.; Lee, J. S.; Park, S. H.; Koo, J.; Lee, G. M. Influence of co-down-regulation of caspase-3 and caspase-7 by siRNAs on sodium butyrate-induced apoptotic cell death of Chinese hamster ovary cells producing thrombopoietin. *Metab. Eng.* **2007**, *9*, 452–464.
33. Denault, J.-B.; Salvesen, G. S. Human caspase-7 activity and regulation by its N-terminal peptide. *J. Biol. Chem.* **2003**, *278*, 34042–34050.
34. Stennicke, H. R.; Renucci, M.; Meldal, M.; Salvesen, G. S. Internally quenched fluorescent peptide substrates disclose the subsite preferences of human caspases 1, 3, 6, 7 and 8. *Biochem. J.* **2000**, *350 Pt 2*, 563–568.
35. McStay, G. P.; Salvesen, G. S.; Green, D. R. Overlapping cleavage motif selectivity of caspases: implications for analysis of apoptotic pathways. *Cell Death Differ* **2008**, *15*, 322–331.
36. Boucher, D.; Blais, V.; Denault, J.-B. Caspase-7 uses an exosite to promote poly(ADP ribose) polymerase 1 proteolysis. *Proc. Natl. Acad. Sci. U.S.A.* **2012**, *109*, 5669–5674.
37. Coleman, M. L.; Sahai, E. A.; Yeo, M.; Bosch, M.; Dewar, A.; Olson, M. F. Membrane blebbing during apoptosis results from caspase-mediated activation of ROCK I. *Nat. Cell Biol.* **2001**, *3*, 339–345.
38. Sebbagh, M.; Renvoizé, C.; Hamelin, J.; Riché, N.; Bertoglio, J.; Bréard, J. Caspase-3-mediated cleavage of ROCK I induces MLC phosphorylation and apoptotic membrane

blebbing. *Nat. Cell Biol.* **2001**, *3*, 346–352.

39. Coleman, M. L.; Olson, M. F. Rho GTPase signalling pathways in the morphological changes associated with apoptosis. *Cell Death Differ* **2002**, *9*, 493–504.

40. Riento, K.; Ridley, A. J. Rocks: multifunctional kinases in cell behaviour. *Nat. Rev. Mol. Cell Biol.* **2003**, *4*, 446–456.

41. Garg, R.; Riento, K.; Keep, N.; Morris, J. D. H.; Ridley, A. J. N-terminus-mediated dimerization of ROCK-I is required for RhoE binding and actin reorganization. *Biochem. J.* **2008**, *411*, 407–414.

42. Charras, G.; Paluch, E. Blebs lead the way: how to migrate without lamellipodia. *Nat. Rev. Mol. Cell Biol.* **2008**, *9*, 730–736.

43. Schnupf, P.; Portnoy, D. A.; Decatur, A. L. Phosphorylation, ubiquitination and degradation of listeriolysin O in mammalian cells: role of the PEST-like sequence. *Cell. Microbiol.* **2006**, *8*, 353–364.

44. Glomski, I. J.; Decatur, A. L.; Portnoy, D. A. *Listeria monocytogenes* mutants that fail to compartmentalize listeriolysin O activity are cytotoxic, avirulent, and unable to evade host extracellular defenses. *Infection and Immunity* **2003**, *71*, 6754–6765.

45. Schnupf, P.; Hofmann, J.; Norseen, J.; Glomski, I. J.; Schwartzstein, H.; Decatur, A. L. Regulated translation of listeriolysin O controls virulence of *Listeria monocytogenes*. *Mol. Microbiol.* **2006**, *61*, 999–1012.

Appendix I

Purpose

The following section contains figures supplemental to the main chapter discussions. Figures A1-A7 were included as supplemental material to the PLoS Pathogens paper, and are referenced in Chapter 2. Figure A8 is an immunoblot demonstrating transient activation of caspase-7 in response to LLO treatment in BMDMs. This data is referenced in Chapter 3. Figure A9 demonstrates that loss of caspase-7 renders BMDMs more permeable to small molecules after treatment with LLO. This is referenced in Chapter 3 and supported by data included in Figure 3.1.

Figure A1.

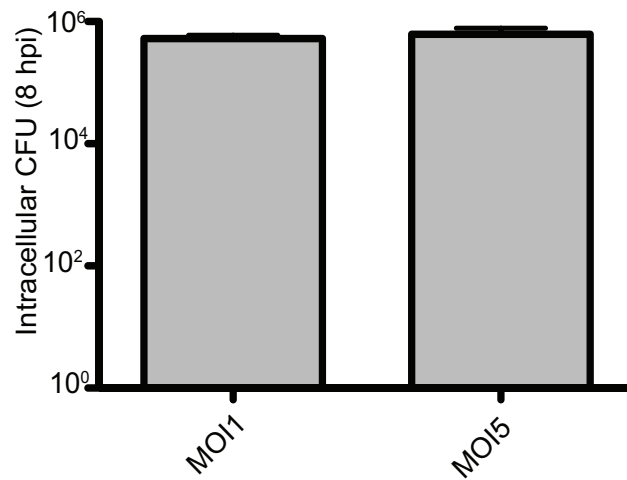


Figure A1. Infection at MOI1 and MOI5 results in equivalent intracellular CFU by 8 h pi. BL/6 BMDMs were infected at the indicated MOI for 30 min, after which 10 μ g/ml gentamicin was added to the cell culture medium to inhibit extracellular bacterial replication. Intracellular CFU were enumerated 8 h pi by osmotic lysis and serial dilution onto LB agar plates.

Figure A2.

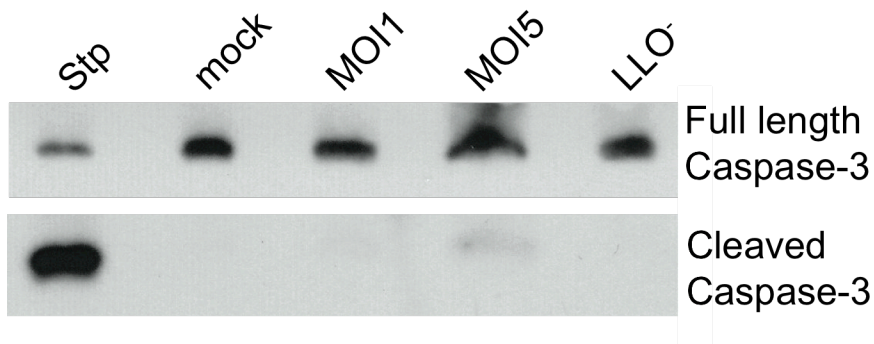


Figure A2. Caspase-3 is weakly cleaved in response to *L. monocytogenes* infection.

BL/6 BMDM were infected with *L. monocytogenes* and cell lysates were probed with an antibody that recognizes full-length and cleaved caspase-3 (Cell Signaling Technology). Cells were treated with 1 μ M staurosporine for 4 h (stp) as a positive control for caspase-3 cleavage.

Figure A3.

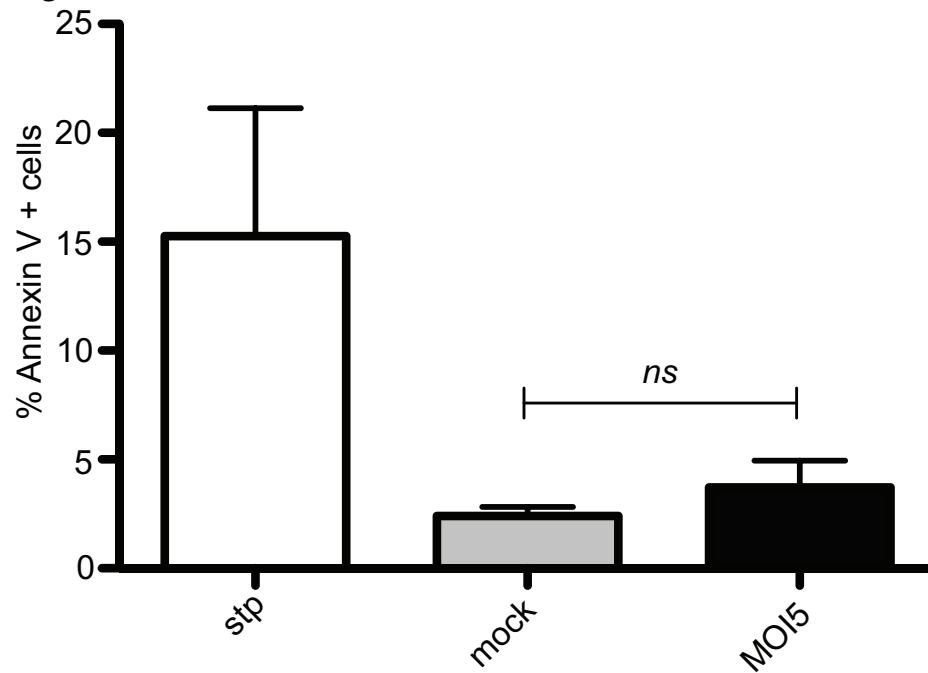


Figure A3. Most *L. monocytogenes* infected cells do not display common markers of apoptosis. BL/6 BMDMs were infected at MOI5 with *L. monocytogenes* for 6 h and then stained for phosphatidyl serine exposure using Annexin V according to the manufacturer's instructions (Biotium, Inc. Hayward, CA). The percentage of cells positive for Annexin V was determined via fluorescence microscopy of duplicate samples $N > 100$ cells per condition. Cells were treated with $1\mu\text{M}$ staurosporine for 4 h (stp) as a positive control for apoptosis. *ns* = not significant by Student's unpaired t-test.

Figure A4.

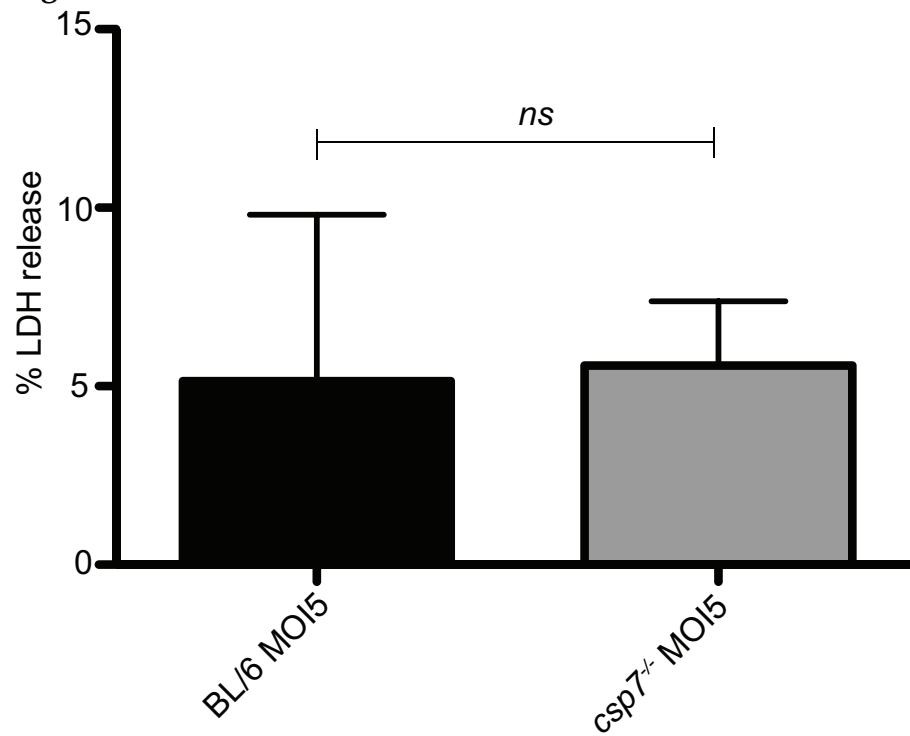


Figure A4. Caspase-7 deficient cells retain LDH at similar levels as BL/6 cells during infection. BMDMs isolated from BL/6 and caspase-7-deficient mice were infected at MOI5 with *L. monocytogenes* for 8 h after which release of lactate dehydrogenase (LDH) into cell culture supernatants was determined. The amount of LDH released as the result of detergent induced lysis was set to 100% and the amount of signal from uninfected cells was set to 0%. *ns* = not significant by Student's unpaired t-test.

Figure A5.

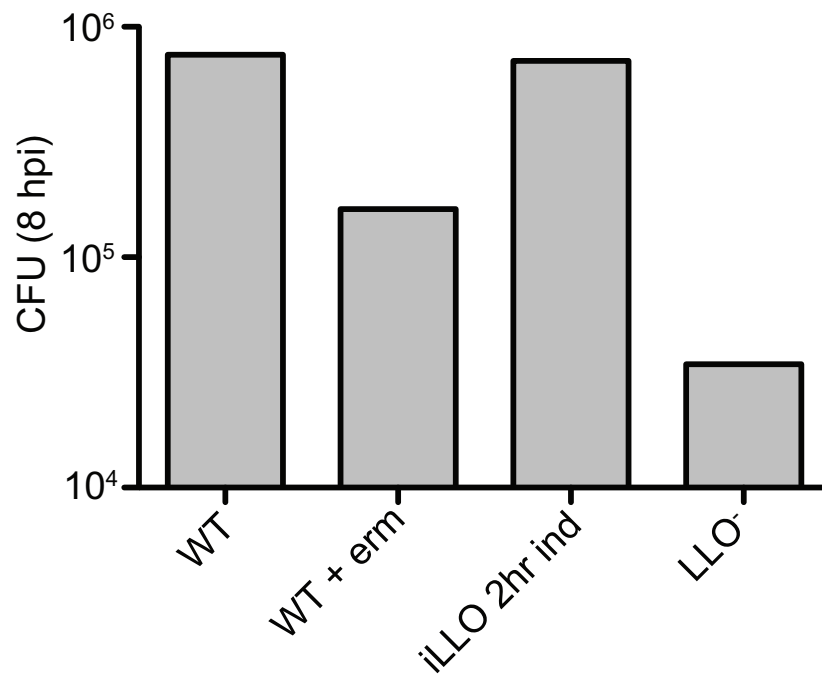


Figure A5. WT and iLLO strains grow to equivalent intracellular CFU by 8 h pi. WT BMDMs were infected using the indicated strains and conditions for 8 h as in Fig. A1. Intracellular CFU were enumerated by osmotic lysis of macrophages and serial dilution onto LB agar plates.

Figure A6.

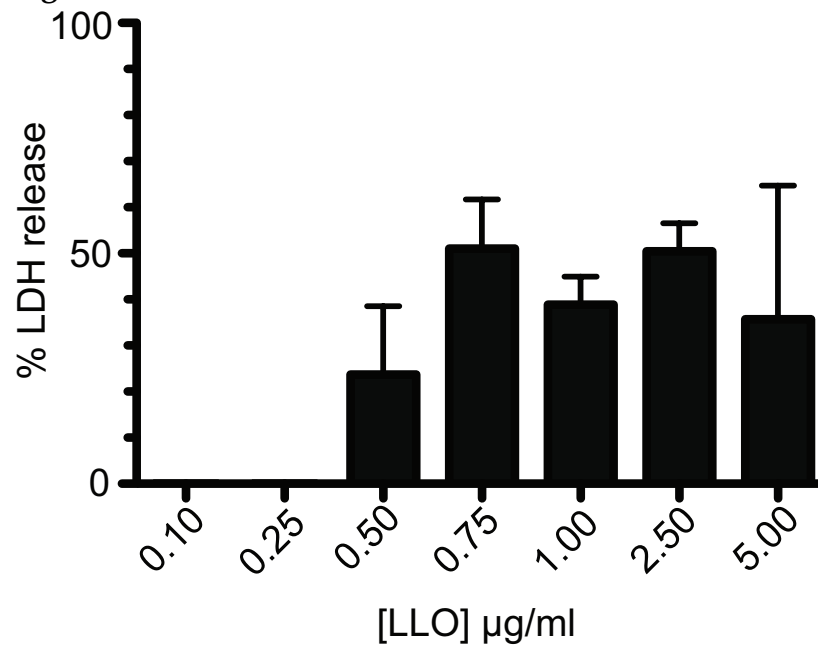


Figure A6. BMDM treated with low concentrations of exogenous LLO do not release LDH by 5 h pi. BMDM cultures from Fig 2.6C were washed 1 h post toxin treatment, after the initial LDH release measurement, and fresh medium was added to the cells. LDH released into the medium was measured after 5 h. The amount of LDH released as the result of detergent induced lysis was set to 100% and the amount of signal from uninfected cells was set to 0%.

Figure A7.

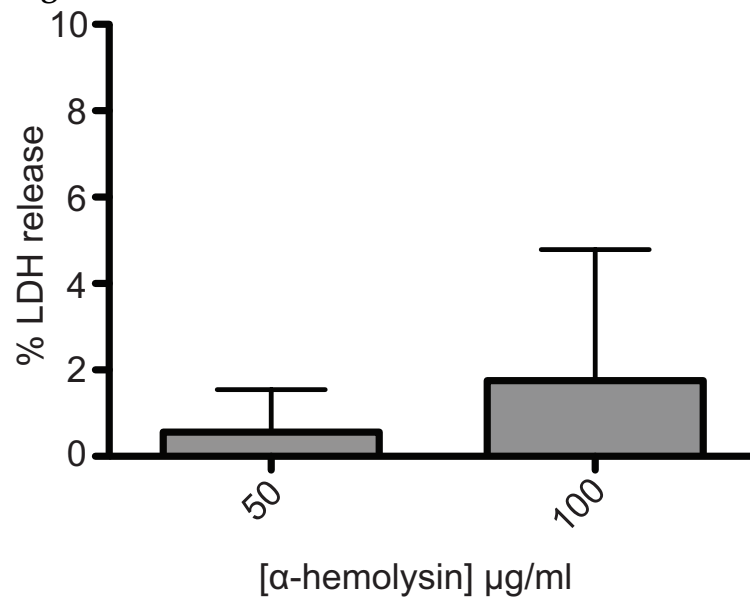


Figure A7. BMDM treated with α -hemolysin release little LDH 8 h post treatment. BMDMs from the experiment shown in Fig. 2.7CD were washed 1 h post toxin treatment, after the initial LDH release measurement, and fresh media was added to the cells. LDH released into the fresh medium was measured 8 h later. The amount of LDH released as the result of detergent induced lysis was set to 100% and the amount of signal from uninfected cells was set to 0%.

Figure A8.

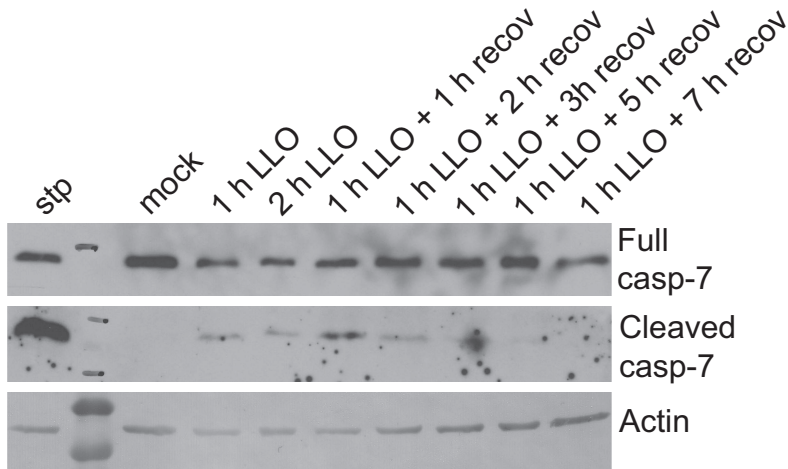


Fig A8. Treatment of BMDMs with LLO results in transient caspase-7 activation. BMDMs were incubated with $0.25\mu\text{g/ml}$ LLO for 1 or 2 h continuously, then lysed and probed for caspase-7 cleavage. For recovery (recov) samples, cells were incubated with $0.25\mu\text{g/ml}$ LLO for 1 h, and then washed and incubated in fresh media without toxin for the time noted. Cells were treated with $1\mu\text{M}$ staurosporine (stp) as a positive control for caspase-7 cleavage. Lysates were probed for actin as a loading control. Full length caspase-7 runs at 35kDa, cleaved caspase-7 runs at 17 kDa, and actin runs at 42kDa.

Figure A9.

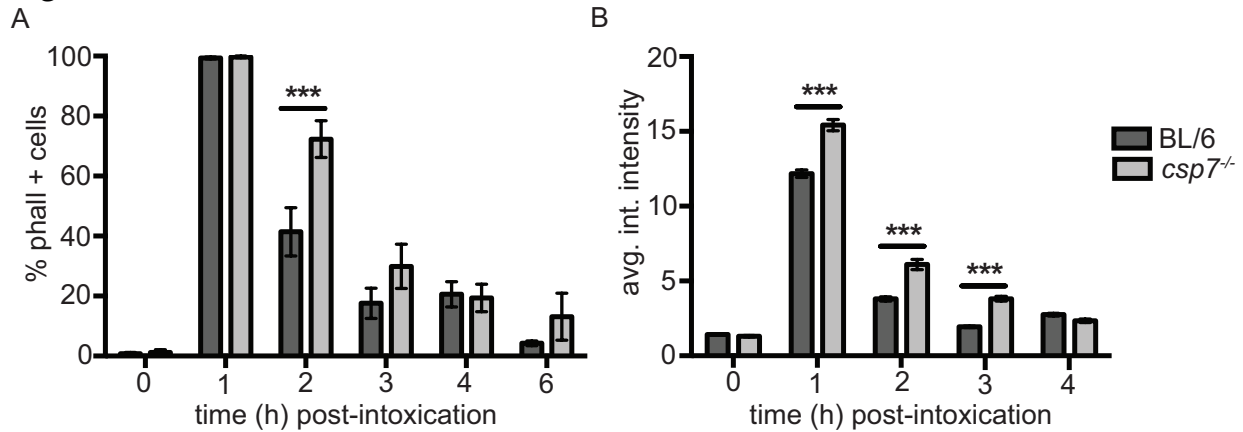


Figure A9. Caspase-7 deficient cells display slower recovery after LLO intoxication compared to BL/6 cells. (A and B) BMDMs were intoxicated with 0.25 μ g/ml LLO, after which they were incubated directly with 1:50 rhodamine-phalloidin (phall) for 15 min, or they were allowed to recover for the indicated time in media without toxin then incubated with phall. BMDMs were fixed and assessed for (A) the percentage of total cells stained positive for phall and (B) the intensity of phall staining as measured by Metamorph software. N > 200 cells per condition, graphs measure data from 3 independent experiments. *** P < 0.0001 by Student's unpaired t-test.